HISTORY OF THE CHUKCHI BORDERLAND AND THE AMERASIA BASIN, ARCTIC OCEAN

By

Ilhan Ibrahim, B.Eng., M.Eng.

A Dissertation Submitted in Partial Fulfillment of the Requirements

for the Degree of

Doctor of Philosophy

in

Geophysics

University of Alaska Fairbanks

August 2018

APPROVED:

Bernard J. Coakley, Committee Chair

Christopher A. Johnson, Committee Member

David W. Houseknecht, Committee Member

Michael T. Whalen, Committee Member

Paul J. McCarthy, Chair

Department of Geosciences

Anupma Prakash, Interim Dean

College of Natural Science and Mathematics

Michael Castellini, Interim Dean

Graduate School

Abstract

Structural and stratigraphic interpretation of 2D multi-channel seismic (MCS) reflection profiles through recognition of the sub-surface reflection patterns and integration of the seismic interpretation with the other geophysical and geological data reveal the history of the Chukchi Borderland. This investigation provides new constraints for the tectonic development of the Amerasia Basin.

North-striking normal faults of the Chukchi Borderland dissect the continental basement into the Chukchi Plateau, Northwind Basin and Northwind Ridge from west to east. A well-developed angular unconformity (Au) separates the stratigraphic section into sub and super-Au seismic units. Sub-Au units include: (1) seaward dipping reflections (SDRs) observed in the juncture between the North Chukchi-Toll Basins and Chukchi Plateau; (2) growth and folded strata in the Northwind Basin; (3) thrust faults in the Northwind Basin and over the Northwind Ridge; and (4) a clinoform sequence that downlaps onto the extended continental crust of the Canada Basin, supported by presence of SDRs and diapiric reflections within the crust. Au is inferred to correlate to the Hauterivian (LCu) and the Middle Jurassic (Ju) unconformities of the Alaska North Slope.

The SDRs indicate that the southwestern margin of the Chukchi Borderland may be a rifted continental margin. Loosely constrained age control of a super-Au unit (inferred condensed section, perhaps correlative to Hauterivian pebble shale or the Jurassic upper Kingak shale units of Alaska North Slope) implies that the rifted margin subsided no later than the earliest Cretaceous, providing a plausible time constraint for Middle Jurassic–earliest Cretaceous rifting in the North Chukchi Basin. The growth strata and north-striking normal faults of the Northwind Basin are continuous with the extensional structures of the Mississippian Hanna Trough, providing a geologic linkage between the two. The folding and thrust faults reveal a phase of contraction confined to sub-Au units of the south and eastern Northwind Basin and Northwind Ridge. The clinoform sequence of the

Northwind Ridge-Canada Basin is inferred to correlate with the Upper Jurassic-Lower Cretaceous Kingak shale unit of Alaska North Slope, implying that the extension of the crust beneath the western Canada Basin occurred no later than the Middle Jurassic.

Super-Au strata (~16 km) onlap the condensed section, SDRs, growth and passive margin strata from west to east, tapering down to a few kilometers north and eastward across the seismic grid. These are part of the Aptian through Cenozoic Brookian megasequence, a series of clinothems, deposited across the foreland of the Chukotka and Brooks Range orogens. These strata were deposited by northward-migrating depositional systems that progressively filled the North Chukchi Basin and buried the southern flank of the Chukchi Borderland, and deposited along the Northwind margin of the Canada Basin. Another unit of growth strata is observed in the Northwind Basin, indicating another phase of extension of the Boderland. The Upper Cretaceous section of the Brookian megasequence is displaced by normal faults over the Chukchi Plateau and inferred age-equivalent strata over the Northwind Ridge. These constrain the second phase of extension of the interior Borderland to the Late Cretaceous to Paleocene.

The recognition of the sub-Au units and continuity of the super-Au units across the area, north-striking normal faults, and the absence of east-directed thrust faults between the Northwind Ridge and Canada Basin invalidate one model proposed for tectonic development of the Amerasia Basin. Models that require significant relative motion between the Chukchi Shelf and Borderland since the Middle Jurassic are precluded by these observations.

Table of contents

List of figures

Acknowledgements

National Science Foundation Award (OPP-0909568) funded acquisition, processing and interpretation of the 2D multi-channel seismic (MCS) reflection profiles collected on board the *R/V Marcus G. Langseth*. ION Geophysical Corporation provided three years of research assistanship. The Geophysical Institute and Graduate School, University of Alaska Fairbanks provided two semesters of research assistantship, and one semester of thesis completion fellowship and one semester of tuition fee award, respectively. The Institute for Geophysics, University of Texas Austin hosted a year of curricular practical training under supervision of Nathan Bangs. Reprocessing of the MCS profiles funded by ExxonMobil and permission to use reprocessed MCS images granted by Brian Horn and Joe Gagliardi from ION are greatly appreciated.

The interpretations of MCS data and written manuscripts making up this dissertation were improved by reviews of David W. Houseknecht, David Stone and Michael T. Whalen, and by conversations with Christopher A. Johnson, Deniz Cukur, Garry D. Karner, Ian Norton, Kristian E. Miesling, Nathan Bangs, and the late Wesley K. Wallace. The AAPG Bulletin and Marine Petroleum Geology journal peer reviews of the manuscripts by David C. Mosher, Kirk W. Sherwood, Steven C. Bergman, Thomas X. Homza, Tim M. O'Brien, William H. Craddock, and the editorial comments by Barry J. Katz and Lawrence B. Aspler are also acknowledged.

These manuscripts benefited from extensive reviews by David W. Houseknecht, whose comprehensive knowledge of the stratigraphy and history of Northern Alaska substantially improved each chapter of this dissertation and are greatly appreciated.

I thank my advisor, Bernard J. Coakley, for providing a great opportunity to work on my Ph.D. thesis project. I greatly appreciate the process.

I would like to take this opportunity to express my gratitude towards those who gave me their helping hands in numerous ways throughout the Ph.D. process. Amupma Prakash, Barbara Day, Batuhan and Julia Osmanoglu, Carla Susi Tomsich, Carol Holz, Deniz and Senay Cukur, Dmitry Nikolsky, Ellen Craig, Emily M. Harbaugh, Elizabeth L. Miller, Franta Majs, Heming Liao, Heiko Mueller, Hyewon Tzvetcoff, Jessica Landry, Jessy Gray, JoAnn M. Cooper, Joanne Heslop, Kamalei and Adalia Otero, Kelly Offield, Kenny Tran, Krishna Ganapuram, Kyle and Paige E. D. Palanuk, Lawrence K. Duffy, Leah Berman, Lise-Marie D. Monroe, Luis Alza, Mario Rivillas, Max and Kathleen K. Maliska, Megan Blanchard, Michael Castellini, Miryung Kim, Ngan Naguyen, Nicholas W. Hayman, Nilesh Dixit, Oyunsuvd Chinbat, Paul Henkart, Paul J. McCarthy, Raelene Wentz, Recep Cakir, Reija Shnoro, Sean P. S. Gulick, Stephen T. Obed, Thomas and Debora D'aquin, Tiffany M. Green, Unuit Nunaat, Vipul Silval, and the late Kirk Mcinctosh.

The last, and surely the most, when I think of family, I think of commitment and love. ''I love you all.''

To my family …

1 Introduction and statement of problem

1.1 Introduction and motivation

The geological history of the Amerasia Basin is not well understood. This is due to remoteness and ice conditions of the Arctic Ocean, which restrict collection of geological and geophysical data to constrain the crust beneath the basin and to develop time constraints for the tectonic deformation. The Chukchi Borderland, a block of extended continental crust (Grantz et al., 1998; Brumley et al., 2015; O'Brien et al., 2016) embedded in the Canada Basin, figures prominently in all tectonic models proposed for the opening of the Amerasia Basin. The Borderland cannot be simply reconstructed back to any of the nearby continental shelves. It complicates any model for the Mesozoic opening of the Amerasia Basin. According to the commonly accepted model, the Canada Basin opened like a pair of scissors (Carey, 1958). This was accomplished by a counter-clockwise rotation of the "Arctic Alaska-Chukotka microplate" (Miller et al., 2010) by 66 degrees. The microplate collided with the Siberian margin, which formed the Early Cretaceous Chukotka and Brooks Range orogens (Moore et al., 1994; Sokolov et al., 2002). Most of the existing models for the development of the Amerasia Basin accept the basic pattern of scissors-like or, classically, the "windshield wiper" opening for the basin. This hypothesis is supported by the identification of a possible relict mid-ocean ridge axis in the central Canada Basin (Brozena, et. al., 2002). Since the continental Borderland creates a space problem for any simple opening model, the greatest differences between models center on how to accommodate that block. Fundamental differences among the proposed models include the paleo-location of the Borderland as well as whether the Borderland is a single entity or instead comprises small terranes which behaved as independent microplates. A consequence of these models is the interpretation that the Borderland is distinct from the continental blocks beneath the Chukchi Shelf basins (Thurston and Theiss, 1987; Sherwood, 1994; Sherwood et al., 2002). Multi-channel seismic (MCS) reflection data collected across the transition between the Chukchi Shelf and Borderland are integrated with other geological and geophysical data to establish new constraints on the timing and phases of deformation across the Borderland and to provide new constraints for the development of the Amerasia Basin.

1.2 Dissertation format

This dissertation comprises three distinct chapters which present manuscripts submitted, accepted for publication and prepared for submission to peer-reviewed journals. All three chapters are related to the structure and stratigraphy of the Chukchi Borderland and adjacent basins, Arctic Ocean.

Chapter 2 objectives are to present observations from new MCS profiles to describe structures and stratigraphy of the Northwind Basin, Chukchi Borderland. This investigation is used to interpret the tectonic and depositional history and to constrain the timing of deformation. This manuscript was submitted on September 13, 2016 and resubmitted on April 21, 2017 after the first revision to the AAPG Bulletin. Having weathered two cycles of review, the manuscript has been invited for resubmission, pending revision, since August 9, 2017.

Chapter 3 documents the structure and stratigraphy of the southwestern margin of the Chukchi Borderland and presents an interpretation of its tectonic evolution. This manuscript was submitted on July 18, 2017 to Marine and Petroleum Geology. This manuscript was revised on April 10, 2018 and accepted for publication on April 17, 2018. It was published on April 18, 2018.

Chapter 4 objectives are to investigate the history of deformation along the southeastern margin of the Chukchi Borderland to to provide new insights for the tectonic development of the Amerasia Basin. This manuscript is planned for submission to the journal "Tectonophysics."

1.3 Conclusions

In the Arctic Ocean, Chukchi Borderland separates the North Chukchi shelf and Toll deep basins to the west and Canada deep basin to the east. Existing plate reconstructions have attempted to restore this north-striking, fragment of the continental crust to all margins of the Amerasia Basin based on sparse geologic and geophysical measurements. Regional multi-channel seismic reflection and potential field geophysics, and geologic data indicate it is a high standing continental block, requiring special accommodation to create a restorable model of the formation of the Amerasia Basin.

The Chukchi Borderland is composed of the Chukchi Plateau, Northwind Basin, and Northwind Ridge divided by mostly north striking normal faults. These offset the basement and bound a sequence of syn-tectonic sediments beneath an angular unconformity (Au). Equivalent strata are, locally, uplifted, deformed and eroded. Seaward dipping reflections (SDRs) are observed in the juncture between the North Chukchi, Toll basins, and southern Chukchi Plateau underlying the Au. Similarly, SDRs and diapiric reflections have been observed within the crust along the southwestern margin of the Canada Basin. These reveal that western and eastern margins of the Chukchi Borderland were rifted due to the associated volcanism.

An inferred condensed section, which is believed to be synchronous with the composite pebble shale and gamma-ray zone (Hauterivian-Aptian), and perhaps the upper Kingak shale unit (Upper Jurasic-Lower Cretaceous) of the Alaska North Slope, forms the basal sediments in the North Chukchi Basin. Along the southwestern margin of the Canada Basin, an inferred Upper Jurasic-Lower Cretaceous clinoform sequence forms the basal sediments. Approximately 16 to 4 km post-rift strata onlap the condensed section, SDRs and, in part, the wedge sequence on the Chukchi Plateau, and the clinoform sequence along the western margin of the Canada Basin from west to east, thinning to the north. All of these stratigraphic units imply that the rifted margin of the North Chukchi Basin subsided no later than the earliest

Cretaceous, and of the Canada Basin no later that the Middle Jurassic, providing a plausible time constraint for Middle to Late Jurassic rifting in this region.

The recognition of SDRs and Hauterivian–Aptian condensed section, inferred Upper Jurassic-Lower Cretaceous clinoform sequence and continuity of the Cretaceous post-rift strata along the margins of the Chukchi Borderland, strike variations of the normal faults, absence of observable east-directed thrust faults along the Northwind Ridge-Canada Basin substantially constrain tectonic models proposed for tectonic development of the Amerasia Basin. Models that require significant relative motion between the Chukchi Shelf and Borderland, and or the Canada Basin since the Middle Jurassic are precluded by these observations.

1.4 References

Brozena, J.M., Lawver, L.A., Kovacs, L.C., Childers V.A., 2002. Aerogeophysical evidence for the rotational opening of the Canada Basin. American Association for Petroleum Geologists Bulletins 86, 1138.

Brumley, K., Miller, E.L., Konstantinou, A., Grove, M., Meisling, K.E., Mayer, L.A., 2015. First bedrock samples dredged from submarine outcrops in the Chukchi Borderland, Arctic Ocean. Geosphere 11, 76-92, doi:10.1130/GES01044.1.

Carey, S., 1958. A tectonic approach to continental drift, in continental drift: a symposium. Australia: University of Tasmania, Hobart, 177-355.

Grantz, A., Clark, D.L., Phillips, R.L., Srivastava, S.P., Blome, C.D., Gray, L.B., Haga, H., Mamet, B.L., McIntyre, D.J., McNeil, D.H., Mickey, M.B., Mullen, M.W., Murchey, B.I., Ross, C.A., Stevens, C.H., Silberling, N.J., Wall, J.H., Willard, D.A., 1998. Phanerozoic stratigraphy of Northwind Ridge, magnetic anomalies in the Canada basin, and the geometry and timing of rifting in the Amerasia basin, Arctic Ocean. Geological Society of America Bulletin 110, 801-820, doi: 10.1130/0016-7606(1998)110<0801:PSONRM>2.3.CO;2.

Miller, E.L., Gehrels, G.E., Pease, V., Sokolov, S., 2010. Stratigraphy and U-Pb detrital zircon geochronology of Wrangel Island, Russia: Implications for Arctic paleogeography. AAPG Bulletin 94, 665-692, doi:10.1306/10200909036.

Moore, T.E., Wallace, W.K., Bird, K.J., Karl, S.M., Mull, C.G., Dillon, J.T., 1994. Geology of northern Alaska, in Plafker, G., Berg, H.C., (Eds.), The Geology of Alaska: Boulder, CO, Geological Society of America, Geology of North America G-1, 49-140, doi:10.1130/DNAG-GNA-G1.49.

O'Brien, T.M., Miller, E.L., Benowitz, J.P., Meisling, K.E., Dumitru, T.A., 2016. Dredge samples from the Chukchi Borderland: Implications for paleogeographic reconstruction and tectonic evolution of the Amerasia Basin of the Arctic. American Journal of Science 316, 873-924, doi: 10.2475/09.2016.03.

Sherwood, K.W., Johnson, P.P., Craig, J.D., Zerwick, S.A., Lothamer, R.T., Thurston, D.K., Hurlbert, S.B., 2002. Structure and stratigraphy of the Hanna Trough, U.S. Chukchi Shelf, Alaska, in Miller, E.L., Grantz, A., Klemperer, S.L. (Eds.), Tectonic Evolution of the Bering Shelf–Chukchi Sea–Arctic Margin and Adjacent Landmasses, Geological Society of America, Boulder, CO, Special Papers 360, 39-66.

Sherwood, K., 1994. Stratigraphy, structure, and origin of the Franklinian, northeast Chukchi basin, Arctic Alaska plate, 1992 Proceedings International Conference on Arctic Margins: US Minerals Management Service OCS Studies, pp. 94-0040.

Sokolov, S.D., Bondarenko, G.Y., Morozov, O.L., Shekhovtsov, V.A., Glotov, S.P., Ganelin, A.V., Kravchenko-Berezhnoy, I.R., 2002. South Anyui suture, northeast Arctic Russia: facts and problems, in Miller, E.L., Grantz, A., Klemperer, S.L. (Eds.), Tectonic Evolution of the Bering Shelf–Chukchi Sea–Arctic Margin and Adjacent Landmasses, Geological Society of America, Boulder, CO, Special Papers 360, 209-224.

Thurston, D.K., Theiss, L.A., 1987. Geologic Report for the Chukchi Sea Planning Area: Anchorage, Alaska, U.S. Department of the Interior, Minerals Management Service Outer Continental Shelf Report 87-0046, 193 p.

2 Structure and stratigraphy of the Northwind Basin, Chukchi Borderland: Constraints on the tectonic development of the Amerasia Basin, Arctic Ocean[1]

2.1 Abstract

The history of Northwind Basin has been described from 2D multi-channel seismic (MCS) reflection data acquired across the transition from the Chukchi Shelf to Borderland. Mapped normal faults of the Borderland strike primarily to the north. The interpreted stratigraphic section can be separated into two major seismic units along a prominent unconformity (Au), which is inferred to be correlative with the Hauterivian (LCu) unconformity of the North Slope Alaska. Sub-Au unit is consistent with an early phase of contraction and extension. Super-Au unit is composed of syn and post-extensional, and glacio-marine strata.

Mapped normal faults of the Chukchi Borderland are consistent with extension. The super-Au syn-extensional strata are distinguished by reflection packages that diverge towards normal faults. Post-extensional strata are characterized by bi-directional onlap onto the underlying unit, consistent with sediment transport along the axis of the basin. These post-extensional strata are dated as lower Eocene by direct correlation of the MCS data to the Crackerjack and Popcorn exploration wells.

The Cretaceous strata (lower Brookian), interpreted to form great thicknesses in the North Chukchi basin, appear to be largely absent from the Northwind basin. The inferred absence of the Cretaceous strata in the Northwind basin and unobservable discontinuity are consistent with the continuity of the Chukchi Shelf and Borderland since the earliest Cretaceous. This combined with absence of east directed thrusts rooted beneath the Northwind Ridge contradict

[1] Ilhan, I., Coakley, B.J., in review. Structure and stratigraphy of the Northwind Basin, Chukchi Borderland: Constraints on the tectonic development of the Amerasia Basin, Arctic Ocean. AAPG Bulletin.

tectonic models that require significant relative motion between the Chukchi Shelf, Canada Basin and Borderland since that time.

2.2 Introduction

The Chukchi Borderland is a high-standing continental fragment (Grantz et al., 1998; Brumley et al., 2015; O'Brien et al., 2016) that projects northward into the Amerasia Basin, Arctic Ocean (Fig. 2.1a). The Borderland is segmented into the Chukchi Plateau, Northwind Basin and Northwind Ridge (Grantz et al., 1979, 1990, 1998). The Northwind basin, which is the main focus of this paper, covers an area of ~50000 km^2 and extends approximately 125 km east-west and over 400 km in north-south directions (Fig. 2.1b).

Not much is known about this region. It is located ~300 km north of the northernmost Popcorn well drilled for hydrocarbon exploration in the Chukchi Sea (Fig. 2.1b). Collecting geological and geophysical data in this part of the Arctic Ocean has been difficult due to sea ice and remoteness. According to previous investigations, the Northwind basin was formed by basin and range style extensional deformation (Hall, 1990; Grantz et al., 1993, 1998, 2011). This interpretation was based on northerly-trending high bathymetric relief, modeling of gravity anomalies, and a few short 2D seismic reflection profiles that did not image the basin itself (Grantz et al., 1998). The timing of the inferred east-west extension required to form the basin has been speculated to be late Paleocene (Grantz et al., 1993, 1998) on the basis of observed stratigraphy from the Chukchi Sea exploration wells (Fig. 2.1b; Sherwood et al., 2002). The distance of these wells from the basin complicates this interpretation.

In multi-channel seismic (MCS) reflection profiles, acquired from the USCGC Icebreaker Healy in 2005 (Fig. 2.1b), Arrigoni (2008) recognized normal faults and reflections that thicken towards these faults. These growth strata support the extension and existence of syn-tectonic sediments in the grabens in the northern Northwind basin.

In this paper, observations from new MCS profiles (Fig. 2.1b) are used to describe structures and stratigraphy of the Northwind basin. The objectives are to interpret tectonic and depositional history, and to constrain the timing of deformation. This investigation extends understanding of the frontier area, north of the exploration wells in the Chukchi Sea, and adjacent basins buried by sediments (Fig. 2.1b). The objectives are accomplished by mapping the continuation of sediment delivery systems across the southern Chukchi Borderland into the Northwind basin.

2.3 Background

The Chukchi Borderland is bounded to the west by the Toll Basin and Alpha–Mendeleev Ridge, to the south by the North Chukchi Basin and to the east by the Canada Basin (Fig. 2.1a). The timing of deformation, amount of crustal extension, stratigraphy and history of sediment delivery to the internal basins of the Borderland have not been previously observed beyond the extent of industry MCS profiles collected for hydrocarbon exploration on the Chukchi Shelf (e.g. Kumar et al., 2011).

There are a number of models for the tectonic development of the Amerasia Basin (Lawver and Scotese, 1990; Lane, 1997; Embry, 2000; Miller et al., 2006; Grantz et al., 2011; Doré et al., 2016; O'Brien et al., 2016; Hutchinson et al., 2017). This divergence of views is partly due to the lack of data and resulting uncertainty about how and where to restore the continental blocks of the Borderland in plate-reconstruction models. The model of Carey (1958), which pre-dates mapping of the Borderland, proposes counter-clockwise rotation of the Arctic Alaska–Chukotka microplate away from the Canadian Arctic Islands around a pole in the Mackenzie Delta (Fig. 2.1a). Implications of this simple rotational opening of the Amerasia Basin include: extension along the continental margins of Arctic Canada and northern Alaska; the presence of a transform fault along an Amerasia Basin margin located at Lomonosov Ridge (Cochran et al., 2006; Evangelatos and Mosher, 2016); and contraction across the southern margin of the microplate, which was accommodated by the formation of the Chukotka and Brooks Range orogens (Moore et al., 1994; Sokolov et al., 2002). This model is controversial (Lane, 1997; Embry, 2000; Doré et al., 2016), but forms the basis for most contemporary understanding of the tectonic history of the Amerasia Basin.

To accommodate the continental Borderland in an oceanic basin (Chian et al., 2016) requires plate boundaries along its edges (Coakley and Ilhan, 2012). Many models for the formation of the Amerasia Basin take the rotational model (Carey, 1958) as a starting point. This rotation of the microplate is supported by paleomagnetic results of oriented piston cores from the Kuparuk formation (Valanginian–Hauterivian; Fig. 2.1a), which supports 65–70 degrees rotation since deposition (Halgedahl and Jarrad, 1987). Rotational models for the formation of the Canada Basin solve the problem of the Borderland by rotating, displacing, and/or distorting this continental block to make a restorable plate model of basin formation.

One popular model (Grantz et al., 2011) attempts to explain the basin history with multiple phases of rotation (Fig. 2.1a). This begins with Jurassic (195-160 Ma) counter-clockwise rotation of the microplate away from the Canadian Arctic Islands around a pole in the Mackenzie Delta, initiating the phase-1 extension of the crust in the proto-Canada basin. This was followed by pre-Valanginian (145.5-140 Ma) clockwise rotation of the Borderland away from the East Siberian Shelf around a pole along the southern Northwind Ridge (Fig. 2.1a). To support this hypothesis, Grantz et al. (1998) interpreted east-directed thrust faults from a seismic profile between the Northwind Ridge and western margin of the Canada Basin. Later, in the Barremian (131-127.5 Ma), the phase-2 extension proceeded by seafloor spreading that formed the central Canada basin. The phase-2 oceanic crust and the timing have been supported by the paired magnetic anomalies (Fig. 2.1a) and the absence of the Early Cretaceous long-normal magnetic anomaly in the central Canada basin (Grantz et al., 2011). During the Barremian–Campanian (127 to 89-75 Ma) northward propagation of seafloor spreading forms the Alpha–Mendeleev large igneous province (Drachev and Saunders, 2006; Fig. 2.1a).

To accommodate the clockwise rotation of the Chukchi Borderland, Grantz et al. (2011) inferred an arcuate left-lateral transform fault and structural discontinuity along the western and northern margins of the Borderland. This rotation requires shortening along the Northwind Ridge, onto crust of the proto-Canada basin (Fig 2.1a).

According to Grantz et al. (2011) the Northwind basin, which dissects the Borderland, formed as a result of extension during the late Paleocene. This age is based on tracking the continuous reflectors from the Chukchi Sea exploration wells (Sherwood et al., 2002) to the basins more than 300 km to the North.

2.4 Regional stratigraphy

This research relies on the stratigraphy documented by five exploration wells on the U.S. Chukchi Shelf. Reflectors observed in the MCS data were dated by synthetic seismogram ties to the Popcorn and Crackerjack wells. These 1989–1991 vintage wells penetrated Cenozoic–Paleozoic strata that correlate to the stratigraphic section of the Alaska North Slope (Sherwood et al., 2002). This work is mainly focused on the Cretaceous–Cenozoic Brookian megasequence.

Orientation of clinoform successions within the Brookian megasequence demonstrate that sediments were derived from the Chukotka and Brooks Range orogens and routed northward into the accommodation of the North Chukchi and Toll basins (Fig. 2.1b; Houseknecht and Bird, 2011; Ilhan and Coakley, 2018).

The Brookian megasequence is divided into lower and upper sequences by the mid-Brookian unconformity, which forms one of the consistent regional correlation and mapping surfaces (MBu; Thurston and Theiss, 1987; Sherwood et al., 2002; Drachev et al., 1999, 2010; Kumar et al., 2011; Granath et al., 2015; and Nikishin et al., 2014, 2017). The lower Brookian sequence is comprised of sediments derived mainly from the Chukotka orogen. These sediments were routed to the north and east across the Chukchi Shelf (western Colville foreland basin) and Arctic Platform (Fig. 2.1b). These sediments filled the North Chukchi and western Colville basins to be deposited in the Canada basin along the rifted margins of Alaska and Canada (Sherwood et al., 2002; Houseknecht et al. 2009; Drachev et al., 2010; Drachev, 2011; Houseknecht and Bird, 2011; Kumar et al., 2011). Lower Brookian strata form large-scale clinothems in the North Chukchi Basin and are presumed to be deposited in the Canada Basin (e.g. Fig. 1 in Houseknecht et al., 2009). The lower Brookian sequence is subdivided into Aptian–Albian and Upper Cretaceous subsequences by the Cenomanian (Cu) unconformity (Craddock and Houseknecht, 2016; Houseknecht et al., 2016). Aptian–Albian strata reflect voluminous sediment influx from tectonic highlands whereas Upper Cretaceous strata reflect less voluminous sediment influx and include widespread volcanic ash falls (Houseknecht and Bird, 2011).

The Cenozoic upper Brookian sequence is comprised of sediments derived from the rejuvenated Chukotka and Brooks Range orogens. It was routed mainly northward to the high-accommodation North Chukchi and Canada basins (Houseknecht and Bird, 2011). Upper Brookian strata form giant clinothems in the North Chukchi and Canada basins, ranging in age from Paleocene through Miocene (Sherwood et al., 2002; Drachev et al., 2010; Houseknecht and Bird, 2011; Kumar et al., 2011; Hegewald and Jokat, 2013a, b; Granath et al., 2015; Nikishin et al., 2014, 2017).

2.5 Data and methods

MCS reflection data were acquired to: image the subsurface geology of the southern Chukchi Borderland; tie the seismic data to the Crackerjack and Popcorn exploration wells on the Chukchi Shelf; and constrain ages of tectonic and sedimentary processes of this region. The ultimate goal was to indirectly test hypotheses for the formation of the Amerasia Basin. To accomplish these scientific objectives, approximately 5,300 km of MCS profiles were acquired in

2011 by the *R/V Marcus G. Langseth* across the transition from the Chukchi Sea to Borderland (Fig. 2.1a).

For the MCS data acquisition, a tuned array of ten airguns was used as a source for generating the acoustic/seismic energy. The total volume of the source was 1,830 cubic inches. Collectively these guns produced a simple, nearly dipole, total source signature. The spectrum of the returned signals, reflected from the subsurface interfaces, ranges between 5 and 125 Hz and falls off rapidly at both ends. A streamer including 468 hydrophones (spaced 12.5 m apart) was used to detect the reflected energy. The recording time was 10s and the sampling rate was 2 ms. The distance between the source and first receiver group was 37.5 m. The source and streamer were towed at 6 and 9 m depths, respectively. The shots were triggered every 37.5 m along the track. The resulting nominal maximum fold, which is the number of recorded signals that sampled the same geometric location at depth, was 78.

After initial data processing at the University of Alaska, a preliminary interpretation was completed. Subsequently, the data set was reprocessed by ION Geophysical. Those reprocessed MCS profiles were used for this work.

While the tuned array guaranteed good quality imaging of individual reflectors, additional processing of the data was necessary to correct for various transient issues encountered during acquisition and to improve the signal to noise ratio. Objectives of the MCS data processing were to attenuate various kinds of random, linear, and coherent noise, in particular multiples, to enhance the deeper returns, and to optimize the source signature. These objectives were accomplished by methods that include: reformatting and resampling of the original SEG-D shot records (2 ms) to ProMAX format at 4 ms. Further processing included: geometry merge, source and streamer static corrections, source system delay correction; source residual bubble energy removal and zero phase application, velocity analysis (4^{th} order), source spherical spreading and absorption corrections, noise attenuation (swell noise, high amplitude noise bursts, etc.), external seismic source interference attenuation, side-scattered energy and refracted linear noise attenuation and receiver amplitude correction. The most important step for the seismic imaging and interpretation was multiple attenuation, which was accomplished by: SPMA (short period multiple attenuation) and SRME (surface related multiple elimination), high-resolution radon demultiple, apex-shifted demultiple (ASMA), F-X deconvolution (common offset), "Larner" noise removal (common offset), and pre-stack time migration. These methods enhanced primary signals and attenuated random, coherent, and linear noise. All of the MCS images shown in this paper are from pre-stack time-migrated profiles reprocessed by ION.

The seismic data interpretation was based on sequence stratigraphic principles of Vail et al. (1977). The MCS data set was used in conjunction with bathymetry (Jakobsson et al., 2012), free-air gravity (Bonvalot et al., 2012) and magnetic (Maus et al., 2009) anomaly maps to supplement and extend our structural interpretation between the 2D profiles.

There is no well control within the survey area. The MCS data were correlated to the nearest available well control, approximately 300 km to the south on the Chukchi Platform (Fig. 2.1b). Ages of formations in the Crackerjack and Popcorn exploration wells were obtained from biostratigraphy (Sherwood et al., 2002; Mickey et al., 2006; J. Bujak, 2018 personal comm.). These age assignments made it possible to date the surfaces that defined the seismic units (Fig. 2.2). A time-depth function developed by Hegewald (2012) and publicly available check-shot survey were used to convert two-way-time in MCS profiles to approximate depth.

2.6 Structure

The basement structure of the southern Chukchi Borderland is revealed on the MCS profiles (Figs. 2.2–7). Based on observed structural and bathymetric relief, we have mapped normal faults of the area. These faults extend to the north along gravimetric and magnetic anomaly gradients (Figs. 2.8a–c), beyond the limit of MCS grid. These faults dissect the Borderland into Chukchi plateau, Northwind basin, Northwind ridge and define the western edge of the Canada basin. These faults define the limits of sedimentary depocenters.

Three sets of basin bounding faults (BF) have been distinguished: north striking, BF1 and BF2; northwest striking (oblique), BF3; and northeast striking (curvilinear), BF4. The north and northwest striking faults (BF2 and BF3) bound the Northwind basin. These faults are consistent with the northwest and north oriented bathymetric features, and gravity and magnetic anomalies (Figs. 2.8a–c). We believe that these two sets of faults support E-W and SW-NE phases of extension.

The total throw and heave observed on these faults are the result of extension. Using the fault offsets, a minimum estimate of the total amount of extension can be made by pinning and restoring the pre-deformation surfaces within the interior Chukchi Borderland. The fault heaves range from 100 m to 10-15 km (Figs. 2.2–7). The maximum total heave occurs along the BF2b (Fig. 2.3) and BF3a (Fig. 2.6b) with 12 km and 12.6 km respectively, and a central fault between these two with 14.3 km (Fig. 2.5b).

Normal fault offsets can be used to restore the pre-deformation structure and constrain thinning of the lithosphere. The stretching or beta factor (McKenzie, 1978) can be estimated from the fault heaves observed on the MCS profiles (Figs. 2.2–7). To quantify the pre-extensional length of the crust, the total sum of the heaves is subtracted from the present-day length within the interior Chukchi Borderland. This is accomplished by restoring the mapped normal faults (Figs. 2.8a–c). Dividing the present-day length by the estimated initial length constrains the stretching factor for the area. This ranges from 1.1 to 1.2.

While this stretching factor (1.1 to 1.2) on its own suggests that only minor extension and weak thermal subsidence occurred in the Northwind basin, it should be recognized that this estimate presumes that the area was initially horizontal and near sea level. Any inherited structures would diminish this estimate. The stretching estimated from the fault heaves is a minimum estimate. The apparent compressional deformation of the sub-Au rocks (Figs. 2.3, 2.5 and 2.7; Ilhan and Coakley, 2018) complicates the history of the Chukchi Borderland.

2.7 Seismic stratigraphy

Critical to understanding this region is correlation of the seismic data to the Crackerjack and Popcorn exploration wells and the ages of the strata observed in the Northwind basin (Fig. 2.2). The distance from these exploration wells to the Northwind basin (~300km) raises questions about diachroneity of individual reflectors. Our model is the best age control available for the region and, within the limits of this uncertainty, offers, at worst, preliminary age constraints of the previously undated basin sediments (Figs. 2.9 and 2.10). The following sections address seismic-well correlation and constraints for these rocks, followed by descriptions and interpretations of the main seismic stratigraphic units.

2.7.1 Age constraints

Mid-Brookian (MBu) unconformity is an erosional surface that separates the Brookian megasequence into a lower sequence of Cretaceous age (Aptian–Albian and Upper Cretaceous; Craddock and Houseknecht, 2016) and an upper sequence of Cenozoic age (Figs. 2.9 and 2.10a). The upper Brookian sequence, contains a stratigraphic section more than 4 seconds of two-way-travel (TWT) or 7-8 km thick in between high-standing blocks of the Crackerjack and Popcorn exploration wells, the North Chukchi basin, and the Northwind basin (Fig. 2.2). This sequence tapers off to zero thickness northward in the Northwind basin, against a reverse slope of the seabed (Figs. 2.1b and 2.8a), indicating its northern limit along the axis of the basin. This succession and the underlying seismic sequences observed in the array of half-grabens in the Northwind basin are the main focus of this paper (Figs. 2.3, 2.4 and 2.6).

The age of the MBu at the exploration wells is constrained by biostratigraphic interpretations (Mickey et al., 2006; J. Bujak, 2018 personal comm.). At Crackerjack, the age of the youngest sub-MBu strata is Turonian and of the oldest super-MBu strata is mid-Paleocene (Figs. 2.9 and 2.10a), indicating a time gap of at least 27 m.y. At Popcorn, where greater exhumation of the lower Brookian sequence occurred (Craddock and Houseknecht, 2016), the age of the youngest sub-MBu strata is Aptian and of the oldest super-MBu strata is early Paleocene (Figs. 2.9 and 2.10a), indicating a time gap of at least 50 m.y. Considering that these two wells are just 50 km apart, ages at Crackerjack are considered to be the most plausible. The estimated age of the MBu at that location falls between Turonian and Paleocene. In the north of these wells, the MBu may overlie Maastrichtian strata in the central North Chukchi basin.

Beyond the eastern flank of the North Chukchi basin, there appears to be uncertainty about stratigraphic position of the MBu due to a structural high shown in Fig. 2.2b. Northward continuation of the MBu shows angular discordance with the rocks beneath, defining an angular unconformity (Au; Figs. 2.2, 2.4 and 2.7). The Au separates the stratigraphic section into sub-Au rocks and super-Au strata in the Northwind basin.

According to the stratigraphic framework of Ilhan and Coakley (2018), the Aptian–Albian strata (PRS1b) pinch out by onlap on the eastern flank of the North Chukchi basin and the underlying inferred pre-Aptian section (PRS1a) appears to be restricted to this basin, resting on the Au (e.g. Fig. 2.4 in Ilhan and Coakley, 2018). The inferred absence of the Aptian–Albian strata in the Northwind basin is likely due to high-standing blocks of the Chukchi Plateau, which appears to have precluded deposition of the most lower Brookian sequence in this basin. The pre-Aptian section is presumed to be either a thin starved section resting on the Au in the Northwind basin or absent. As a result, the Au in the Northwind basin can be correlated to the Hauterivian (LCu) or the Jurassic (Ju) unconformity, which is considered to be Mid-Jurassic on the Chukchi Shelf and Alaska North Slope (Sherwood et al., 2002). All of reasoning suggests that the sub-Au rocks are pre-Hauterivian in age. The super-Au strata are Cretaceous through Cenozoic in age.

Three distinctive seismic units are recognized beneath the Au. The oldest unit A (Fig. 2.4) is acoustically transparent except for rare, discontinuous reflections that display apparently unoriented dips (Figs. 2.2 and 2.3). Beneath the Chukchi plateau, the top of unit A is as shallow as 1s (750 m, Fig. 2.4). It extends to the bottom of the seismic record at 10s (20 km) in the North Chukchi basin (e.g. Fig. 4 in Ilhan and Coakley, 2018). The transparent rocks commonly are overlain by either alternating high-and-low amplitude stratified rocks (unit B; Figs. 2.2-7) or poorly defined, mostly low-amplitude stratified rocks (unit SRS1) that thicken laterally from a zero edge where they terminate beneath the Au to as much as 1 sec. (~1 km, Figs. 2.4 and 2.5) where they terminate abruptly against steeply dipping offsets. Strata within unit B display folding (Figs. 2.2, 2.3, 2.5 and 2.7), whereas strata within unit SRS1 display subtle lateral thickening towards the steep offsets (Figs. 2.4 and 2.5). These display laterally variable, low to moderate dips and locally display normal or reverse offsets (Ilhan and Coakley, 2018). Units A, B, and SRS1 are briefly described and interpreted here, but they are not the primary focus of this paper.

Beneath the Au, unit A is interpreted as crystalline basement based on stratigraphic position, regional geology, and transparent acoustic character. This basement rock may be equivalent in part to the Franklinian megasequence of the Alaska North Slope and Chukchi Shelf (Sherwood et al., 2002; Kumar et al., 2011) or may be part of the Pearya terrane that was documented recently in the northern

Chukchi plateau (O'Brien et al., 2016). The overlying rocks of unit B are interpreted as pre-extensional strata deformed by contractional folding (Figs. 2.5 and 2.7) and of unit SRS1 are interpreted as growth strata deposited during normal faulting (steep offsets). All of the sub-Au rocks deformed by contractional folding and both normal and thrust faulting (Fig. 5 in Ilhan and Coakley, 2018). The only age constraint is that the Au is overlain by Brookian and perhaps Beaufortian strata, so unit B could be coeval with parts of the Franklinian or Ellesmerian megasequence and unit SRS1 could be coeval with parts of the Ellesmerian or Beaufortian megasequence (Fig. 2.10a).

In the Popcorn well we have identified five surfaces of discordance based on locally observed truncation and onlap terminations (Figs. 2.2 and 2.6). These continue into the Northwind basin, providing the basis for age control. Four of these surfaces are consistent with biostratigraphy (Sherwood et al., 2002; Mickey et al., 2006; J. Bujak, 2018 personal comm.) and tie to mid-Paleocene (MPu), late Paleocene (LPu), mid-Eocene (MEu), and Miocene (Mu) unconformities at the Crackerjack and Popcorn wells (Fig. 2.9). The fifth one is inferred to be a Plio-Pleistocene (PPu) unconformity recognized mostly beyond the shelf and in the deep basins (Figs. 2.2-4). Tracing the LPu, MEu and Mu correlative surfaces from these wells into the Northwind basin establishes continuity and subdivision of the Cenozoic strata (Figs. 2.2, 2.6, 2.9 and 2.10). This constrains age of the identified seismic sequences observed in the array of grabens in Northwind Basin (Fig. 2.10b).

2.7.2 Super-Au strata in Northwind Basin

This section describes and interprets the succession restricted to the half-grabens of the Northwind basin that onlaps the Au (Figs. 2.4, 2.6 and 2.7; SRS2). The succession is composed of high-amplitude discontinuous and chaotic, and low-amplitude continuous reflections that rest on the east and west dipping relief of the Au in the deepest parts of the half-grabens (Figs. 2.3–7).

Strata in SRS2 are as much as 1s (1 km) thick in higher accommodation parts of the basin (e.g. along bounding faults, BF2b and BF3a in Fig. 2.3) and pinch out against the correlative surface of the LPu in lower accommodation areas (Fig. 2.6). In the eastern half-grabens of the Northwind basin, the top of SRS2 (LPu) has been correlated to the Popcorn well and the basal strata overlying this surface are constrained to be lower Eocene in age (PRS2a; Figs. 2.2 and 2.9).

The sediments in SRS2 are interpreted as growth strata (e.g. Nøttvedt et al., 1995) that were deposited during a phase of extensional deformation (Fig. 2.4). The overlying basal strata (within PRS2a) are inferred to be lower Eocene in age, which constrains the age of extension to be pre-Eocene (Figs. 2.2, 2.6, 2.9 and 2.10).

Within the growth strata (SRS2), stratal stacking pattern changes from discontinuous (high-amplitude) to continuous (low amplitude) reflections in down-dip direction on the hanging-wall block (e.g. SRS2a and SR2b units in Fig. 2.6c). The continuous reflections (SRS2b) onlap onto the discontinuous (SRS2a) reflections, which indicate a surface of discordance (SRu, Fig. 2.6c). The discontinuous reflections are oriented perpendicular to the basin-bounding fault (BF3a, Fig. 2.7). Along the footwalls of the basin, locally, high-amplitude and chaotic reflections are observed (near the fault planes, e.g. SRS2a-b at BF2b and BF2a in Fig 2.3).

The discontinuous reflections of SRS2a indicate a progradational trend from the hanging wall towards the footwall, which is interpreted as a clinoform sequence. This implies deposition of locally derived shallow marine sediments sourced from the hanging-wall and deposited into the available accommodation created during the extension (e.g. Prosser, 1993). The chaotic reflections are interpreted as un-stratified, alluvial fans. These deposits were likely shed into the basin from the footwall (e.g. Leeder and Gawthorpe, 1987). The top of the SRS2a (SRu) is interpreted as a marine transgressive surface based on retrogradational onlaps of the overlying reflections within SRS2b on the eastern hanging wall of the Northwind basin (Fig. 2.6c). This transgression may be consistent with the southward onlap of the lower Paleocene strata onto the MBu (e.g. southeast of Popcorn well on Figs. 2.9b and 2.10a; Mickey et al., 2006; J. Bujak, 2018 personal comm.). The continuous reflections within SRS2b are interpreted as stratified sediments. This implies a marine depositional setting as opposed to footwall and hanging-wall dominated, locally derived, sediment source for SRS2b. The inferred change from shallow to deep marine depositional setting is consistent with the interpretation of a marine transgression sometime in the early Paleocene. Following the marine transgression, the overlying upper Brookian strata downlap the MBu in the North Chukchi basin or onlap the Au laterally beyond the northeastern margin of this basin and both sides of the half-grabens in the Northwind basin (Fig. 2.2b).

Strata overlying the LPu (or its correlative surface) display acoustic character ranging from high-amplitude in the lower part to alternating low to high amplitude, laterally continuous reflections (Figs. 2.4-7; PRS2a-c). These reflections appear to stack most in the deepest parts of the half-grabens along the basin axis (Fig. 2.5), stack and terminate by onlap against the underlying units. These strata are as much as 3 seconds (~3 km) thick in the deepest part of the basin, thin to less than 1.5 seconds (~1.5 km) in the distal part of the seismic survey, and taper off to zero thickness northward in the Northwind Basin against a reverse slope of the seabed (Fig. 2.1b). The top of this unit (PRS2a-c) is concordant with overlying strata on the shelf and discordant at the shelf edge and in the Northwind basin. This surface has been inferred to correlate to the Plio-Pleistocene (PPu) unconformity (Fig. 2.2).

Strata in PRS2a-c are interpreted to be coeval with the Paleocene through Miocene upper Brookian succession, which form a clinothem on the Chukchi Shelf and Alaska North Slope (Sherwood et al., 2002; Houseknecht et al., 2009; Houseknecht and Bird, 2011; Hegewald and Jokat, 2013a, b). Seismic data show that the topset and foreset facies of the clinothem on the shelf grade into exclusively bottomset facies in the Northwind basin (Fig. 2.2). Therefore, PRS2a-c is interpreted in the study area to comprise exclusively deep water facies, likely including mudstone and sandstone deposited in basin-floor fan and related environments. The pinchout by onlap of PRS2a-c against both flanks of the host grabens and northward in the Northwind basin indicate axial deposition from the south (Figs. 2.2, 2.3 and 2.5).

Strata in PRS2a display high amplitude in the lower part and mainly alternating medium to low amplitude in the upper part, laterally continuous reflections that are parallel to the base of the unit (Figs. 2.4-7). PRS2a is as much as 2 seconds (~2 km) thick in the deepest part of the basin and thins progressively onto the sides of the half-grabens and northward in the Northwind basin (Figs. 2.2 and 2.5). This unit can be traced directly into the upper Brookian clinothem (Figs. 2.2 and 2.6). The oldest strata within PSR2a that overtop SRS2 are constrained to be lower Eocene in age in the eastern half-grabens (Figs. 2.2 and 2.6). In the deepest part of the Northwind basin, the basal strata may be as old as early Paleocene and coeval with the earliest sediments in the upper Brookian clinothem at Popcorn well (Figs. 2.5, 2.9 and 2.10a). The top of PRS2a is discordant with the underlying strata at the Popcorn well (Fig. 2.9) and the overlying strata in the half-grabens, where the lowermost high-amplitude reflections within PRS2b onlap the PRS2a (Fig. 2.6). Therefore this surface is consistent with the middle Eocene (MEu) unconformity (Figs. 2.2, 2.9 and 2.10). The most important seismic-stratigraphic characteristic of PRS2a is lateral onlap terminations onto the underlying units (Fig. 2.5b). PRS2a is also cut by minor faults (Figs. 2.4 and 2.6-7).

The continuity, basin-axis thickening, and lateral onlap terminations of the reflections within the PRS2a indicate bottomset facies of the upper Brookian clinothem deposited in deep water setting, likely to include sandstone and mudstone, in a basin-floor fan and related environments through axial transport. The normal faults within PRS2a and the offset of the MEu (Figs. 2.4 and 2.6–7) indicate a phase of deformation that post-dates the deposition.

Strata in PRS2b display high amplitude in the lower part and mainly alternating medium to low amplitude in the upper part, laterally continuous reflections that are parallel to the base of the unit (Fig. 2.4-7). Locally, high-amplitude and chaotic reflections are observed in this unit (e.g. west of the central high in Fig. 2.3). PRS2b is as much as 1 second (~1 km) thick in the deepest part of the basin and pinches out on intrabasin uplifts and basin margins (Figs. 2.2 and 2.5). This unit can be traced directly into the upper Brookian clinothem (Fig. 2.2). The upper boundary of PRS2b is concordant on the shelf, but locally discordant with the underlying and overlying strata (e.g. erosion label on Fig. 2.2 and onlap on Fig. 2.6). This surface correlates to the Miocene (Mu) unconformity and is consistent with the stratigraphy (Sherwood et al., 2002; Mickey et al., 2006; J. Bujak, 2018 personal comm.). The most important observation of PRS2b is apparent uplift of the strata at the basin margins (Figs. 2.2–7).

PRS2b is interpreted as a combination of bottomset facies of the uppper Brookian clinothem and drape sediments deposited in a deep water setting, most likely to include sandstone and mudstone, in basin-floor fan and related environments through axial transport and vertical settling (Figs. 2.6 and 2.7). Strata on the footwalls of bounding faults and steep tilt indicate a phase of post-depositional deformation that is likely to be due to reactivation of the bounding faults (Figs. 2.3, 2.4, 2.6 and 2.7).

Strata in PRS2c display mostly low to medium amplitude, laterally continuous reflections that are parallel to the base of the unit (Fig. 2.4-7). PRS2a is as much as 0.3s (300 m) thick in the deepest part of the basin, yet it is 0.7s and 1s (700 m to 1 km) thick beneath the shelf and along the bounding fault on the Chukchi plateau (Figs. 2.3 and 2.4). PRS2c pinches out on intrabasin uplifts and basin margins (Figs. 2.5-7). There is no evidence of deformation on this unit (Fig. 2.6b).

The continuity and low amplitude of the reflections indicate bottomset facies of the uppper Brookian clinothem deposited in deep water setting, likely to include mudstone dominated sediments, in basin-floor fan and related environments through axial transport. The unusual thickening of PRS2c, but absence of divergence along the normal fault on the Chukchi plateau (e.g. BF1 on Fig. 2.4), is consistent with reactivation of the bounding faults sometime after the deposition of PRS2b, inferred to be mid-to-late Miocene (Figs. 2.3, 2.4, 2.6 and 2.7).

Strata within unit (GMS) are composed of both parallel-continuous and chaotic reflections, and recognized mostly in off-shelf depressions (Fig. 2.2). This unit is as much as 0.3 seconds (~300 m) thick in depressions near the shelf edge and along the axis of the Northwind basin (Figs. 2.3–5). These strata onlap a surface of discordance (PPu) and pinch out against the Northwind basin flanks.

Chaotic and continuous reflections within unit GMS are interpreted as un-stratified and stratified sediments, respectively. The thickening of this unit towards the margins of the Northwind basin implies a rapid increase in sediment supply to the basin. This unit is interpreted as glacio-marine sediments, supported by pervasive erosion of the Chukchi Shelf by grounded ice sheets (Dove et al., 2014; Jakobsson et al., 2016). The basal surface of discordance correlates to the PPu unconformity, which forms the upper boundary of the upper Brookian sequence (Fig. 2.2). The eroded seafloor was the source for the overlying glacio-marine sediments. Sediments derived from glacial erosion appear to have filled lows on the shelf and in deeper water off the shelf, grading into turbidites. The GMS is thin to absent on the shelf owing to glacial scouring. Analogous behavior has been inferred in association with the West Antarctic Ice Sheet in the Ross Sea, Antarctica (Bart, 2003).

2.8 Discussion

2.8.1 Pre-Au history

Sub-Au rocks are composed of acoustically transparent (unit A), locally continuous (unit B) and low amplitude (SRS1) reflections. In some locations, the continuous reflections appear to be folded (Figs. 2.2b, 2.3b, 2.5b and 2.7b) and the low amplitude reflections thicken into normal faults (Figs. 2.4 and 2.5). The composition and age of these rocks are unknown, but they appear to have sustained significant compression (Fig. 2.7) and a subsequent episode of extension (Fig. 2.4).

Direct sampling of the sub-Au rocks has taken place in two ways; by drilling during the exploration of the Chukchi Shelf (Sherwood et al., 2002) and by dredging from escarpments in the northern and eastern margins of the Chukchi Borderland (O'Brien et al., 2016; Brumley et al 2015; Grantz et al., 1998). On the shelf, the Crackerjack and Popcorn wells penetrated the Ellesmerian and Beaufortian megasequences (Upper Devonian to earliest Cretaceous) beneath the Early Cretaceous Brookian (Bu) unconformity (Sherwood et al., 2002; Figs. 2.9b and 2.10a). These megasequences appear to diminish towards the north, pinching out on the west flank of the North Chukchi high (Fig. 2.1b) or buried beyond seismic recognition beneath the North Chukchi basin (Figs. 2.6 and 2.7 in Sherwood et al., 2002). In northern Alaska, rocks of the Franklinian megasequence (Proterozoic to Upper Devonian) were sampled at the NPRA-Husky (Peard-1) well and numerous wells near Point Barrow (Dumoulin, 2001). This megasequence forms the "basement" to the Arctic platform (Sherwood, 1994; Fig. 2.1b), deformed during the Early to Middle Devonian (Ellesmerian Orogeny) by mostly east-directed thrust faults (Kumar et. al., 2011). At that location, rocks within the Franklinian megasequence lie directly beneath the Hauterivian (LCu) unconformity, where rocks of the Beaufortian and Ellesmerian megasequences (Upper Devonian to earliest Cretaceous) are absent (Sherwood, 1994; Kumar et al., 2011). Near the northern margin of the Borderland, Brumley et al.

(2015) identified "Cambro-Ordovician magmatic and metamorphic rocks" and "I-type granites" among the recovered seafloor samples. Brumley et al. (2015) and O'Brien et al. (2016) related these rocks to similar outcrops mapped in the Pearya Terrane (Trettin, 1987; Bjørnerud and Bradley, 1994) on northern Ellesmere Island on the opposite side of the Arctic Ocean. These rocks may constrain the nature of the sub-Au rocks of the interior Borderland. But, the connection between these regions and the relationship between the sub-Au rocks and the Franklinian, Ellesmerian and Beaufortian megasequences recognized to the south in the Hanna Trough (Fig. 2.1b) is not clear.

Critical constraints for models of the formation of Canada basin come from the history of relative motion between the Chukchi Shelf and Borderland. Considering the possibility that the extensional structures of the Borderland may join those in the North Chukchi basin (Drachev, 2016; Ilhan and Coakley, 2018) or the Hanna Trough (Sherwood et al., 2002; Kumar et al., 2011), it appears that any relative motion of the North Chukchi basin and the flanking Chukchi plateau must pre-date the sub-Au SDRs (seaward dipping reflections) and the overlying, inferred pre-Aptian strata (PRS1a; Ilhan and Coakley, 2018), as well as the growth strata (SRS1) observed along the western bounding fault of the Northwind basin (BF2a in Figs. 2.4 and 2.8). This implies any relative motion between the two occurred no later than the earliest Cretaceous.

Based on variation in strikes of the bounding faults of the Chukchi Borderland (e.g. north-striking BF1 and BF2a oppose to northwest-striking BF3a, Fig. 2.8), we suggest that there may have been two phases of extension resulting in two growth strata preserved in the Northwind basin (sub-Au, SRS1; super-Au, SRS2a–b; Fig. 2.4b). Absence of east-directed thrust faults, required for compressional deformation, along Northwind Ridge and the western margin of the Canada Basin (Fig. 2.5) is inconsistent with the postulated clockwise rotation of the Borderland away from the East Siberian shelf proposed by Grantz et al. (2011). The north-striking normal faults are consistent with the Mississippian rift-phase faults of the Hanna Trough. If the extension of the Borderland is either synchronous, in part, with the North Chukchi basin or the Hanna Trough, the Northwind Ridge is likely to have developed by these events or during opening of the Amerasia Basin.

In the models for rotational opening of the Amerasia Basin, the Northwind Ridge is commonly placed adjacent to the Arctic Canadian margin (Embry, 1990; Lane, 1997; Grantz et al., 1998, 2011; Miller et al., 2006). If the Chukchi Borderland has not been displaced relative to the Chukchi Shelf since the earliest Cretaceous, this becomes a new constraint for the interpretation of basin history.

2.8.2 Post-Au history

Fault motion on the basin bounding faults of the Northwind basin that is responsible for the growth strata (SRS2) cannot be directly observed in the upper Brookian sediments (Paleocene through Miocene; PRS2a-c), which seem to be filling accommodation without reference to the fault motion (Fig. 2.2). The very restricted growth strata that thicken into the bounding faults suggest that the locally sourced syn-tectonic sediments (SRS2a), in a shallow marine setting, were deposited during a relatively brief interval early in the Northwind basin history. This implies a substantial period of sediment starvation, lasting until the upper Brookian sediments arrived to begin filling the North Chukchi basin (Fig. 2.2; Sherwood et al., 2002; Drachev et al., 2010; Houseknecht and Bird, 2011; Kumar et al., 2011; Hegewald and Jokat, 2013a,b; Granath et al., 2015; Nikishin et al., 2014, 2017; Ilhan and Coakley, 2018). This interpretation is supported by pinch out by onlap of the lower Brookian strata (most of the Cretaceous) along the northeastern margin of the North Chukchi basin and on the flanking Chukchi plateau (Figs. 2.3 and 2.4; PRS1b-c in Figs. 4 and 8 in Ilhan and Coakley, 2018). This implies that the Northwind basin was sediment starved during most of the Cretaceous.

Age constraints of PRS2a of the Northwind basin rely on correlating reflectors from the Popcorn and Crackerjack wells on the Chukchi Shelf. The basal strata that onlap the growth strata (SRS2b) in the eastern half-graben of the Northwind basin are constrained to be lower Eocene in age (Figs. 2.2 and 2.6). Clearly these growth strata (SRS2b) are pre-Eocene in age (pre-date the LPu), but further constraint is necessary to relate the timing of the Northwind basin extension to events elsewhere.

To the north, O'Brien et al. (2016) measured latest Cretaceous to Paleocene (68-61 Ma) apatite fission track ages from dredge rocks collected along faults of the Northwind ridge. To the south, north-trending normal faults of the Chukchi plateau displace the Upper Cretaceous section of the lower Brookian strata about (0.7–1.3 sec or 500 m to 1 km) on the northern flank of the North Chukchi basin (Figs. 2.3 and 2.4; Fig. 8 in Ilhan and Coakley, 2018). Further south in the Hanna trough, Lothamer (1994) shows that north-striking normal faults (likely reactivated Late Paleozoic rift-phase faults) displace the lower Brookian and pre-late Eocene part of the upper Brookian strata (Fig. 3 in Sherwood et al., 2002). These observations may suggest progression of extension from north to south and constrain the Northwind basin extension sometime between the Upper Cretaceous to Paleocene. This constraint with the recognition of the sub-Au SDRs along the southwestern Chukchi Borderland and the growth strata (SRS1) found in the western Northwind basin along the BF2 (Fig. 2.4) constrain two phases of extension: inferred pre-Cretaceous and Upper Cretaceous–Paleocene. The latter event may be synchronous with the "wrench" faulting in the Chukchi platform west of the Wainwright dome of Thurston and Theiss (1987).

Changes in sediment transport directions are distinguished by eastward oriented high-amplitude, discontinuous reflections (SRS2a) and low amplitude, continuous reflections (SRS2b) on the hanging wall (Fig. 2.6c). The former implies locally-sourced sediment deposition, thus a shallow-marine depositional setting. The latter indicates retrogradational onlap, suggesting a marine transgression. This is consistent with southward onlap of the lower Paleocene strata onto the middle Brookian (MBu) unconformity (Turonian to early Paleocene) between the Crackerjack and Popcorn wells (Fig. 2.9b). Following marine transgression at that location, the overlying upper Brookian clinothems (Paleocene through Miocene) downlap the MBu in the North Chukchi basin (Fig. 2.2). Beyond the northeastern margin of the North Chukchi basin and in the Northwind basin, the Paleocene strata are characterized by bi-directional lateral onlap onto the Au (Figs. 2.2 and 2.5). These strata may be coeval with the growth strata (SRS2b) overlying the SRu (Fig. 2.6c), where retrogradational onlaps on the eastern hanging-wall of the Northwind basin are consistent with marine transgression. These sediments were likely to have been delivered to the basin by progradation of the upper Brookian clinothems. This basal deposition youngs to the north. The limit is indicated by a reversal in the slope of the seafloor along axis and an increase in seafloor roughness (Figs. 2.1b and 2.8a).

Integration of published information and new observations of this study permit an interpretation of regional sediment dispersal patterns for the upper Brookian sequence across the study area. On a regional scale, Upper Cretaceous and Cenozoic sediment transport was mainly northward from the resurgent Brooks Range orogen and the moribund Chukotka orogen (Houseknecht and Bird, 2011). On a sub-regional scale, the Chukchi Shelf was influenced during the Upper Cretaceous and Paleogene by north-trending wrench faults that reactivated older, rift-phase normal faults of the Hanna Trough in strike-slip motion (Thurston and Theiss, 1987; Lothamer, 1994). South of the Popcorn well, these wrench faults dissected the MBu surface into pull-apart basins that channeled sediment routing northward. Seismic images included in the reports cited above show north-dipping foresets and bi-directional onlap onto the lateral margins of the grabens, indicating that sediment was routed axially northward during the Paleocene and Eocene.

Within the North Chukchi basin, the Paleogene wrench faults are expressed as growth faults in the thick upper Brookian clinothem. These faults evidently did not restrict sediment routing as individual depositional sequences. Lowstand shelf margins in the clinothem can be correlated as spatially linear to curvilinear features across broad areas (Hegewald and Jokat, 2013a, b). These subsequences demonstrate that the clinoform depositional system prograded generally northward across the North Chukchi basin. Distinctive fluctuations in relative sea level are marked by lowstand shelf margins generally oriented west-east.

Aggradation of the upper Brookian succession eventually filled the North Chukchi basin, and overtopped the southwestern horst of the Chukchi plateau. This deposition prograded onto the fragmented Chukchi Borderland, which was characterized by highly variable accommodation inherited from its extensional history. The greatest contrast in accommodation was between the high-standing blocks of the Chukchi plateau and Northwind ridge, and the deep Northwind basin, which is composed of sub-basins and high-standing blocks. The upper Brookian depositional system initially prograded into the southern end of the Northwind basin and sediment routing was immediately restricted by the irregular accommodation. Thus, the seismic observations of north-dipping foresets and bi-directional onlap onto the lateral margins of the grabens are consistent with axial sediment routing (Fig. 2.2). As the depositional system continued to prograde and aggrade to higher levels as the sediments filling, graben basins at shallower seafloor depths were progressively accessible to the sediment dispersal system. This is supported by thickest sediments found along the basin axial deep, which achieves maximum depth in the middle of the basin (Fig. 2.5). This depositional system is extant, as indicated by the active shelf margin, which obliquely crosses the southern Chukchi Borderland from southeast to northwest.

2.9 Conclusions

The structural and stratigraphic development of the Northwind basin has been investigated with the MCS data constrained by correlation of these data to the Crackerjack and Popcorn exploration wells (Figs. 2.1b, 2.9 and 2.10).

North, northwest and northeaest striking normal faults (BF1 and BF2; oblique, BF3a; BF4; Fig. 2.8) dissect the Chukchi Borderland into Chukchi Plateau, Northwind Basin and Northwind Ridge.

The strike variations of the normal faults (Fig. 2.8) indicate E-W and SW-NE extension, suggesting two phases of deformation. The north-striking faults are parallel to the structural trend of the Mississippian Hanna Trough buried beneath the Chukchi Shelf between the Chukchi and Arctic platforms. The low (1.2) stretching factor of the continental Borderland complicates a simple extensional model for the basin history, indicating earlier contractional deformation of the area.

Stratigraphy of the Northwind basin can be separated into sub-Au rocks and super-Au strata along an angular (Au) unconformity. The Au can be correlated with the Hauterivian (LCu) or perhaps the Jurassic (Ju) unconformity. The sub-Au rocks are inferred to be pre-Hauterivian in age and super-Au strata are inferred to be Cretaceous through Cenozoic in age.

Inferred pre-Hauterivian rocks are grouped into acoustically transparent "basement" (unit A) locally continuous reflections that indicate folding (unit B), and growth strata (SRS1). The folding and growth strata are consistent with a phase of earlier contraction and extension. The contraction of the sub-Au rocks is consistent with the deformed rocks of the Franklinian megasequence (Proterozoic to Upper Devonian) in the Arctic platform. The earlier extension of the sub-Au rocks are either consistent with the rift-phase deposits drilled to the south in the Hanna Trough, the Ellesmerian megasequence (Upper

Devonian to Jurassic); or the rift deposits equivalent to the Beaufortian megasequence (Upper Jurassic to earliest Cretaceous) and may be coeval with the SDRs observed along the eastern margin of the North Chukchi basin.

The hypothesized absence of Aptian-Albian and Upper Cretaceous sections of the lower Brookian strata in the Northwind basin are likely due to basement highs of the southern Chukchi Borderland (e.g. Chukchi plateau and Northwind ridge) and trapping of these sediments (PRS1b-c) in the North Chukchi basin. This implies that the Northwind basin has experienced a substantial period of sediment starvation during most of the Cretaceous.

Super-Au strata in the Northwind basin are grouped into growth (SRS2), post-growth (PRS2a-c), and glacio-marine units. The growth strata are found along the north-striking and oblique faults (BF2a-b and BF3a-b; Fig. 2.8) along the flank and interior of the Northwind basin. These strata record the Northwind basin second phase extension (Figs. 2.3, 2.4, 2.6, and 2.8), constrained to be Upper Cretaceous to Paleocene in age.

SRS2 is separated into SRS2a and SRS2b along an unconformity (SRu), interpreted as a marine transgressive surface based on retrogradation onlaps observed on the eastern half-graben of the Northwind basin (Fig. 2.6c). This appears to be consistent with marine transgression observed at Popcorn well above the middle Brookian (MBu) unconformity (Turonian to early Paleocene).

SRS2a is dominated by shallow marine sediments, mostly derived from the hanging walls and footwalls of the Northwind basin.

SRS2b is dominated by deep water sediments, derived from the south along the basin axis, inferred to be mostly bottomset facies of the earliest sediments (lower Paleocene) of upper Brookian clinothem.

The post-extensional strata (PRS2a-c) are characterized by bi-directional, lateral onlap onto sides of the half-grabens in the

Northwind basin. These strata are constrained to be early Eocene in the eastern half-graben and may be older in the deepest part of the Northwind basin and consistent with bottomset deposits of the upper Brookian clinothem (Paleocene - Miocene). This clinothem is separated from the overlying glacio-marine deposits along the PPu (Fig. 2.2).

The evolution of the Northwind basin is partly revealed by syn-extensional, growth (SRS1 and SRS2) sequences. Subsequent evolution of the basin is primarily a history of axially prograding distal shelf deposits filling massive accommodation created by extension.

Based on absence of an obvious structural discontinuity between the Chukchi Shelf and Borderland and continuous deposition of the inferred Aptian-Albian (lower Brookian) and pre-Aptian sediments in the adjacent North Chukchi basin (Ilhan and Coakley, 2018), we argue against any significant relative motion between the Chukchi Shelf and Borderland since the earliest Cretaceous.

2.10 References

Arrigoni, V., 2008. Origin and Evolution of the Chukchi Borderland, MS Thesis, Texas A&M University, College Station, 74 p.

Bart, P. J., 2003, Were West Antarctic ice sheet grounding events in the Ross Sea a consequence of East Antarctic ice sheet expansion during the middle Miocene?: Earth and Planetary Science Letters, v. 216, p. 93-107, doi:10.1016/S0012-821X(03)00509-0.

Bjørnerud, M., and D. Bradley, 1994, Silurian foredeep and accretionary prism in northern Ellesmere Island: implications for the nature of the Ellesmerian Orogeny, in D.K. Thurston and K. Fujita eds., 1992, Proceedings of the 1992 International Conference on Arctic Margins: Anchorage, Alaska, Minerals Management Service Outer Continental Shelf Report 94-0040, p. 2-4, https://www.boem.gov/ICAM92-129/.

Bonvalot, S., G. Balmino, A. Briais, M. Kuhn, A. Peyrefitte, N. Vales et al., 2012, World Gravity Map, Paris, Bureau Gravimetrique International (BGI), map, CGMW-BGI-CNES-IRD Ed.

Brozena, J. M., L. A. Lawver, L.C. Kovacs, and V. A. Childers, 2002, Aerogeophysical evidence for the rotational opening of the Canada Basin: AAPG Bulletin, v. 86, p.1138.

Brumley, K., E. L. Miller, A. Konstantinou, M. Grove, K. E. Meisling, and L. A. Mayer, 2015, First bedrock samples dredged from submarine outcrops in the Chukchi Borderland, Arctic Ocean: Geosphere, v. 11, p. 76-92, doi:10.1130/GES01044.1.

Carey, S. W., 1958, A tectonic approach to continental drift, in continental drift: a symposium: Australia: University of Tasmania, Hobart, p. 177–355.

Chian, D., H. R. Jackson, D. R. Hutchinson, J. W. Shimeld, G. N. Oakey, N. Lebedeva-Ivanova, Q. Li, R. W. Saltus, and D. C. Mosher, 2016, Distribution of crustal types in Canada Basin, Arctic Ocean: Tectonophysics, v. 691, p. 8-30, http://dx.doi.org/10.1016/j.tecto.2016.01.038.

Coakley, B., and I. Ilhan, 2012, Developing geophysical constraints on the history of the Amerasian Basin of the Arctic Ocean: Proceeding, OTC23795, Arctic Technology Conference, Houston, TX.

Cochran, J. R., M. H. Edwards, and B. J. Coakley, 2006, Morphology and structure of the Lomonosov Ridge, Arctic Ocean: Geochemistry, Geophysics, Geosystems, v. 7, Q05019, doi:10.1029/2005GC001114.

Craddock, W. H., and D. W. Houseknecht, 2016, Cretaceous–Cenozoic burial and exhumation history of the Chukchi shelf, offshore Arctic Alaska: AAPG Bulletin, v. 100, p. 63-100, doi:10.1306/09291515010.

Doré, A. G., E. R. Lundin, A. Gibbons, T. O. Sømme, and B. O. Tørudbakken, 2016, Transform margins of the Arctic: a synthesis and re-evaluation: Geological Society, London, Special Publications, v. 431, p. 63-94, http://doi.org/10.1144/SP431.8.

Dove, D., L. Polyak, and B. Coakley, 2014, Widespread, multi-source glacial erosion on the Chukchi margin, Arctic Ocean: Quaternary Science Reviews, v. 92, p. 112-122, http://dx.doi.org/10.1016/j.quascirev.2013.07.016.

Drachev, S. S., 2016, Fold belts and sedimentary basins of the Eurasian Arctic: Arktos, v. 2(1), p. 1-30, doi:10.1007/s41063-015-0014-8.

Drachev, S. S., 2011, Chapter 25 Tectonic setting, structure and petroleum geology of the Siberian Arctic offshore sedimentary basins: Geological Society, London, Memoirs, v. 35, p. 369-394, doi: 10.1144/M35.25.

Drachev, S. S., N. A. Malyshev, and A. M. Nikishin, 2010, Tectonic history and petroleum geology of the Russian Arctic Shelves: an overview: Geological society, London, petroleum geology conference series, p. 591-619, doi:10.1144/0070591.

Drachev, S., and A. Saunders, 2006, The Early Cretaceous Arctic LIP: Its geodynamic setting and implications for Canada Basin opening: Proceeding, Fourth International Conference on Arctic Margins, Dartmouth, Nova Scotia, p. 216-223.

Drachev, S., G. Johnson, S. Laxon, D. McAdoo, and H. Kassens, 1999, Main structural elements of Eastern Russian Arctic continental margin derived from satellite gravity and multichannel seismic reflection data, Land-Ocean Systems in the Siberian Arctic, Springer, p. 667-682.

Dumoulin, J. A., 2001, Lithologies of the basement complex (Devonian and older) in the National Petroleum Reserve–Alaska, in Houseknecht, D.W., ed., NPRA Core Workshop: Petroleum Plays and Systems in the National Petroleum Reserve–Alaska: SEPM (Society for Sedimentary Geology) Core Workshop 21, p. 201–214.

Embry, A., 2000, Counterclockwise rotation of the Arctic Alaska Plate: Best available model or untenable hypothesis for the opening of the Amerasia Basin: Polarforschung, v. 68, p. 247-255.

Embry, A. F., 1990, Geological and geophysical evidence in support of the hypothesis of anticlockwise rotation of northern Alaska: Marine Geology, v. 93, p. 317-329.

Evangelatos, J., and D. C. Mosher, 2016, Seismic stratigraphy, structure and morphology of Makarov Basin and surrounding regions: tectonic implications: Marine Geology, v. 374, p. 1-13, http://dx.doi.org/10.1016/j.margeo.2016.01.013.

Granath, J. W., K.-J. McDonough, E. J. Sterne, and B. W. Horn, 2015, Contrasting extensional basin styles and sedimentary fill across the eastern Russian Arctic shelf as imaged in crustal-scale PSDM reflection data: American Association of Petroleum Geologists Datapages, Search and Discovery Article, v. 10811.

Grantz, A., P. E. Hart, and V. A. Childers, 2011, Chapter 50 Geology and tectonic development of the Amerasia and Canada Basins, Arctic Ocean: Geological Society, London, Memoirs, v. 35, p. 771-799, doi:10.1144/M35.50.

Grantz, A., D. L. Clark, R. L. Phillips, S. P. Srivastava, C. D. Blome, L. B. Gray, H. Haga, B. L. Mamet, D. J. McIntyre, D. H. McNeil, M. B. Mickey, M. W. Mullen, B. I. Murchey, C. A. Ross, C. H. Stevens, N. J. Silberling, J. H. Wall, and D. A. Willard, 1998, Phanerozoic stratigraphy of Northwind Ridge, magnetic anomalies in the Canada basin, and the geometry and timing of rifting in the Amerasia basin, Arctic Ocean: Geological Society of America Bulletin, v. 110, p. 801-820, doi:10.1130/0016-7606(1998)110<0801:PSONRM>2.3.CO;2.

Grantz, A., S. May, M. Mullen, L. Gray, J. Lull, D. Clark, and C. Stevens, 1993, Northwind Ridge: A continental fragment isolated by Tertiary rifting in the Amerasia basin: Arctic Ocean: Eos (Transactions, American Geophysical Union), v. 74, p. 614.

Grantz, A., S. D. May, P. T. Taylor, and L. A. Lawver, 1990, Canada Basin, *in* A. Grantz, L. Johnson, and J. F. Sweeney, eds., The Arctic Ocean Region, Geological Society of America, https://doi.org/10.1130/DNAG-GNA-L.379.

Grantz, A., S. Eittreim, and D. A. Dinter, 1979, Geology and tectonic development of the continental margin north of Alaska, Developments in Geotectonics, v. 15, Elsevier, p. 263-291.

Halgedahl, S., and R. Jarrard, 1987, Paleomagnetism of the Kuparuk River Formation from oriented drill core: evidence for the rotation of the Arctic Alaska plate, in I. Tailleur, and P. Weimer, eds., Alaskan North Slope Geology, Pacific Section: Society for Sedimentary Geology, Santa Barbara, CA, p. 581-617.

Hall, J. K., 1990, Chukchi borderland, in A. Grantz, L. Johnson, and J.F. Sweeney, eds., The arctic ocean region, The Geology of North America, Boulder/Colorado, v. 50, p. 337-350.

Hegewald, A., and W. Jokat, 2013a, Tectonic and sedimentary structures in the northern Chukchi region, Arctic Ocean: Journal of Geophysical Research: Solid Earth, v. 118, p. 3285-3296, doi:10.1002/jgrb.50282.

Hegewald, A., and W. Jokat, 2013b, Relative sea level variations in the Chukchi region - Arctic Ocean - since the late Eocene: Geophysical Research Letters, v. 40, p. 803-807, doi:10.1002/GRL.50182, 2013.

Hegewald, A., 2012, The Chukchi Region-Arctic Ocean-Tectonic and Sedimentary Evolution, Ph.D. Thesis, Alfred Wegener Institute, Kiel, Germany 130 p.

Houseknecht, D. W., W. H. Craddock, and R. O. Lease, 2016, Upper Cretaceous and Lower Jurassic strata in shallow cores on the Chukchi Shelf, Arctic Alaska: Chapter C in Studies by the US Geological Survey in Alaska, vol. 15, US Geological Survey, https://doi.org/10.3133/pp1814C.

Houseknecht, D. W., and K. J. Bird, 2011, Chapter 34 Geology and petroleum potential of the rifted margins of the Canada Basin: Geological Society, London, Memoirs, v. 35, p. 509-526, doi:10.1111/j.1365-2117.2008.00392.x.

Houseknecht, D. W., K. J. Bird, and C. J. Schenk, 2009, Seismic analysis of clinoform depositional sequences and shelf-margin trajectories in Lower Cretaceous (Albian) strata, Alaska North Slope: Basin Research, v. 21, p. 644-654, doi: 10.1111/j.1365-2117.2008.00392.x.

Hutchinson, D. R., H. R. Jackson, D. W. Houseknecht, Q. Li, J. W. Shimeld, D. C. Mosher, D. Chian, R. W. Saltus, and G. N. Oakey, 2017, Significance of Northeast-Trending Features in Canada Basin, Arctic Ocean: Geochemistry, Geophysics, Geosystems, v. 18, p. 4156-4178, https://doi.org/10.1002/2017GC007099.

Ilhan, I., and B. J. Coakley, 2018, Meso–Cenozoic evolution of the southwestern Chukchi Borderland, Arctic Ocean: Marine and Petroleum Geology, v. 95, p. 100-109, https://doi.org/10.1016/j.marpetgeo.2018.04.014.

Jakobsson, M., L. Mayer, B. Coakley, J. A. Dowdeswell, S. Forbes, B. Fridman, H. Hodnesdal, R. Noormets, R. Pedersen, M. Rebesco, H. W. Schenke, Y. Zarayskaya, D. Accettella, A. Armstrong, R. M. Anderson, P. Bienhoff, A. Camerlenghi, I. Church, M. Edwards, J. V. Gardner, J. K. Hall, B. Hell, O. Hestvik, Y. Kristoffersen, C. Marcussen, R. Mohammad, D. Mosher, S. V. Nghiem, M. T. Pedrosa, P. G. Travaglini, and P. Weatherall, 2012, The International Bathymetric Chart of the Arctic Ocean (IBCAO) Version 3.0: Geophysical Research Letters, v. 39, L12609, doi:10.1029/2012GL052219.

Kumar, N., J. W. Granath, P. A. Emmet, J. A. Helwig, and M. G. Dinkelman, 2011, Stratigraphic and tectonic framework of the US Chukchi Shelf: Exploration insights from a new regional deep-seismic reflection survey: Geological Society, London, Memoirs, v. 35(1), p. 501-508, doi:10.1144/M35.33.

Lane, L. S., 1997, Canada Basin, Arctic Ocean: evidence against a rotational origin: Tectonics, v. 16, p. 363-387.

Lawver, L., and C. Scotese, 1990, A review of tectonic models for the evolution of the Canada Basin: The Geology of North America, v. 50, p. 593-618.

Leeder, M. R., and R. L. Gawthorpe, 1987, Sedimentary models for extensional tilt-block/half-graben basins: Geological Society, London, Special Publications, v. 28, p. 139-152, doi:10.1144/GSL.SP.1987.028.01.11.

Lothamer, R., 1994, Early tertiary wrench faulting in the North Chukchi basin, Chukchi sea, Alaska, in D.K. Thurston and K. Fujita eds., 1992, Proceedings of the 1992 International Conference on Arctic Margins: Anchorage, Alaska, Minerals Management Service Outer Continental Shelf Report 94-0040, p. 251–256, https://www.boem.gov/ICAM92-129/.

Maus, S., U. Barckhausen, H. Berkenbosch, N. Bournas, J. Brozena, V. Childers, F. Dostaler, J. D. Fairhead, C. Finn, R. R. B. von Frese, C. Gaina, S. Golynsky, R. Kucks, H. Lühr, P. Milligan, S. Mogren, R. D. Müller, O. Olesen, M. Pilkington, R. Saltus, B. Schreckenberger, E. Thébault, and F. Caratori Tontini, 2009, EMAG2: A 2-arc min resolution Earth Magnetic Anomaly Grid compiled from satellite, airborne, and marine magnetic measurements: Geochemistry, Geophysics, Geosystems, v. 10, Q08005, doi:10.1029/2009GC002471.

McKenzie, D., 1978, Some remarks on the development of sedimentary basins: Earth and Planetary science letters, v. 40, p. 25-32.

Mickey, M.B., Haga, H., Bird, K.J., 2006. Micropaleontology of selected wells and seismic shot holes, northern Alaska: U. S. Geological Survey Open-File Report 2006-1055, CDROM, http://pubs.usgs.gov/of/2006/1055/.

Miller, E. L., G. E. Gehrels, V. Pease, and S. Sokolov, 2010, Stratigraphy and U-Pb detrital zircon geochronology of Wrangel Island, Russia: Implications for Arctic paleogeography: AAPG Bulletin, v. 94, p. 665-692, doi: 10.1306/10200909036.

Miller, E. L., J. Toro, G. Gehrels, J. M. Amato, A. Prokopiev, M. I. Tuchkova, V. V. Akinin, T. A. Dumitru, T. E. Moore, and M. P. Cecile, 2006, New insights into Arctic paleogeography and tectonics from U-Pb detrital zircon geochronology: Tectonics, v. 25, TC 3013, doi:10.1029/2005TC001830.

Nikishin, A. M., E. I. Petrov, N. A. Malyshev, and V. P. Ershova, 2017, Rift systems of the Russian Eastern Arctic shelf and Arctic deep water basins: link between geological history and geodynamics: Geodynamics & Tectonophysics, v. 8, p. 11-43.

Nikishin, A. M., N. A. Malyshev, and E. I. Petrov, 2014, Geological structure and history of the Arctic Ocean, EAGE Publications, Houten, The Netherlands 88 pp.

Moore, T. E., W. K. Wallace, K. J. Bird, S. M. Karl, C. G. Mull, and J. T. Dillon, 1994, Geology of northern Alaska, in G. Plafker, and H. C. Berg, eds., The Geology of Alaska: Geological Society of America, Geology of North America, v. G-1, p. 49–140, doi:10.1130 /DNAG-GNA-G1.49.

Nøttvedt, A., R. Gabrielsen, and R. Steel, 1995, Tectonostratigraphy and sedimentary architecture of rift basins, with reference to the northern North Sea: Marine and Petroleum Geology, v. 12, p. 881-901.

O'Brien, T. M., E. L. Miller, J. P. Benowitz, K. E. Meisling, and T. A. Dumitru, 2016, Dredge samples from the Chukchi Borderland: Implications for paleogeographic reconstruction and tectonic evolution of the Amerasia Basin of the Arctic: American Journal of Science, v. 316, p. 873-924, doi:10.2475/09.2016.03.

Prosser, S., 1993, Rift-related linked depositional systems and their seismic expression: Geological Society, London, Special Publications, v. 71, p. 35-66, doi:10.1144/GSL.SP.1993.071.01.03.

Sherwood, K. W., P. P. Johnson, J. D. Craig, S. A. Zerwick, R. T. Lothamer, D. K. Thurston, and S. B. Hurlbert, 2002, Structure and stratigraphy of the Hanna Trough, U.S. Chukchi Shelf, Alaska, in E.L. Miller, A. Grantz, and S.L. Klemperer, eds., Tectonic Evolution of the Bering Shelf–Chukchi Sea–Arctic Margin and Adjacent Landmasses: Geological Society of America, Boulder, CO, Special Papers, v. 360, p. 39-66.

Sherwood, K., 1994, Stratigraphy, structure, and origin of the Franklinian, northeast Chukchi basin, Arctic Alaska plate: in D.K. Thurston, and K. Fujita, eds.,1992, Proceedings International Conference on Arctic Margins: US Minerals Management Service Outer Continental Shelf Report 94-0040, p. 245-250.

Sokolov, S. D., G. Y. Bondarenko, O. L. Morozov, V. A. Shekhovtsov, S. P. Glotov, A. V. Ganelin, and I. R. Kravchenko-Berezhnoy, 2002, South Anyui suture, northeast Arctic Russia: Facts and problems: in Miller, E. L., and A. Grantz, eds., Tectonic Evolution of the Bering Shelf–Chukchi Sea–Arctic Margin and Adjacent Land masses: Geological Society of America Special Paper, 360, p. 209–224.

Thurston, D., and L. Theiss, 1987, Geologic Report for the Chukchi Sea Planning Area, Alaska Regional Geology: Petroleum Geology, and Environmental Geology: US Minerals Management Service Outer Continental Shelf Report 87-0046, 193 p.

Trettin, H., 1987, Pearya: a composite terrane with Caledonian affinities in northern Ellesmere Island: Canadian Journal of Earth Sciences, v. 24, p. 224-245.

Vail, P. R., Mitchum, R. M., and Thompson, S., III, 1977, Seismic stratigraphy and global changes of sea level, Part 3: Relative changes of sea level from coastal onlap, Application of seismic reflection configuration to stratigrapic interpretation: AAPG Memoir, 26, p. 63-81.

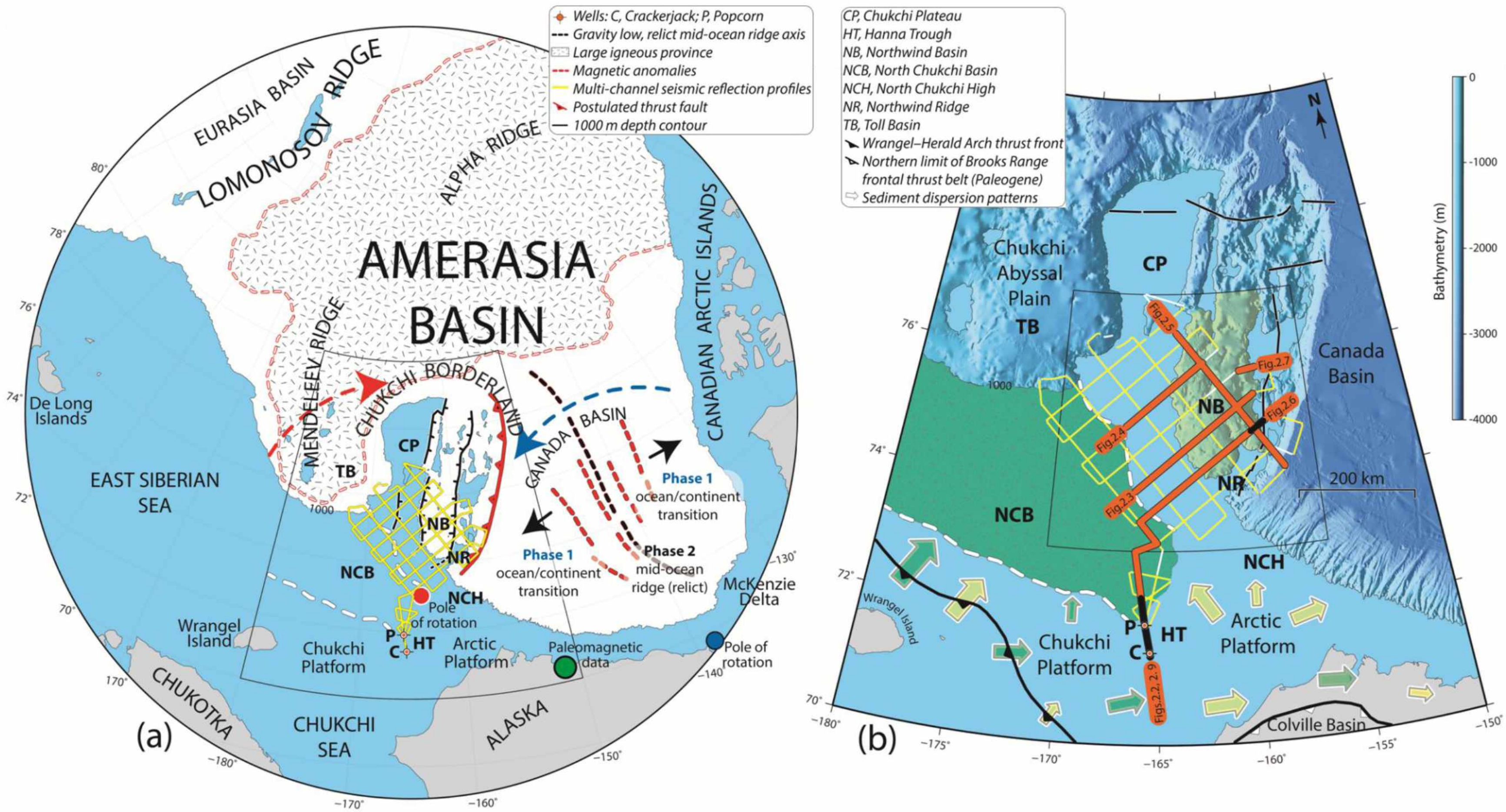

Figure 2.1 Overview of the study area

(a) Physiographic and tectonic elements of the Amerasia Basin, Arctic Ocean (modified from Grantz et al., 2011). The 1000 m contour (basinward boundary of blue; Jakobsson et al., 2012) approximates the present-day shelf edge and is a proxy for northern boundary of the Arctic Alaska-Chukotka microplate (Miller et al., 2010), the Arctic Canada and Lomonosov Ridge. Blue and red arrows track proposed counter-clockwise and clockwise rotations of the microplate away from the Canadian Arctic Islands around a pole in the McKenzie Delta, and of the Chukchi Borderland away from the East Siberian Shelf around a pole south of the Northwind Ridge (Grantz et al., 2011).

Figure 2.1 cont.
The green circle indicates the location of paleomagnetic data from the Kuparuk Formation (Valanginian–Hauterivian). Black arrows, first phase extensional deformation of the proto-Canada Basin (Grantz et al., 2011); red thrust fault, postulated compressional deformation along the Northwind Ridge required by the proposed clockwise rotation of the Borderland (Grantz et al., 2011); black and red dashed lines, gravity and magnetic anomalies (Brozena et al., 2002) indicating the second phase deformation "relict mid-ocean ridge" in the central Canada Basin; filled pattern indicates the large igneous province (Drachev and Saunders, 2006) which includes the Mendeleev and Alpha Ridges; normal faults, postulated late Paleocene east-west extensional deformation of the Borderland (Grantz et al., 2011). Yellow lines indicate 2011 tracks of *R/V Marcus Langseth*, multi-channel seismic (MCS) reflection profiles that were acquired and interpreted for this study. Also shown are the Crackerjack (C) and Popcorn (P) exploration wells (Sherwood et al., 2002). CP, Chukchi Plateau; NB, Northwind Basin; NR, Northwind Ridge; NCH, North Chukchi High; HT, Hanna Trough; NCB, North Chukchi Basin; TB, Toll Basin. **(b)** Bathymetry of the deepwater areas northwest of Alaska (Jakobsson et al., 2012). The 1000 m depth contour outlines the Chukchi Borderland and adjacent major basins, highs, and pertinent structural elements of the study area, contractional deformation fronts to the south (Drachev et al., 2010), and Cretaceous (green arrows) and Cenozoic (yellow arrows) sediment dispersion patterns flanking the Chukotka–Brooks Range (Houseknecht and Bird, 2011). Small map frame, area of detail maps shown in Fig. 2.8; black lines, tracks of *USCGC Healy* MCS profiles (Arrigoni, 2008); yellow lines, MCS profiles from ION Geophysical; bold black and orange lines, figures shown in this paper.

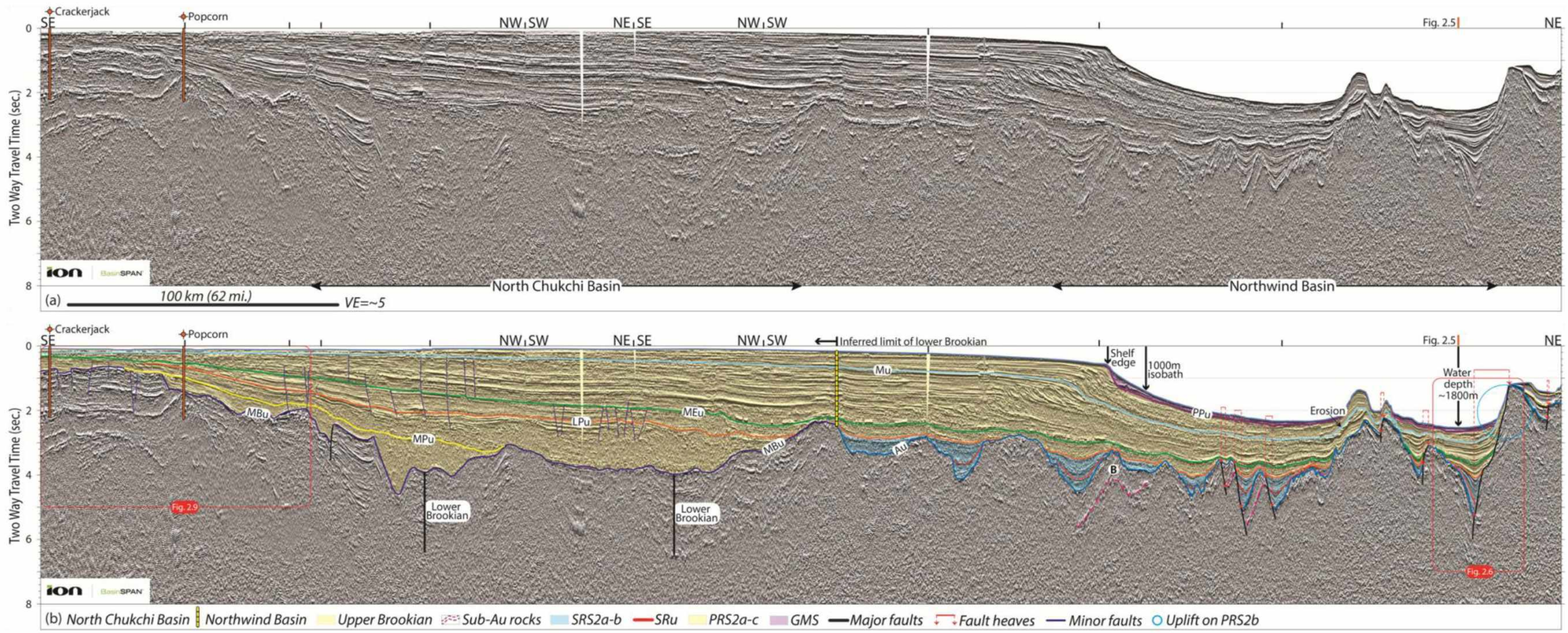

Figure 2.2 MCS profile-1

(a) MCS profile crossing the Crackerjack and Popcorn exploration wells (orange bars), southern edge of the North Chukchi Basin, and the southern Northwind Basin. Black bars indicate crossing points of the other MCS profiles. This is a crooked profile and the annotated directions indicate changes in profile directions (Fig. 2.1b). **(b)** Interpreted section illustrates the Cenozoic (upper Brookian) strata (yellow unit), downlapping onto the mid-Brookian unconformity (MBu) in the North Chukchi basin, and subdivision of the Northwind basin stratigraphy separated by unconformities or their correlative surfaces tied to the exploration wells. Yellow bar indicates the depositional limit of the Cretaceous (lower Brookian) strata in the North Chukchi basin, and the basin-flanking high. Unconformities include: Angular, Au; Syn-rift, SRu; mid-Paleocene, MPu; late Paleocene, LPu; mid-Eocene, MEu; Miocene, Mu; Plio-Pleistocene, PPu. Northwind basin-fill subdivision: SRS, syn-extensional sequence; PRS, post-extensional sequence; GMS, glacio-marine sequence. Boxes indicate sections of the profile shown in Figs. 2.6 and 2.9.

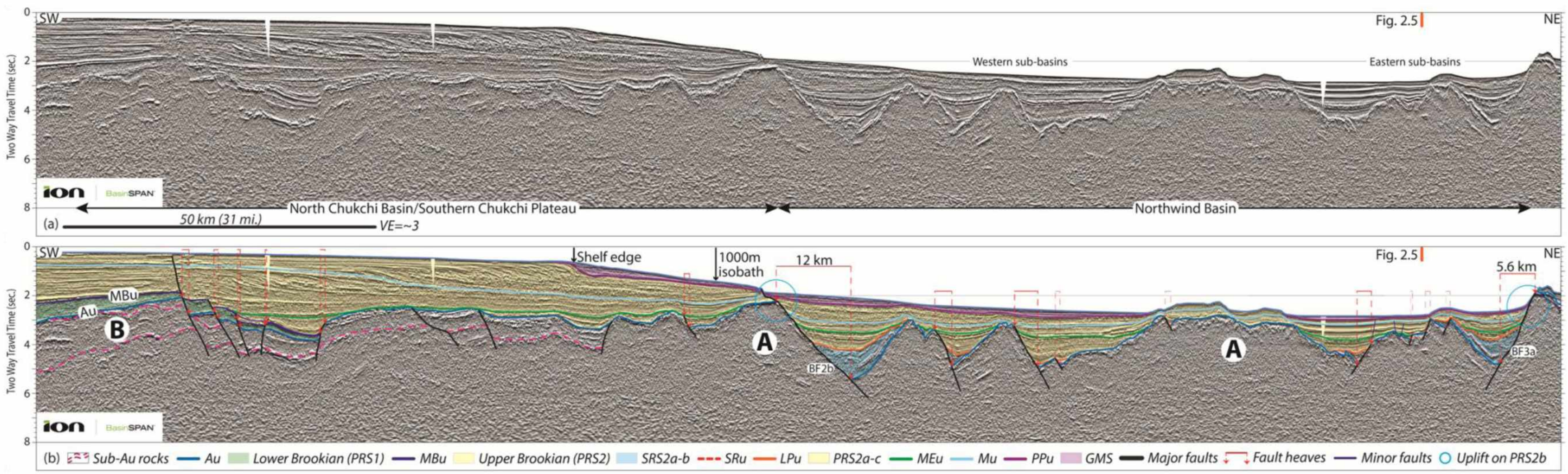

Figure 2.3 MCS profile-2

(a) MCS profile crossing eastern margin of the North Chukchi Basin, southern Chukchi Plateau and Northwind Basin. See Fig. 2.1b for location. **(b)** Interpreted section illustrates subdivision of the stratigraphy across the profile and extensional deformation of the Northwind basin depicted along two bounding faults (BF2b and BF3a). Unconformities include: Angular, Au; mid-Brookian, MBu; Syn-rift, SRu; late Paleocene, LPu; mid-Eocene, MEu; Miocene, Mu; Plio-Pleistocene, PPu. Northwind basin-fill subdivision: SRS, syn-extensional sequence; PRS, post-extensional sequence; GMS, glacio-marine sequence.

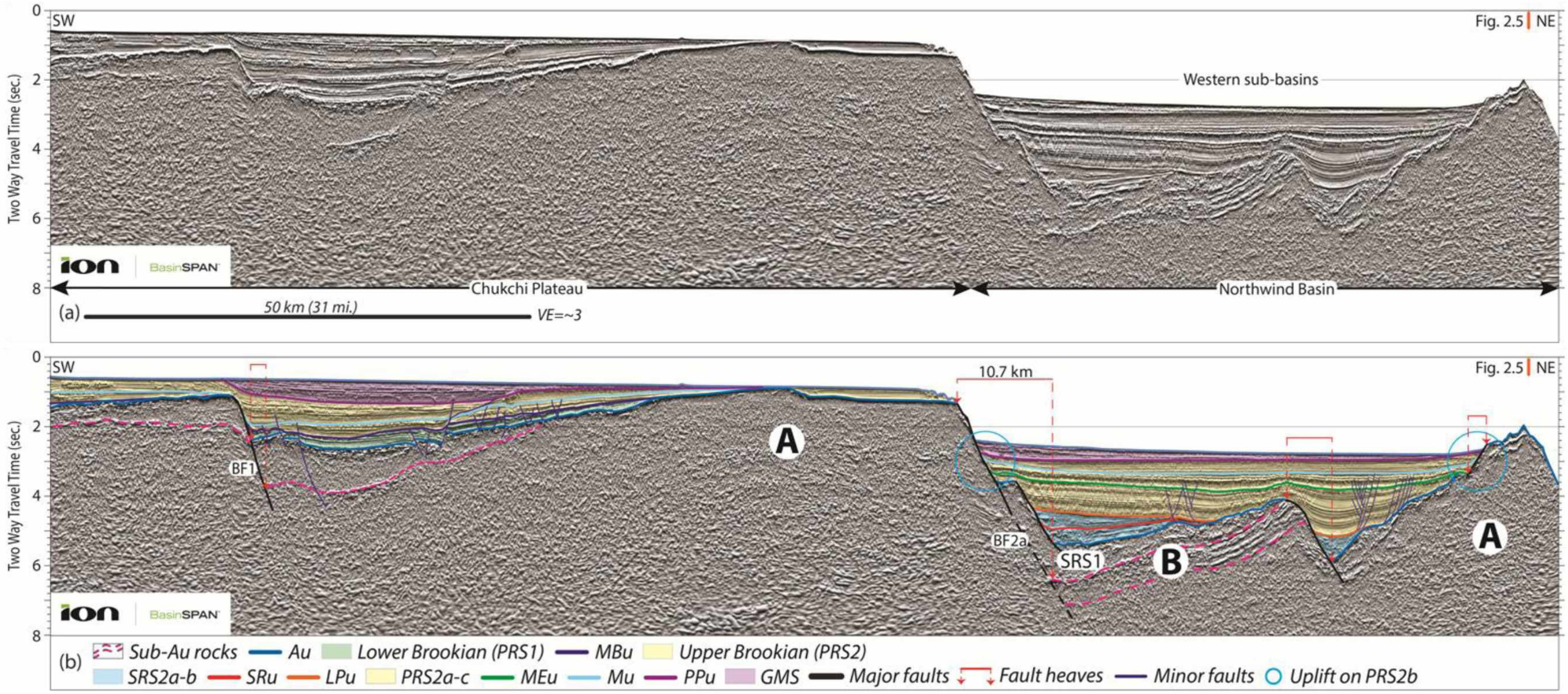

Figure 2.4 MCS profile-3

(a) MCS profile crossing the Chukchi Plateau and western sub-basins of the Northwind Basin. See Fig. 2.1b for location. **(b)** Interpreted section illustrates subdivision of the stratigraphy across two bounding faults (BF1 and BF2a) that dissect the Chukchi plateau into basement blocks. Unconformities include: Angular, Au; mid-Brookian, MBu; Syn-rift, SRu; late Paleocene, LPu; mid-Eocene, MEu; Miocene, Mu; Plio-Pleistocene, PPu. Northwind basin-fill subdivision: SRS, syn-extensional sequence; PRS, post-extensional sequence; GMS, glacio-marine sequence.

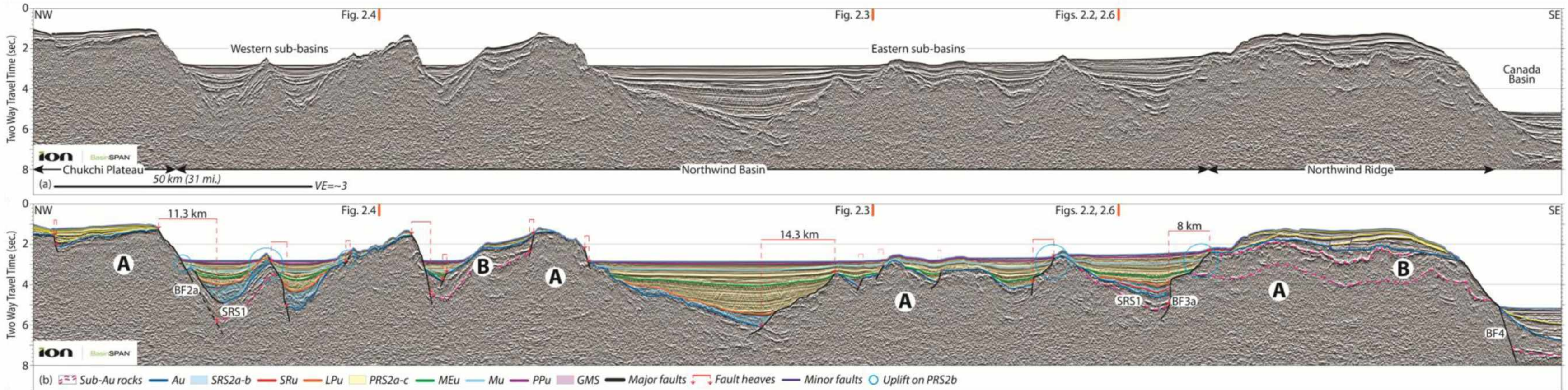

Figure 2.5 MCS profile-4

(a) MCS profile from the Chukchi Plateau to Canada Basin. See Fig. 2.1b for location. **(b)** Interpreted section illustrates subdivision of the stratigraphy across the Northwind basin and three bounding faults (BF2a, BF3a and BF4). Unconformities include: Angular, Au; Syn-rift, SRu; late Paleocene, LPu; mid-Eocene, MEu; Miocene, Mu; Plio-Pleistocene, PPu. Northwind basin-fill subdivision: SRS, syn-extensional sequence; PRS, post-extensional sequence; GMS, glacio-marine sequence.

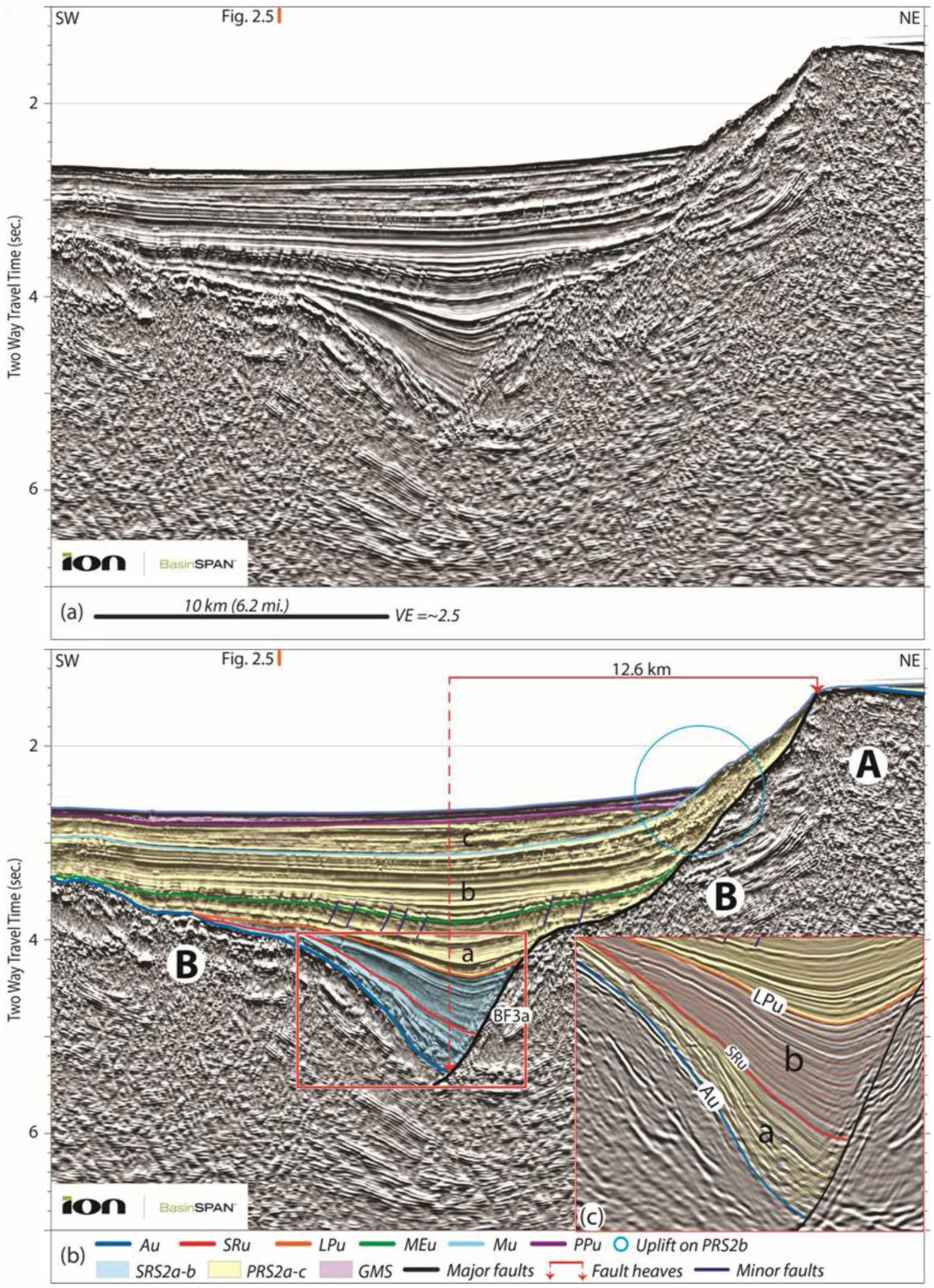

Figure 2.6 MCS profile-5

(a) MCS profile crossing the southeastern margin of the Northwind Basin. See Figs. 2.1b and 2.2b for location. **(b)** Interpreted section illustrates subdivision of the stratigraphy along southeastern bounding fault (BF3a). **(c)** Enlarged section of the profile depicts the detail stratigraphy. Unconformities include: Angular, Au; Syn-rift, SRu; late Paleocene, LPu; mid-Eocene, MEu; Miocene, Mu; Plio-Pleistocene, PPu. Northwind basin-fill subdivision: SRS, syn-extensional sequence; PRS, post-extensional sequence; GMS, glacio-marine sequence.

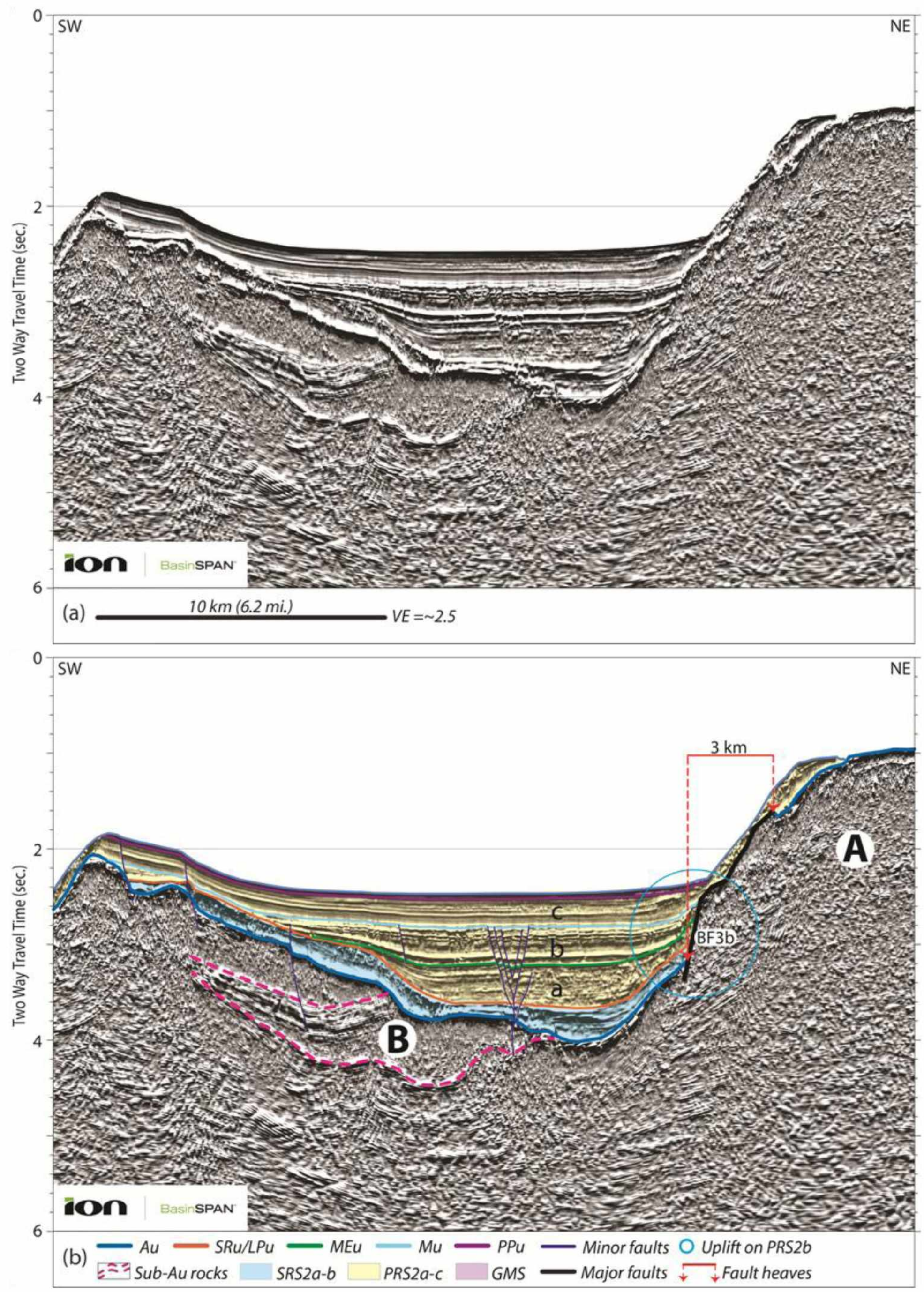

Figure 2.7 MCS profile-6

(a) MCS profile crossing the northeastern margin of the Northwind Basin. See Fig. 2.1b for location. **(b)** Interpreted section illustrates subdivision of the stratigraphy along northeastern bounding fault (BF3b) and angular truncation of the sub-Au rocks. Unconformities include: Angular, Au; Syn-rift and late Paleocene (amalgamated), SRu/LPu; mid-Eocene, MEu; Miocene, Mu; Plio-Pleistocene, PPu. Northwind basin-fill subdivision: SRS, syn-extensional sequence; PRS, post-extensional sequence; GMS, glacio-marine sequence.

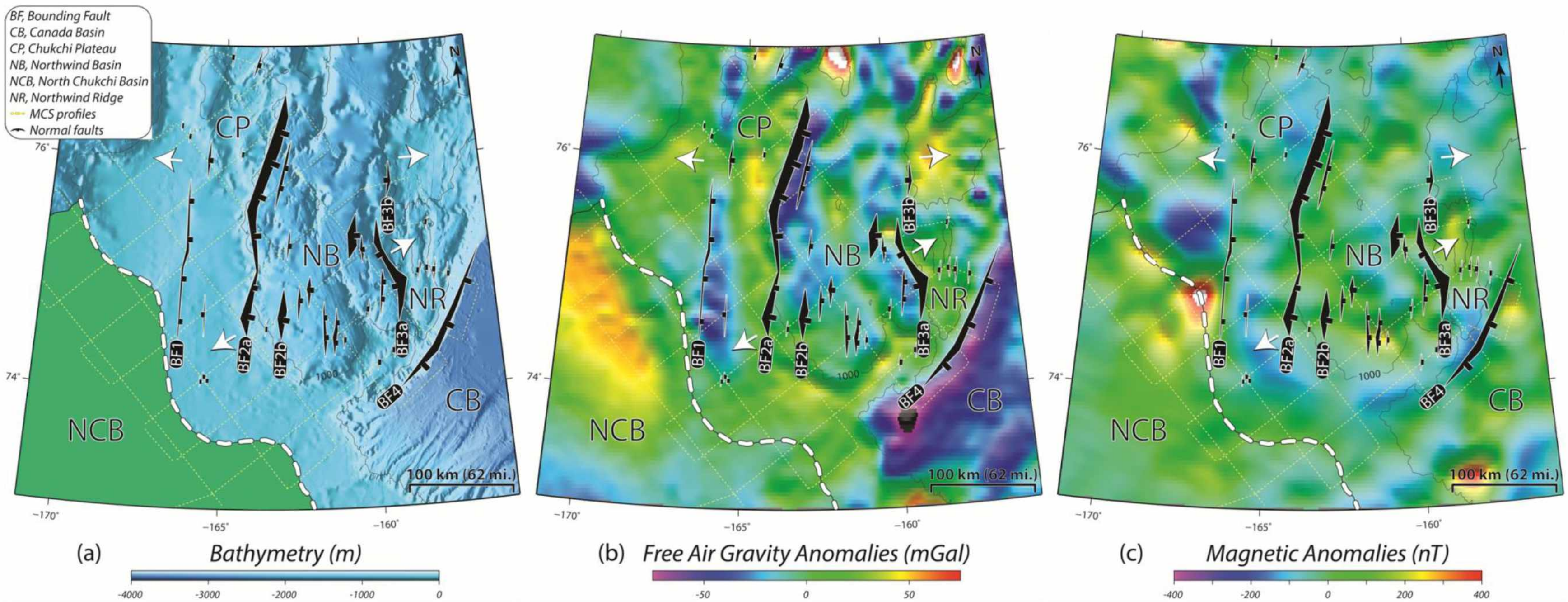

Figure 2.8 Bathymetry and potential field maps
(a) Normal faults superimposed on bathymetry (Jakobsson et al., 2012), **(b)** free air gravity (Bonvalot et al., 2012) and **(c)** magnetic (Maus et al., 2009) anomaly maps. These maps illustrate strikes, dips and relative heaves of the faults. White arrows indicate E-W and SW-NE extensional trends. White dashed line is the approximate depositional limit of the inferred Aptian-Albian lower Brookian strata (PRS2b; Ilhan and Coakley, 2018) along the eastern margin of the North Chukchi Basin.

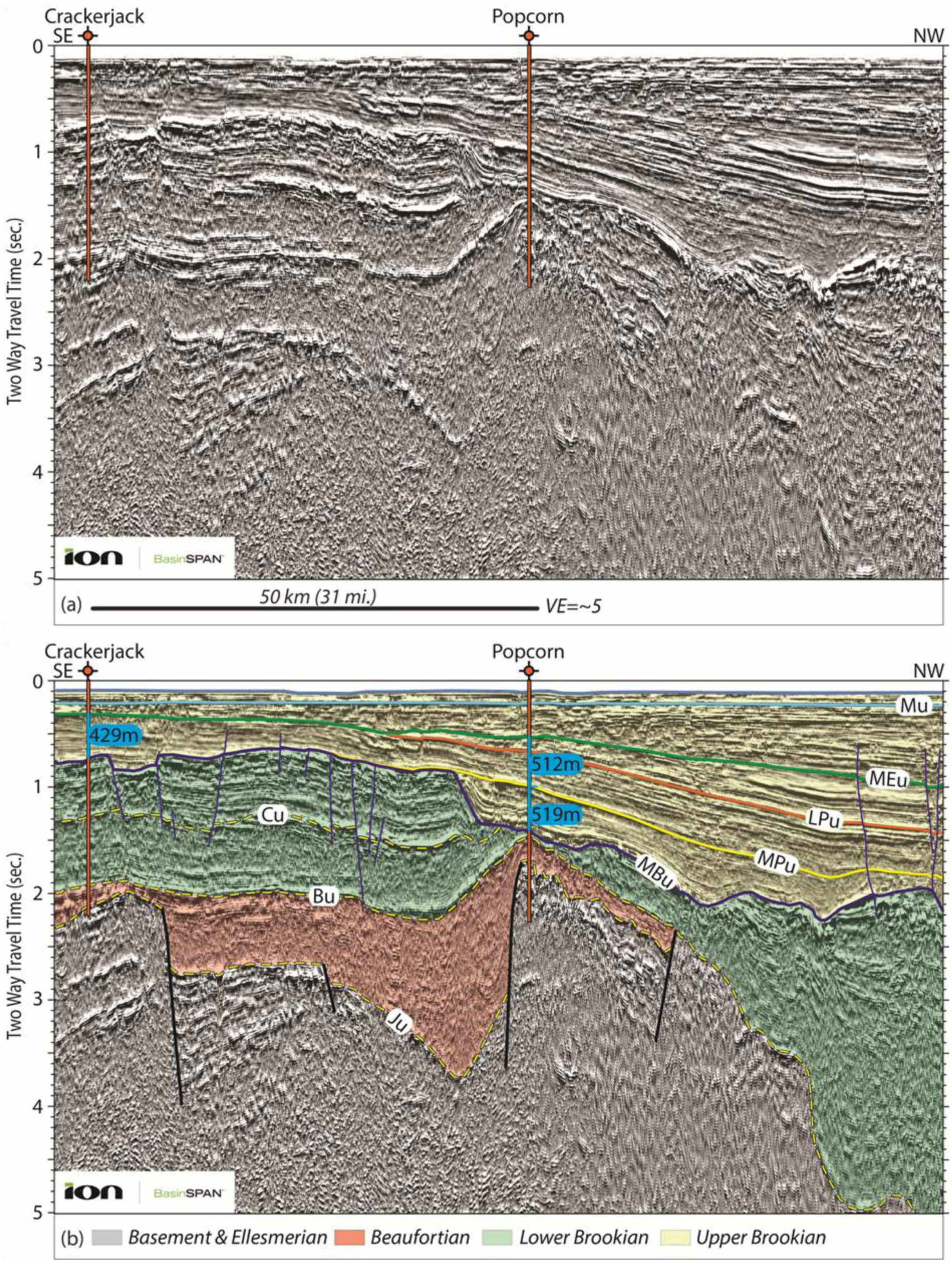

Figure 2.9 MCS profile-7

(a) MCS profile crossing the Crackerjack and Popcorn exploration wells. See Figs. 2.1b and 2.2b for location.

Figure 2.9 cont.
(b) Interpreted section illustrates subdivision of the Chukchi Shelf stratigraphy observed in these wells (Sherwood et al., 2002). Mid-Brookian (MBu) unconformity is draped across ~500 m of erosional relief along its surface between the lower and upper Brookian strata. Blue bars indicate the mid-Paleocene to mid-Eocene strata (419 m) at Crackerjack and lower Paleocene to mid-Eocene strata (519 m and 512 m) at Popcorn wells obtained from the biostratigraphy reports (Mickey et al., 2006; J. Bujak, 2018 personal comm.). Unconformities observed in these wells include: Jurassic, Ju; Brookian, Bu (lower Cretaceous); Cenomanian, Cu; mid-Brookian, MBu (basal Paleocene); mid-Paleocene, MPu; late Paleocene, LPu; mid-Eocene, MEu; Miocene, Mu. Northwind basin-fill subdivision: SRS, syn-extensional sequence; PRS, post-extensional sequence; GMS, glacio-marine sequence. The Cenozoic unconformities (or their correlative surfaces) are traced across the Chukchi Shelf as continuous surfaces through the MCS grid making it possible to constrain the ages of the upper Brookian strata in the Northwind basin.

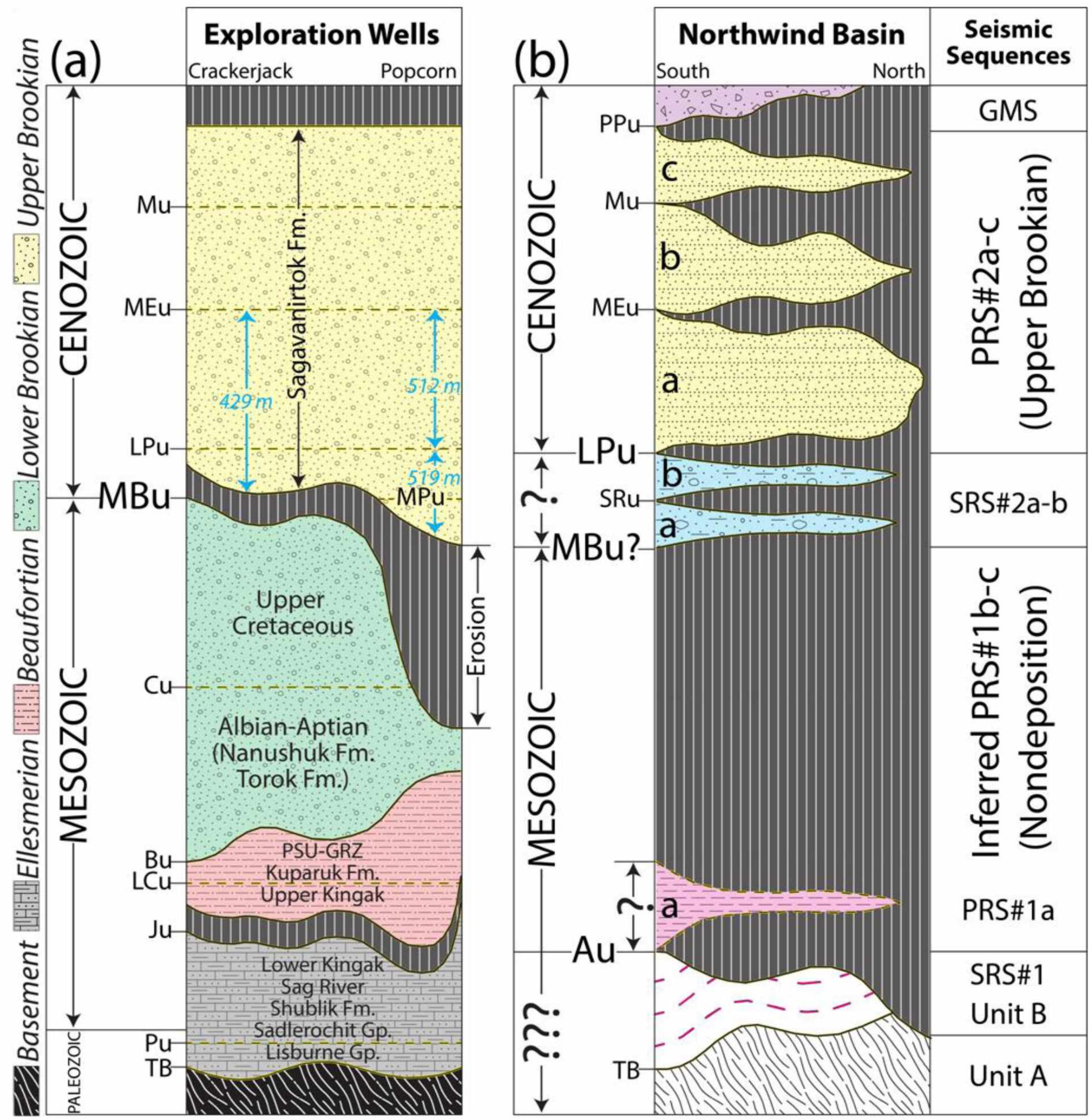

Figure 2.10 Simplified stratigraphic sections of the study area
(a) A simplified stratigraphic section across the Crackerjack and Popcorn exploration wells (modified from Sherwood et al., 2002). Blue bars indicate the thickness of early Paleocene to mid-Eocene strata as dated in the biostratigraphy reports of these wells (Mickey et al., 2006; J. Bujak, 2018 personal comm.). Unconformities include: Top basement, TB; Permian, Pu; Jurassic, Ju; lower Cretaceous, LCu; Brookian, Bu; Cenomanian, Cu (Craddock and Houseknecht, 2016); mid-Paleocene, MPu; late Paleocene, LPu; mid-Eocene, MEu; and Miocene, Mu. **(b)** A simplified stratigraphic column of the Northwind basin. Unconformities include: Top basement, TB; Angular, Au; Syn-rift, SRu; late Paleocene, LPu; mid-Eocene, MEu; Miocene, Mu; Plio-Pleistocene, PPu. Northwind basin-fill subdivision: SRS, syn-extensional sequence; PRS, post-extensional sequence; GMS, glacio-marine sequence.

3 Meso-Cenozoic evolution of the Chukchi Shelf and North Chukchi Basin, Arctic Ocean[1]

3.1 Abstract

A regional stratigraphic framework is developed for the North Chukchi Basin and southern margin of the Chukchi Borderland based on a grid of 2D multi-channel seismic reflection profiles tied to exploration wells on the U.S. Chukchi Shelf. The northern flank of the North Chukchi Basin displays a 16 km succession of mainly Cretaceous and Cenozoic strata that progressively onlap an unconformity (Au) on the southern margin of the Borderland. Rocks beneath the unconformity are inferred to represent (A) crystalline basement that may have affinity to the Peary terrane, (B) deformed growth strata that may be related to Carboniferous to Jurassic strata on the Chukchi Shelf, and (C) seaward dipping reflections (SDRs) likely related to oceanic igneous rocks or exhumed mantle beneath the North Chukchi Basin. The SDRs indicate that the southwestern margin of the Borderland is a rifted continental margin and loosely constrained age control suggests that rifting occurred between Middle Jurassic and earliest Cretaceous.

Cretaceous through Cenozoic strata that fill the North Chukchi Basin are part of the Brookian megasequence deposited across the foreland of the Chukotka and Brooks Range orogens. These strata form a series of clinothems deposited by northward-migrating depositional systems that progressively filled the North Chukchi Basin and buried the southern flank of the Borderland. Onlap of the Au by bottomset facies indicates that deep water conditions prevailed along the northern basin margin during Aptian–Oligocene. Foreset and topset facies onlap and overtop the highest standing part of the Borderland and indicate that marine slope and shallow marine to deltaic

[1] Ilhan, I., Coakley, B.J., 2018. Meso-Cenozoic evolution of the southwestern Chukchi Borderland, Arctic Ocean. Marine and Petroleum Geology 95, 100-109, https://doi.org/10.1016/j.marpetgeo.2018.04.014.

environments reached the Borderland during the Oligocene and persisted thereafter.

3.2 Introduction

The tectonic evolution of the Chukchi Borderland has been the subject of much speculation, fueled largely by sparse seismic data of limited quality with which to constrain its history. The objectives of this paper are to document the stratigraphy and structure of the south-western margin of the Borderland and to interpret its tectonic evolution. This is achieved through interpretation of a regional grid of 2D multi-channel seismic (MCS) reflection profiles and ancillary data. These profiles are tied to well-dated stratigraphy of exploration wells on the Chukchi Shelf, which constrain the timing of events in and around the Borderland. With these data and correlations, structural boundaries are described and interpreted; age, extent, and thickness of regional strata are determined; and sediment routing systems are examined.

3.3 Tectonic setting and models for opening of Amerasia Basin

The Chukchi Borderland is a continental block located in the Amerasia Basin (Brumley et al., 2015; O'Brien et al., 2016), northwest of Arctic Alaska (Fig. 3.1a). The crust beneath the Amerasia Basin is, in part, constrained to be oceanic (Chian et al., 2016). The presence of the Borderland in an ocean basin (Døssing et al., 2013) requires plate boundaries along its edges, although characterization of those boundaries is controversial (Coakley and Ilhan, 2012). The Borderland is dissected by normal faults into the Chukchi Plateau, Northwind Basin, and Northwind Ridge (Grantz et al., 1979, 1998, 1990). Most of the normal faults are sub-parallel to the rift axis of the Upper Devonian (?) to Mississippian Hanna Trough beneath the Chukchi Shelf (Sherwood et al., 2002).

Where and how the Chukchi Borderland restores to margins of the Arctic continents in plate-tectonic models of the Amerasia Basin has been controversial. The earliest model, which pre-dated the discovery of the Borderland, implied counter-clockwise rotation of the Arctic Alaska–Chukotka microplate away from the Canadian Arctic Islands around a pole in the Mackenzie Delta region (Carey, 1958, Fig. 3.1a). A majority of subsequent models similarly incorporate rotational opening of the Amerasia Basin, although several alternatives have been proposed (Lawver and Scotese, 1990; Lane, 1997; Embry, 2000; Miller et al., 2006; Grantz et al., 2011; Doré et al., 2016; O'Brien et al., 2016; Hutchinson et al., 2017). Implications of rotational opening of the Amerasia Basin include: (1) extension along the Arctic continental margins of Canada and Alaska; (2) the presence of a transform fault along an Amerasia Basin margin located at Lomonosov Ridge (Cochran et al., 2006; Evangelatos and Mosher, 2016); and (3) contraction across the southern margin of the microplate that was accommodated by the formation of the Chukotka and Brooks Range orogens (Moore et al., 1994; Sokolov et al., 2002).

Rotational models solve the problems of provenance and movement of the Chukchi Borderland by rotating, displacing, and/or distorting this continental block to make a restorable plate model of Amerasia Basin formation. In one of these models, Grantz et al. (2011) solved these problems with multiple phases of rotation (Fig. 3.1a). The initial phase involved Jurassic counter-clockwise rotation of the Arctic Alaska–Chukotka microplate away from the Canadian Arctic around a pole in the Mackenzie delta region. This episode was followed by pre-Valanginian clockwise rotation of the Borderland away from the East Siberian Shelf around a pole near the southern Northwind Ridge (Fig. 3.1a). Subsequently, Barremian seafloor spreading formed the central Canada Basin. Finally, northward propagation of seafloor spreading from the Atlantic Ocean formed the Alpha–Mendeleev large igneous province during the Barremian to Campanian (Grantz et al., 2011, Fig. 3.1a).

To accommodate the clockwise rotation of the Chukchi Borderland, Grantz et al. (2011) inferred an arcuate left-lateral transform fault and structural discontinuity along the western and northern edges of the Borderland. This rotation requires contractional deformation along the eastern edge of the Borderland, where the Northwind Ridge would impinge onto the proto-Canada Basin (Fig. 3.1a).

The counter-clockwise rotation of the Alaska–Chukotka microplate is supported by a paleomagnetic study of Valanginian to Hauterivian rocks in the Kuparuk River oil field near the northern coast of Alaska, which documented 65–70 degrees of post-depositional rotation (Halgedahl and Jarrard, 1987). This result contradicts the Jurassic rotation of the microplate proposed by Grantz et al. (2011). In addition, seismic reflection images across the boundary between Northwind Ridge and Canada Basin do not display evidence for contraction (e.g., Fig. 5 in Hutchinson et al., 2017). This constraint contradicts the postulated clockwise rotation of the Chukchi Borderland away from the East Siberia Shelf proposed by Grantz et al. (2011).

At the southwestern margin of the Chukchi Borderland, the tectonic boundary at the juncture of the Chukchi Plateau, North Chukchi Basin, and Toll Basin is unknown. To the south of this area, earlier investigations interpret structural geometry to suggest that the North Chukchi Basin is asymmetric and structurally continuous with the underfilled Toll Basin to the north. This has been interpreted to indicate that the North Chukchi Basin formed by rifting, and that it is floored by either oceanic crust or exhumed mantle (Grantz et al., 1979; Grantz and May, 1983; Granath et al., 2015; Drachev, 2016). Although MCS profiles have been published of the North Chukchi Basin north of Wrangel Island (Granath et al., 2015; Nikishin et al., 2017), there is no equivalent documentation of the relationship between the Chukchi Plateau and Toll Basin. Drachev et al. (2010) and Drachev (2016) interpreted the stratigraphy of the North Chukchi Basin on the Russia side, yet there is no documentation of the stratal geometry, thickness, and inferred ages on the U.S. side of the basin, nor of the structural relationship between the North Chukchi Basin and the Chukchi Plateau.

3.4 Regional stratigraphy

This research relies on the stratigraphy documented by five exploration wells on the U.S. Chukchi Shelf and correlated regionally using MCS data tied to those wells. These 1989–1991 vintage wells penetrated Cenozoic–Paleozoic strata that correlate to the stratigraphic section of the Alaska North Slope (Fig. 3.2a; Sherwood et al., 2002), and this work is focused mainly on the Cretaceous–Cenozoic Brookian megasequence. Orientations of clinoform successions in the Brookian megasequence demonstrate that sediment was derived from the Chukotka and Brooks Range orogens and routed generally northward into the large accommodation North Chukchi – Toll Basin and Canada Basin (Houseknecht and Bird, 2011).

The Brookian megasequence is divided into lower and upper sequences by the mid-Brookian unconformity, which commonly has been used as a regional correlation and mapping surface (MBu; Thurston and Theiss, 1987; Sherwood et al., 2002; Drachev et al., 1999, 2010; Kumar et al., 2011; Granath et al., 2015; and Nikishin et al., 2014, 2017). The lower Brookian sequence comprises sediment derived mainly from the Chukotka orogen and routed to the north and east across the Chukchi Shelf (western Colville foreland basin) and Arctic Platform (Fig. 3.1b). These sediments filled the North Chukchi Basin, western Colville Basin, and presumed to be deposited in the Canada Basin (Fig. 3.1b; Sherwood et al., 2002; Houseknecht et al., 2009; Drachev et al., 2010; Houseknecht and Bird, 2011; Kumar et al., 2011). Lower Brookian strata form large-scale clinothems in the North Chukchi and Canada Basins, although the northward extent and internal facies of the clinothems were unknown prior to this study because of sparse and poor-quality seismic data. The lower Brookian sequence is subdivided into Aptian–Albian and Upper Cretaceous subsequences by the Cenomanian (Cu) unconformity (Fig. 3.2; Craddock and Houseknecht, 2016; Houseknecht et al., 2016). Aptian–Albian strata reflect voluminous sediment influx from tectonic highlands whereas Upper Cretaceous strata reflect lower sedimentation rate and widespread volcanic ash falls (Houseknecht and Bird, 2011).

The Cenozoic upper Brookian sequence comprises sediment derived from the rejuvenated Chukotka and Brooks Range orogens, and routed mainly northward to the high-accommodation North Chukchi and Canada Basins (Houseknecht and Bird, 2011). Upper Brookian strata form giant clinothems in the North Chukchi and Canada Basins, and range in age from Paleocene through Miocene (Sherwood et al., 2002; Drachev et al., 2010; Houseknecht and Bird, 2011; Kumar et al., 2011; Hegewald and Jokat, 2013a, b; Granath et al., 2015; Nikishin et al., 2014, 2017).

3.5 Data and methods

MCS reflection data were acquired to: (1) image the subsurface geology of the southern Chukchi Borderland; (2) tie the seismic data to wells on the Chukchi Shelf; and (3) constrain ages of tectonic and sedimentary processes of this region. The ultimate goal was to indirectly test hypotheses for the formation of the Amerasia Basin. To accomplish these scientific objectives, approximately 5300 km of MCS profiles were acquired in 2011 by the R/V Marcus G. Langseth across the transition from the Chukchi Shelf to Borderland. Additional MCS profiles cross the width of the eastern North Chukchi Basin to tie to exploration wells (Fig. 3.1a). The MCS profiles were interpreted based on sequence stratigraphic principles of Vail et al. (1977). By interpreting the patterns of reflections throughout the region and integrating the other geophysical and geological constraints, a seismic stratigraphic framework has been developed for the area. Correlation of interpreted reflections to biostratigraphic data from exploration wells made it possible to assign ages to the seismic sequences (Fig. 3.2; Mickey et al., 2006; J. Bujak, 2018 personal comm.; Ilhan and Coakley, in review). A time-depth function developed by Hegewald (2012) is used to convert two-way-time in MCS profiles to approximate depth. Bathymetry (Jakobsson et al., 2012), free-air gravity (Bonvalot et al., 2012) and magnetic (Maus et al., 2009) anomaly maps were used to extend our structural interpretation beyond the limits of the MCS grid (Figs. 3.1b and 3.3a–b).

For the MCS data acquisition, a tuned array of ten airguns with total volume of 1830 cubic inches was used. These guns produced a simple, nearly dipole, total source signature. The spectrum of the returned signals, reflected from the subsurface interfaces, ranges between 5 and 125 Hz and falls off rapidly at both ends. The streamer included 468 hydrophones spaced 12.5 m apart that recorded 10s of returns with a sampling rate of 2ms. The distance between the source and first hydrophone group was 37.5 m. The source and streamer were towed at 6 and 9 m depths, respectively. The shots were triggered every 12.5 m along the track. The resulting nominal maximum fold, which is the number of recorded signals that sampled the same geometric location at depth, was 78.

After initial data processing at the University of Alaska, a preliminary interpretation was completed. Subsequently, the data set was reprocessed by ION Geophysical and those reprocessed MCS profiles were used for this work. Objectives of the MCS data processing were to attenuate various kinds of random, linear, and coherent noise, in particular multiples, to enhance the deeper returns, and to optimize the source signature. These objectives were accomplished by methods that include: (1) reformat SEG-D to ProMAX format and resample data from 2ms to 4ms, geometry merge, source and streamer static corrections, source system delay correction; (2) source residual bubble energy removal and zero phase application, velocity analysis (4^{th} order), source spherical spreading and absorption corrections, noise attenuation (swell noise, high amplitude noise bursts, etc.), external seismic source interference attenuation, side-scattered energy and refracted linear noise attenuation, receiver amplitude correction; and (3) multiple attenuation: SPMA (short period multiple attenuation) and SRME (surface related multiple elimination), high-resolution radon demultiple, apex shifted demultiple (ASMA), F-X deconvolution (common offset), "Larner" noise removal (common offset), and pre-stack time migration. These methods enhanced primary signals and attenuated random, coherent, and linear noise. All of the MCS profile images shown in this paper are from pre-stack time-migrated profiles reprocessed by ION.

3.6 Seismic stratigraphy

This work is focused on strata in the northern part of the North Chukchi basin and in basins on the Chukchi Borderland (Fig. 3.1). The following sections address age constraints for these strata followed by descriptions and interpretations of the main seismic stratigraphic units.

3.6.1 Age constraints

The southern to southwestern part of the study area is the northern margin of the North Chukchi basin (Figs. 3.1 and 3.3; NCB), which contains a stratigraphic section more than 8 seconds of two-way-travel (TWT) or 16 km thick (Fig. 3.4). This succession and coeval strata on the Chukchi Borderland are the main focus of this paper. At the southwestern end of the seismic image in Fig. 3.4, strata shallower than ~7 seconds (14 km) have been correlated directly to the Popcorn and Crackerjack wells using MCS data collected during the 2011 *R/V Marcus Langseth* cruise and documented across the interior Borderland (Ilhan and Coakley, in review). Seismic-to-well correlations using public-domain check-shot surveys, regional stratigraphic correlations (Sherwood et al., 2002), biostratigraphic data from the wells (Mickey et al., 2006; J. Bujak, 2018 personal comm.), and local geochronological constraints (Houseknecht et al., 2016) indicate that the succession shallower than ~7 seconds (14 km) ranges from Aptian to Miocene in age. The deeper section is more difficult to correlate to well control and may be as old as Upper Jurassic or as young as Aptian. Based on the age and seismic character of correlative strata in the Popcorn and Crackerjack wells, the strata shallower than ~7 seconds (14 km) are interpreted as part of the Brookian megasequence (Fig. 3.2). Deeper strata may include part of the Beaufortian megasequence and the lowermost part of the Brookian megasequence.

3.6.2 Tectono-stratigraphic framework of southwestern margin of borderland

The stratigraphic succession described above thins to the northeast and much of the succession pinches out against a reflective surface of discordance (Fig. 3.4). This pinchout progresses upward within the succession, reflection by reflection. Three distinctive rock units are recognized beneath the primary reflective surface. The oldest unit A (Fig. 3.4) is acoustically transparent except for rare, discontinuous reflections that display apparently unoriented dips. Beneath the Chukchi Plateau, the top of unit A is as shallow as 1 second (~750 m, Fig. 3.4). It extends to the bottom of the seismic record at 10 seconds (~20 km). The transparent rocks commonly are overlain by poorly defined, low-amplitude stratified rocks (unit B) that thicken laterally from a zero edge where they terminate beneath the surface of discordance to as much as 1 second (~1 km, Fig. 3.4) where they terminate abruptly against steeply dipping fault offsets. These strata thicken towards the steep offsets. These low-amplitude reflections are laterally variable, low to moderate dipping and locally display normal or reverse offsets. Units A and B are briefly described and interpreted here, but they are not the primary focus of this paper.

The third rock unit (C) beneath the surface of discordance has been observed only in the southwestern margin of the MCS grid at the juncture of the Chukchi Plateau, Toll Basin, and North Chukchi Basin (Figs. 3.1b and 3.6). These rocks occur in a wedge-shaped unit characterized by semi-continuous, moderate to high-amplitude reflections that display clinoform-like dip to the west or southwest towards the Toll and North Chukchi Basins (Fig. 3.6). The lower boundary of this unit is not well imaged, so the relationship with underlying rocks is unconstrained (Fig. 3.5). Unit C thickens westward towards the Toll and North Chukchi Basins to a maximum of about 1.5 seconds (~4 km).

Based on the properties described above, the surface of discordance is interpreted as an angular unconformity (Au) that was progressively onlapped by Brookian strata. Beneath the Au, unit A is interpreted as crystalline basement based on stratigraphic position, regional geology, and transparent acoustic character. This basement rock may be equivalent in part to the Franklinian megasequence of the Alaska North Slope and Chukchi Shelf (Sherwood et al., 2002; Kumar et al., 2011) or may be part of the Pearya terrane that was documented recently in the northern Chukchi Plateau (O'Brien et al., 2016). The overlying rocks of unit B are interpreted as growth strata deposited during normal faulting (steep offsets), and later deformed by contractional folding and both normal and thrust faulting (Fig. 3.5). The only age constraint is that the Au is overlain by Brookian and perhaps Beaufortian strata, so unit B could be coeval with parts of the Ellesmerian or Beaufortian megasequence (Fig. 3.2).

Based on acoustic properties, internal geometry, and stratigraphic position, unit C is interpreted as stratified magmatic rocks in a volcanic accretionary sequence, commonly known as seaward dipping reflections (SDRs; Mutter, 1985; Pindell et al., 2014; Paton et al., 2017). Alternatively, unit C could be interpreted as a sedimentary clinothem. However, the maximum observed thickness (1.5 seconds thick (~4 km) at a depth greater than 7 seconds (~20 km)) is excessive for a clinothem (Hubbard et al., 2010) whereas such a thickness is not unusual for SDRs (Pindell et al., 2014).

3.6.3 Post-Au strata in North Chukchi Basin

This section provides descriptions and interpretations of the thick succession in the North Chukchi Basin that onlaps the Au on the southwestern margin of the Chukchi Plateau, as described above. The basal strata range from acoustically transparent to low amplitude reflections and rest on irregular relief of the Au in the deepest part of the basin (Figs. 3.4 and 3.7; PRS1a). This unit is as much as 250 msec (over 500m) thick in higher accommodation parts of the basin and pinches out against the Au in lower accommodation areas. The top of PRS1a has been correlated to the Brookian unconformity (Bu in Fig. 3.2; Sherwood et al., 2002) in the Popcorn and Crackerjack wells (Ilhan and Coakley, in review).

These basal strata are interpreted to be mainly coeval with the Hauterivian pebble shale unit of the Chukchi Shelf and Alaska North Slope, although the lower part may be coeval with the Kingak Shale (Sherwood et al., 2002, Fig. 3.2). Across Arctic Alaska, the pebble shale unit is considered a transgressive systems tract deposited during subsidence of crust that had been thermally elevated during rift opening of the Canada Basin (Hubbard et al., 1987).

Strata overlying the Bu display acoustic character ranging from mainly transparent in the lower part to mainly medium to high amplitude, laterally continuous reflections in the upper part; all reflections are parallel or sub-parallel to the base of the unit (Figs. 3.4 and 3.7; PRS1b). These strata are as much as 1.5 seconds (~3 km) thick in the deepest part of the basin, thin to a progressive pinchout against the Au on the flank of the Chukchi Plateau (Fig. 3.4), and thin to less than 1 second (~2 km) in the distal part of the seismic survey in the southeastern Toll Basin (Fig. 3.7). The top of this unit is concordant with overlying strata in the deep basin and displays subtle discordance in lower accommodation areas, with apparent truncation of the uppermost reflections in the overlying sequence PRS1b (Fig. 3.7). This surface has been correlated to the Cenomanian unconformity (Cu; Craddock and Houseknecht, 2016) in the Popcorn and Crackerjack wells (Ilhan and Coakley, in review).

Strata in PRS1b are interpreted to be coeval with the Aptian-Cenomanian Torok and Nanushuk Formations, which form a clinothem on the Chukchi Shelf and Alaska North Slope (Sherwood et al., 2002; Houseknecht et al., 2009). Seismic data show that the topset (Nanushuk) and foreset (upper Torok) facies of the clinothem grade into exclusively bottomset facies between the Chukchi Shelf and the north flank of the North Chukchi Basin. Therefore, PRS1b is interpreted in the study area to comprise exclusively deep water facies, likely including mudstone and sandstone deposited in basin-floor fan and related environments. The onlap pinchout of PRS1b against the Au on the Chukchi Plateau (Fig. 3.4) indicates that these deep water deposits were banked against the steep northern flank of the basin bounded by the Chukchi Plateau.

Strata overlying the Cu display mainly medium to high amplitude, laterally continuous reflections that are parallel to the base of the unit, although relatively transparent intervals are present locally (Figs. 3.4, 3.5, 3.7 and 3.8; PRS1c). Chaotic reflections occur in the upper one-third to one-half of PRS1c, mostly in areas where this unit thins by onlap directly onto the Au (Figs. 3.4, 3.5, 3.7 and 3.8). PRS1c is as much as 2.3s (4 km) thick in the deepest part of the basin and thins progressively onto the Au on the flank of the Chukchi Plateau. PRS1c is the oldest unit to overtop the southernmost horst on the plateau in the central part of the study area (Figs. 3.4 and 3.8). The top of the unit is concordant with overlying strata in the deep basin and displays discordance in lower accommodation areas, with clear truncation of the uppermost reflections (e.g., Fig. 3.5, near and southwest of tie with Fig. 3.4). This surface has been correlated to the Middle Brookian unconformity (MBu; Sherwood et al., 2002) in the Popcorn and Crackerjack wells (Ilhan and Coakley, in review).

Strata in PRS1c are interpreted to be Cenomanian and younger Cretaceous strata, which have been recognized only recently on the Chukchi Shelf. Upper Cretaceous strata are thin to absent across the Chukchi Shelf and western North Slope, where they comprise non-marine to shallow marine deposits where present (Houseknecht et al., 2016). These strata thicken eastward on the North Slope and northward into the North Chukchi Basin and form clinothems that grade basinward into exclusively bottomset facies (Decker, 2010; Hubbard et al., 2010; Houseknecht and Bird, 2011). Unit PRS1c is interpreted to be bottomset seismic facies comprising mudstone and sandstone deposited in basin-floor fan and related environments. The onlap pinchout of PRS1c against the Au on the Chukchi Plateau (Fig. 3.4) indicates that these deep water deposits were banked against the steep northern flank of the basin formed by the Chukchi Plateau. The chaotic reflections in the upper part of the unit and near the onlap onto the plateau are interpreted as mass wasting that occurred where unconsolidated deposits were near the rigid underlying substrate formed by the pre-Au rocks.

Strata overlying the MBu comprise in ascending order medium amplitude reflections that dip gently to the north-northwest, high amplitude reflections that dip more steeply to the north-northwest, and medium to high amplitude reflections that are nearly horizontal (Figs. 3.4, 3.5, 3.7 and 3.8; PRS2a-b). Locally, chaotic reflections are present and the more steeply dipping reflections display synform geometry where the unit thins abruptly onto the Chukchi Plateau (Fig. 3.4, near tie with Figs. 3.5 and 3.8, near southwest of tie with Fig. 3.5). Within PRS2a-b, the nearly horizontal reflections thin northward and westward by rolling over into the steeply dipping reflections or by abrupt termination. This unit is nearly 3 seconds (~6.5 km) thick in the deep basin. It thins by onlap onto the MBu on the Chukchi Plateau (Figs. 3.4 and 3.7). In the southeastern part of the study area, PRS2a-b thickens to as much as 4.5 seconds (~8.5 km) into graben-like accommodation (Fig. 3.7). The top of the unit is concordant with overlying strata in the deep basin and displays discordance in lower accommodation areas, with clear truncation of underlying reflections (Figs. 3.4 and 3.5). This surface has been correlated to a Miocene unconformity in the Popcorn and Crackerjack wells (Ilhan and Coakley, in review).

PRS2a-b is interpreted as a clinothem containing in ascending order bottomset (low dip reflections, basin floor deposits), foreset (steeply dipping reflections, marine slope deposits), and topset (near horizontal reflections, shallow marine to nonmarine deposits) facies.

The foreset and topset reflections include geometries and stacking patterns that reflect numerous lowstand, transgressive, and highstand systems tracts, and the foreset dip and thinning of topsets indicate the depositional system migrated northward from the North Chukchi Basin to the Chukchi Plateau (Hegewald and Jokat, 2013b). The synform foresets displayed on SW-NE seismic profiles (Figs. 3.4 and 3.8) and the northwest foreset dips displayed on SE-NW seismic profiles (Figs. 3.5 and 3.7) indicate that the direction of progradation changed abruptly when the depositional system encountered the high-standing plateau. In other words, the plateau acted as an accommodation sill. As the depositional system prograded northward until the sill forced the system to switch to northwestern progradation. Truncation of strata in the upper part of PRS1c (e.g., Fig. 3.5 near and west of tie with Fig. 3.4) is interpreted as erosion and localized incision on the MBu prior to deposition of PRS2a-b on the low accommodation plateau.

Strata overlying the Mu in the North Chukchi Basin are mainly medium to high amplitude, near horizontal reflections, although thin intervals of inclined reflections that display moderate north dip are present locally (Figs. 3.4, 3.7 and 8; PRS2c). Near horizontal reflections also are common in some areas of the Chukchi Plateau (Fig. 3.5). However, in many parts of the southern plateau the Mu displays 1 second of relief and truncates underlying reflections in PRS2a-b (Fig. 3.4). In these areas, PRS2c displays, in ascending order, medium amplitude reflections that dip gently to the north-northwest, high amplitude reflections that dip more steeply to the north (Fig. 3.8) or northwest (Fig. 3.5), and medium to high amplitude reflections that are nearly horizontal (Figs. 3.5 and 3.8). In the northwestern part of the study area, the middle, steeply dipping reflections and the upper, near horizontal reflections terminate and only the lower, gently dipping reflections are present, and these acoustic characteristics are accompanied by a significant increase in interpreted water depth (Fig. 3.5). The top of PRS2c corresponds to the sea floor across much of the study area. PRS2c is interpreted as a clinothem. In the North Chukchi Basin only topset facies are present, and the small scale inclined reflections are interpreted as delta-front deposits. Above the Chukchi Plateau low angle reflections are interpreted as basin floor deposits (likely including basin-floor fan facies) and overlying, larger scale and steeply dipping reflections are interpreted as foresets deposited on a marine slope. The basinward termination of steeply dipping and horizontal reflections define the modern shelf margin, with terminal marine slope and shallow marine deposits entering the modern Toll deep water basin (Fig. 3.5).

3.7 Discussion

3.7.1 Rifted margin of the southwestern Chukchi Borderland

The boundary between the southwestern Chukchi Plateau and the North Chukchi Basin is characterized by a northwest-trending positive gravity anomaly (>50 mGal; Fig. 3.3a). This anomaly diminishes southwestward into the North Chukchi Basin. To the east of the gravity anomaly, where it tapers off (Fig. 3.3a), there are three circular positive magnetic anomalies (>200 nT; Fig. 3.3b). This magnetic pattern can be attributed to uplifted shallow basement blocks of the Chukchi Plateau (Fig. 3.4).

The northwest-trending gravity pattern is interpreted to be the expression of the shallow limit of a block of continental crust that thins and dips to the southwest beneath the North Chukchi Basin (Figs. 3.4, 3.5 and 3.8). From the shallow basement of the Chukchi Plateau, the sediments rapidly thicken to the south beyond the MCS survey into the North Chukchi Basin (Figs. 3.2a and 3.4). In this area the north-west trending gravity anomaly may be due to a change in the crustal type (e.g., continental vs. oceanic) underlying the North Chukchi Basin or approximate outline of the SDRs. A negative north-trending gravity anomaly (0 to 50 mGal; Fig. 3.3a) is associated with the Chukchi Plateau normal fault (BF1; Figs. 1b, 3a and 4). The density contrast between the basement rock and the graben fill (Figs. 3.3b, 3.4 and 3.8) can account for this anomaly.

Basement beneath the North Chukchi Basin has been interpreted as exhumed mantle or oceanic crust by Granath et al. (2015) and as serpentinized mantle by Drachev (2016). The northern end of a MCS profile just 30 km west of Fig. 3.6 is interpreted as part of the Alpha-Mendeleev Ridge oceanic large igneous province (Granath et al., 2015). Thus our interpretation of SDRs at the southwestern margin of the Chukchi Borderland is consistent with oceanic igneous rocks or exhumed mantle a short distance basinward, and reinforces our interpretation that this margin of the Borderland is a rifted margin. The stratified magmatic edifice of the SDRs is interpreted to extend southeast along the southwestern margin of the MCS grid and it may extend along the entire boundary between the North Chukchi Basin and the Chukchi Plateau.

The approximate age of inferred rifting along the southwestern margin of the Chukchi Borderland can be constrained using our seismic stratigraphic framework. The major surface of discordance (Au) separates the SDRs from overlying strata (Fig. 3.6) and the oldest strata at that location (PRS1b) are inferred to be no younger than Aptian (Fig. 3.2). However, in nearby areas of higher accommodation, older strata (PRS1a) rest directly on the Au (Figs. 3.4, 3.7 and 3.8) and those strata are inferred to be Hauterivian or older. This evidence indicates that the Au may be coeval with the Hauterivian LCu or perhaps with the Jurassic unconformity (Ju), which is considered to be Mid-Jurassic on the Chukchi Shelf and Alaska North Slope (Sherwood et al., 2002, Fig. 3.2). The rate at which rifted margins subside and, therefore, the lag time between rifting and the accumulation of sediment on the unconformity (Au) may range between a few and a few tens of millions of years, depending on the tectonic setting (e.g., Pindell et al., 2014; Sclater and Christie, 1980) and sediment supply. This reasoning suggests that rifting along the southwestern margin of the Borderland likely occurred between the Middle Jurassic and earliest Cretaceous.

Once the southern margin of the Chukchi Borderland subsided below sea level, the North Chukchi Basin was progressively filled during the Cretaceous and Cenozoic by northward prograding shelf-margin systems that deposited a series of clinothems across the basin. Seismic stratigraphic interpretations indicate that deep water depositional systems persisted along the margin of the Borderland from the Aptian through the Paleogene and that basin-floor deposits progressively onlapped the Au (Figs. 3.4 and 3.8). As the basin filled, marine slope and shallow marine conditions reached the Borderland during the Oligocene and clinoform foresets and topsets completed the burial of the highstanding crustal block along the margin of the Chukchi Plateau (Figs. 3.4 and 3.8).

3.8 Conclusions

Along the Southwestern margin of the Chukchi Borderland, more than 16 km of mostly Cretaceous and Cenozoic strata in the North Chukchi Basin progressively onlap an angular unconformity (Au) developed on a highstanding block of the Chukchi Plateau. Rocks beneath the unconformity are interpreted as (A) acoustically transparent crystalline basement rocks that may be part of the Pearya terrane, (B) deformed growth strata that may be coeval with Ellesmerian or Beaufortian strata of the Chukchi Shelf, and (C) seaward dipping reflections (SDRs). The SDRs likely are laterally related to oceanic igneous rocks or exhumed mantle underlying the North Chukchi and Toll Basins.

The southwestern margin of the Chukchi Borderland is interpreted as a rifted margin formed during opening of the North Chukchi Basin. A poorly constrained, basal stratigraphic unit resting on the Au is interpreted to be coeval to the Hauterivian pebble shale unit and perhaps the Jurassic Kingak Shale of the Chukchi Shelf. The presence of this unit provides tentative age control on the development of the rifted continental margin, which is inferred to have occurred between the Middle Jurassic and earliest Cretaceous.

The Cretaceous and Cenozoic fill of the North Chukchi Basin are part of the Brookian megasequence that comprises a series of giant clinothems deposited across the foreland region north of the Chukotka and Brooks Range orogens. These clinothems were deposited by northward-migrating depositional systems that progressively filled the North Chukchi Basin and buried the southern flank of the Chukchi Borderland. Basin-floor deposits (bottomset facies) onlapped the southern Borderland and filled most of the accommodation along the northern flank of the basin. Marine slope (foreset facies) and shallow marine – deltaic (topset facies) reached the Borderland during the Oligocene, completed the filling of the North Chukchi Basin, and overtopped the highstanding basement block of the southern Borderland.

3.9 References

Bonvalot, S., Balmino, G., Briais, A., Kuhn, M., Peyrefitte, A., Vales N. et al., 2012. World Gravity Map, Paris, Bureau Gravimetrique International (BGI), map, CGMW-BGI-CNES-IRD Ed.

Brozena, J.M., Lawver, L.A., Kovacs, L.C., Childers V.A., 2002. Aerogeophysical evidence for the rotational opening of the Canada Basin. American Association for Petroleum Geologists Bulletins 86, 1138.

Brumley, K., Miller, E.L., Konstantinou, A., Grove, M., Meisling, K.E., Mayer, L.A., 2015. First bedrock samples dredged from submarine outcrops in the Chukchi Borderland, Arctic Ocean. Geosphere 11, 76-92, doi:10.1130/GES01044.1.

Carey, S., 1958. A tectonic approach to continental drift, in continental drift: a symposium. Australia: University of Tasmania, Hobart, 177-355.

Chian, D., Jackson, H.R., Hutchinson, D.R., Shimeld, J.W., Oakey, G.N., Lebedeva-Ivanova, N., Li, Q., Saltus, R.W., Mosher, D.C., 2016. Distribution of crustal types in Canada Basin, Arctic Ocean. Tectonophysics 691, 8-30, http://dx.doi.org/10.1016/j.tecto.2016.01.038.

Coakley, B., Ilhan, I., 2012. Developing geophysical constraints on the history of the Amerasian Basin of the Arctic Ocean, Proceeding, OTC23795, Arctic Technology Conference, Houston, TX.

Cochran, J.R., Edwards, M.H., Coakley, B.J., 2006. Morphology and structure of the Lomonosov Ridge, Arctic Ocean. Geochemistry, Geophysics, Geosystems 7, Q05019, doi: 10.1029/2005GC001114.

Craddock, W.H., Houseknecht, D.W., 2016. Cretaceous–Cenozoic burial and exhumation history of the Chukchi shelf, offshore Arctic Alaska. AAPG Bulletin 100, 63-100, doi: 10.1306/09291515010.

Decker, P., 2010. Brookian sequence stratigraphic framework of the northern Colville foreland basin, central North Slope, Alaska (poster and presentation): DNR Spring Technical Review Meeting, Anchorage, April 21–22, 2010. Alaska Division of Geological & Geophysical Surveys, 30p., 1 sheet, accessed July 6, 2017, http://doi.org/10.14509/21861.

Doré, A.G., Lundin, E.R., Gibbons, A., Sømme, T.O., Tørudbakken, B.O., 2016. Transform margins of the Arctic: a synthesis and re-evaluation. Geological Society, London, Special Publications 431, 63-94.

Døssing, A., Jackson, H.R., Matzka, J., Einarsson, I., Rasmussen, T.M., Olesen, A.V., Brozena, J.M., 2013. On the origin of the Amerasia Basin and the High Arctic Large Igneous Province—Results of new aeromagnetic data. Earth and Planetary Science Letters 363, 219-230.

Drachev, S.S., Johnson, G.L., Laxon, S.W., McAdoo, D.C., Kassens, H., 1999. Main structural elements of eastern Russian Arctic continental margin derived from satellite gravity and multichannel seismic reflection data: Main structural elements of the Eastern Russian Arctic Continental Margin derived from satellite gravity and multichannel seismic reflection data, in: Kassens, H., Bauch, H. A. et al. (Eds.), Land–Ocean Systems in the Siberian Arctic: Dynamics and History. Springer, Berlin, 667–682.

Drachev, S., Saunders, A., 2006. The Early Cretaceous Arctic LIP: its geodynamic setting and implications for Canada Basin opening, Proc. Fourth Int. Conf. on Arctic Margins, Dartmouth, Nova Scotia, pp. 216-223.

Drachev, S.S., Malyshev, N.A., Nikishin, A.M., 2010. Tectonic history and petroleum geology of the Russian Arctic Shelves: an overview. Geological society, London, petroleum geology conference series, 591-619, doi: 10.1144/0070591.

Drachev, S.S., 2016. Fold belts and sedimentary basins of the Eurasian Arctic. Arktos 2(1), 1-30, doi: 10.1007/s41063-015-0014-8.

Embry, A., 2000. Counterclockwise rotation of the Arctic Alaska Plate: best available model or untenable hypothesis for the opening of the Amerasia Basin. Polarforschung 68, 247-255.

Evangelatos, J., Mosher, D.C., 2016. Seismic stratigraphy, structure and morphology of Makarov Basin and surrounding regions: Tectonic implications. Marine Geology, 374, 1–13.

Granath, J.W., McDonough, K-J., Sterne, E.J., and Horn, B.W., 2015. Contrasting extensional basin styles and sedimentary fill across the eastern Russian Arctic shelf as imaged in crustal-scale PSDM reflection data: American Association of Petroleum Geologists, Search and Discovery Article 10811, 28 p., http://www.searchanddiscovery.com/pdfz/documents/2015/10811granath/ndx_granath.pdf.html.

Grantz, A., Eittreim, S., Dinter, D.A., 1979. Geology and tectonic development of the continental margin north of Alaska, Developments in Geotectonics. Elsevier, pp. 263-291, https://doi.org/10.1016/B978-0-444-41851-7.50019-4.

Grantz, A., Eittreim, S., Whitney, O.T., 1981. Geology and physiography of the continental margin north of Alaska and implications for the origin of the Canada Basin, in Nairn, A.E.M., Churkin, M., Stehli, F.T. (Eds.), The Arctic Ocean, The Ocean Basins and Margins, 5. Plenum, New York, 439-492.

Grantz, A., May, S.D., 1983. Rifting history and structural development of the continental margin north of Alaska. American Association of Petroleum Geologists, Mem. 34, 77–102.

Grantz, A., Johnson, G.L., Sweeney, J.F., 1990. Canada Basin, in Grantz, A., Johnson, G.L., Sweeney, J. F. (Eds), The Arctic Ocean Region. The Geology of North America, L. Geological Society of America, Boulder, CO, 379–402.

Grantz, A., May, S.D., Hart, P.E., 1994. Geology of the Arctic continental margin of Alaska, in Plafker, G., Berg, H.C. (Eds.), The Geology of North America, The Geology of Alaska. Geological Society of America G-1, 17-48.

Grantz, A., Clark, D.L., Phillips, R.L., Srivastava, S.P., Blome, C.D., Gray, L.B., Haga, H., Mamet, B.L., McIntyre, D.J., McNeil, D.H., Mickey, M.B., Mullen, M.W., Murchey, B.I., Ross, C.A., Stevens, C.H., Silberling, N.J., Wall, J.H., Willard, D.A., 1998. Phanerozoic stratigraphy of Northwind Ridge, magnetic anomalies in the Canada basin, and the geometry and timing of rifting in the Amerasia basin, Arctic Ocean. Geological Society of America Bulletin 110, 801-820, doi:10.1130/0016-7606(1998)110<0801:PSONRM>2.3.CO;2.

Grantz, A., Scott, R.A., Drachev, S.S., Moore, T.E., 2009. Map Showing the Sedimentary Successions of the Arctic Region (58°-64° to 90°) that May be Prospective for Hydrocarbons. American Association of Petroleum Geologists, Open-File Spatial Library, http://gisudril.aapg.org/gisdemo/.

Grantz, A., Hart, P.E., Childers, V.A., 2011. Geology and tectonic development of the Amerasia and Canada Basins, Arctic Ocean, in Spencer, A.M., Embry, A.F., Gautier, D.L., Stoupakova, A.V., Sørensen, K. (Eds.), Arctic Petroleum Geology: Geological Society, London, Memoirs 35, 771-799, doi:10.1144/M35.50.

Halgedahl, S., Jarrard, R., 1987. Paleomagnetism of the Kuparuk River Formation from oriented drill core: Evidence for rotation of the Arctic Alaska plate, in Tailleur, I., Weimer, P. (Eds.), Alaskan North Slope Geology, Pacific Section, Society for Sedimentary Geology, Santa Barbara, CA, 581-617.

Hegewald, A., 2012. The Chukchi Region-Arctic Ocean-Tectonic and Sedimentary Evolution. Ph.D. Thesis, Alfred Wegener Institute, Kiel, Germany, 130 p.

Hegewald, A., Jokat, W., 2013a. Tectonic and sedimentary structures in the northern Chukchi region, Arctic Ocean. Journal of Geophysical Research: Solid Earth 118, 3285-3296, doi:10.1002/jgrb.50282.

Hegewald, A., Jokat, W., 2013b. Relative sea level variations in the Chukchi region – Arctic Ocean – since the late Eocene. Geophysical Research Letters 40, 803-807.

Houseknecht, D.W., Bird, K.J., 2011. Geology and petroleum potential of the rifted margins of the Canada Basin, in Spencer, A.M., Embry, A.F., Gautier, D.L., Stoupakova, A.V., Sørensen, K. (Eds.), Arctic Petroleum Geology: Geological Society, London, Memoirs 35, 509-526, doi:10.1111/j.1365-2117.2008.00392.x.

Houseknecht, D.W., Bird, K.J., Schenk, C.J., 2009. Seismic analysis of clinoform depositional sequences and shelf-margin trajectories in Lower Cretaceous (Albian) strata, Alaska North Slope. Basin Research 21, 644-654.

Houseknecht, D.W., Craddock, W.H., Lease, R.O., 2016. Upper Cretaceous and Lower Jurassic strata in shallow cores on the Chukchi shelf, Arctic Alaska, *in* Dumoulin, J.A. (Ed.), Studies by the U.S. Geological Survey in Alaska, vol. 15: U.S. Geological Survey Professional Paper 1814–C, 37 p., http://dx.doi.org/10.3133/pp1814C.

Hubbard, S.M., Fildani, A., Romans, B.W., Covault, J.A., McHargue, T.R., 2010. High-Relief Slope Clinoform Development: Insights from Outcrop, Magallanes Basin, Chile. Journal of Sedimentary Research 80, 357-375, doi:10.2110/jsr.2010.042.

Hubbard, R.J., Edrich, S.P., Rattey, R.P., 1987. Geologic evolution and hydrocarbon habitat of the 'Arctic Alaska microplate.' Marine and Petroleum Geology 4, 2-34.

Hutchinson, D.R., Jackson, H.R., Houseknecht, D.W., Li, Q., Shimeld, J.W., Mosher, D., Chian, D., Saltus, R.W., and Oakey, G.N., 2017. Significance of northeast-trending features in the Canada Basin, Arctic Ocean. Geochemistry, Geophysics, Geosystems (G3), 18, p. 4156–4178. http://doi.org/10.1002/2017GC007099.

Ilhan, I., Coakley, B.J., in review. Structure and stratigraphy of the Northwind Basin, Chukchi Borderland: Constraints on the tectonic development of the Amerasia Basin, Arctic Ocean. AAPG Bulletin.

Jakobsson, M., Mayer, L., Coakley, B., Dowdeswell, J.A., Forbes, S., Fridman, B., Hodnesdal, H., Noormets, R., Pedersen, R., Rebesco, M., Schenke, H.W., Zarayskaya, Y., Accettella, D., Armstrong, A., Anderson, R.M., Bienhoff, P., Camerlenghi, A., Church, I., Edwards, M., Gardner, J.V., Hall, J.K., Hell, B., Hestvik, O., Kristoffersen, Y., Marcussen, C., Mohammad, R., Mosher, D., Nghiem, S.V., Pedrosa, M.T., Travaglini, P.G., Weatherall, P., 2012. The International Bathymetric Chart of the Arctic Ocean (IBCAO) Version 3.0. Geophysical Research Letters 39, L12609, doi:10.1029/2012GL052219.

Kumar, N., Granath, J.W., Emmet, P.A., Helwig, J.A., Dinkelman, M.G., 2011. Stratigraphic and tectonic framework of the US Chukchi Shelf: exploration insights from a new regional deep-seismic reflection survey, in Spencer, A.M., Embry, A.F., Gautier, D.L., Stoupakova, A.V., Sørensen, K. (Eds.), Arctic Petroleum Geology: Geological Society, London, Memoirs 35, 501-508, doi:10.1144/M35.33.

Lane, L.S., 1997. Canada Basin, Arctic Ocean: evidence against a rotational origin. Tectonics 16, 363-387.

Lawver, L., Scotese, C., 1990. A review of tectonic models for the evolution of the Canada Basin. The Geology of North America 50, 593-618.

Maus, S., Barckhausen, U., Berkenbosch, H., Bournas, N., Brozena, J., Childers, V., Dostaler, F., Fairhead, J.D., Finn, C., von Frese, R.R.B., Gaina, C., Golynsky, S., Kucks, R., Lühr, H., Milligan, P., Mogren, S., Müller, R.D., Olesen, O., Pilkington, M., Saltus, R., Schreckenberger, B., Thébault, E., Caratori Tontini, F., 2009. EMAG2: A 2-arc min resolution Earth Magnetic Anomaly Grid compiled from satellite, airborne, and marine magnetic measurements. Geochemistry, Geophysics, Geosystems 10, Q08005, doi:10.1029/2009GC002471.

Mickey, M.B., Haga, H., Bird, K.J., 2006. Micropaleontology of selected wells and seismic shot holes, northern Alaska: U. S. Geological Survey Open-File Report 2006-1055, CDROM, http://pubs.usgs.gov/of/2006/1055/.

Miller, E.L., Gehrels, G.E., Pease, V., Sokolov, S., 2010. Stratigraphy and U-Pb detrital zircon geochronology of Wrangel Island, Russia: Implications for Arctic paleogeography. AAPG Bulletin 94, 665-692, doi:10.1306/10200909036.

Miller, E.L., Toro, J., Gehrels, G., Amato, J.M., Prokopiev, A., Tuchkova, M.I., Akinin, V.V., Dumitru, T.A., Moore, T.E., Cecile, M.P., 2006. New insights into Arctic paleogeography and tectonics from U-Pb detrital zircon geochronology. Tectonics 25, TC 3013, doi:10.1029/2005TC001830.

Moore, T.E., Wallace, W.K., Bird, K.J., Karl, S.M., Mull, C.G., Dillon, J.T., 1994. Geology of northern Alaska, in Plafker, G., Berg, H.C., (Eds.), The Geology of Alaska: Boulder, CO, Geological Society of America, Geology of North America G-1, 49-140, doi:10.1130/DNAG-GNA-G1.49.

Mutter, J.C., 1985. Seaward dipping reflectors and the continent-ocean boundary at passive continental margins. Tectonophysics 114, 117-131.

Nikishin A.M., Malyshev, N.A., and Petrov, E.I., 2014, Geological structure and history of the Arctic Ocean: EAGE Publications, Houten, The Netherlands, 88 p.

Nikishin, A.M., Petrov, E.I., Malyshev, N.A., Ershova, V.P., 2017. Rift systems of the Russian Eastern Arctic shelf and Arctic deep water basins: link between geological history and geodynamics. Geodynamics & Tectonophysics 8, 11-43.

O'Brien, T.M., Miller, E.L., Benowitz, J.P., Meisling, K.E., Dumitru, T.A., 2016. Dredge samples from the Chukchi Borderland: Implications for paleogeographic reconstruction and tectonic evolution of the Amerasia Basin of the Arctic. American Journal of Science 316, 873-924, doi: 10.2475/09.2016.03.

Paton, D.A., Pindell, J., McDermott, K., Bellingham, P., Horn, B., 2017. Evolution of seaward-dipping reflectors at the onset of oceanic crust formation at volcanic passive margins: Insights from the South Atlantic. Geology 45, 439-442, doi:10.1130/G38706.1.Sclater, J.G., Christie, P.A., 1980.

Pindell, J., Graham, R., Horn, B., 2014. Rapid outer marginal collapse at the rift to drift transition of passive margin evolution, with a Gulf of Mexico case study. Basin Research 26, 701-725, doi:10.1111/bre.12059.

Sclater, J.G., Christie, P.A., 1980. Continental stretching: An explanation of the post-Mid-Cretaceous subsidence of the central North Sea Basin. Journal of Geophysical Research: Solid Earth 85, 3711-3739.

Sherwood, K.W., Johnson, P.P., Craig, J.D., Zerwick, S.A., Lothamer, R.T., Thurston, D.K., Hurlbert, S.B., 2002. Structure and stratigraphy of the Hanna Trough, U.S. Chukchi Shelf, Alaska, in Miller, E.L., Grantz, A., Klemperer, S.L. (Eds.), Tectonic Evolution of the Bering Shelf–Chukchi Sea–Arctic Margin and Adjacent Landmasses, Geological Society of America, Boulder, CO, Special Papers 360, 39-66.

Sokolov, S.D., Bondarenko, G.Y., Morozov, O.L., Shekhovtsov, V.A., Glotov, S.P., Ganelin, A.V., Kravchenko-Berezhnoy, I.R., 2002. South Anyui suture, northeast Arctic Russia: facts and problems, in Miller, E.L., Grantz, A., Klemperer, S.L. (Eds.), Tectonic Evolution of the Bering Shelf–Chukchi Sea–Arctic Margin and Adjacent Landmasses, Geological Society of America, Boulder, CO, Special Papers 360, 209-224.

Thurston, D.K., Theiss, L.A., 1987. Geologic Report for the Chukchi Sea Planning Area: Anchorage, Alaska, U.S. Department of the Interior, Minerals Management Service Outer Continental Shelf Report 87-0046, 193 p.

Vail, P. R., Mitchum, R. M., Thompson, S., III, 1977. Seismic stratigraphy and global changes of sea level, Part 3: Relative changes of sea level from coastal onlap, Application of seismic reflection configuration to stratigrapic interpretation: AAPG Memoir 26, 63-81.

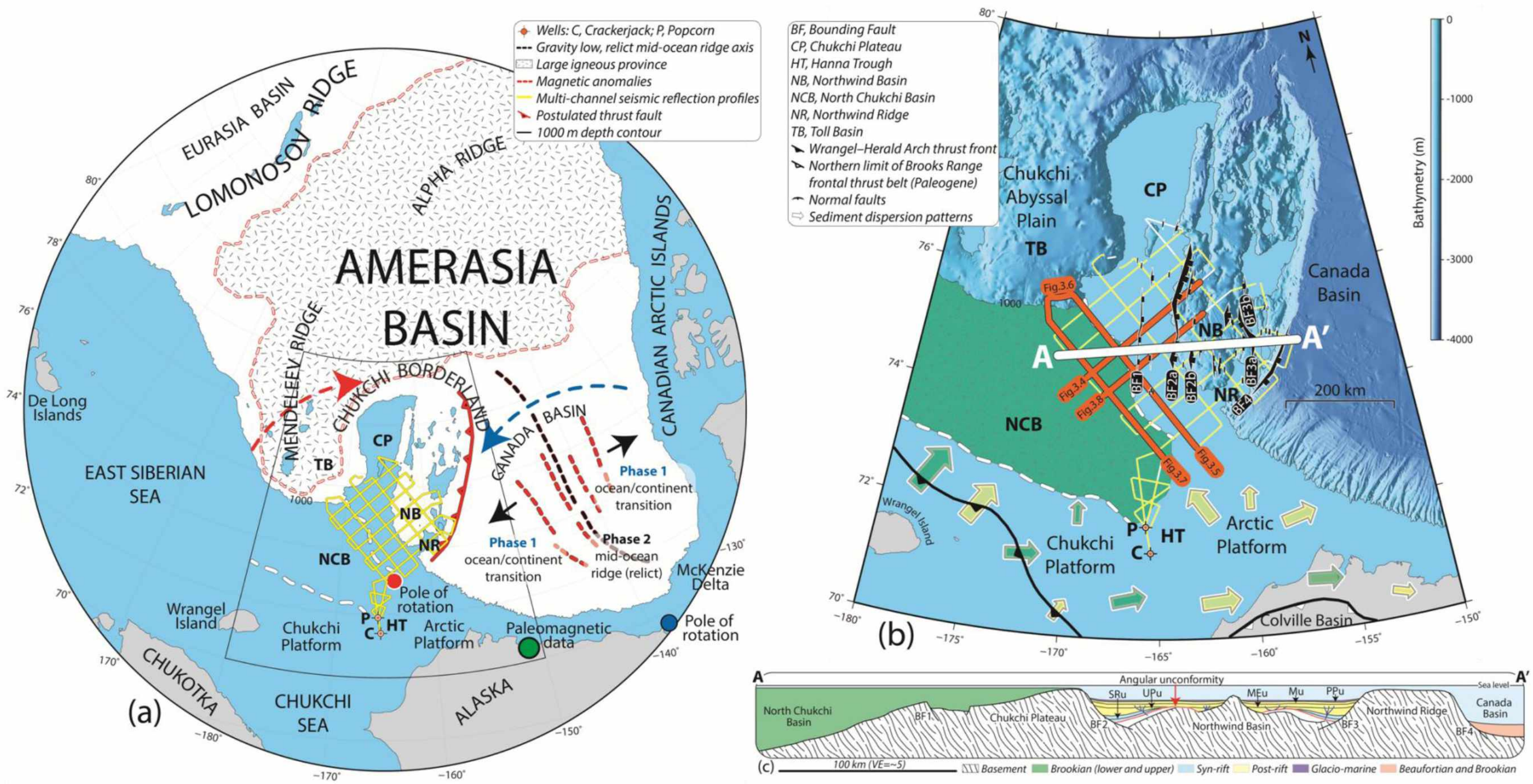

Figure 3.1 Overview of the study area

(**a**)Physiographic and tectonic elements of the Amerasia Basin, Arctic Ocean (modified from Grantz et al., 2011). The 1000 m bathymetric contour (basinward boundary of blue; Jakobsson et al., 2012) outlines the approximate northern boundary of the Arctic Alaska–Chukotka microplate (Miller et al., 2010), the Arctic Canada and Lomonosov Ridge. Blue and red arrows track proposed counter-clockwise and clockwise rotations of the microplate away from the Canadian Arctic Islands around a pole in the McKenzie Delta, and of the Chukchi Borderland away from the East Siberian Shelf around a pole south of the Northwind Ridge (Grantz et al., 2011). The 1000 m bathymetric contour

Figure 3.1 cont.
(basinward boundary of blue; Jakobsson et al., 2012) outlines the approximate northern boundary of the Arctic Alaska–Chukotka microplate (Miller et al., 2010), the Arctic Canada and Lomonosov Ridge. Blue and red arrows track proposed counter-clockwise and clockwise rotations of the microplate away from the Canadian Arctic Islands around a pole in the McKenzie Delta, and of the Chukchi Borderland away from the East Siberian Shelf around a pole south of the Northwind Ridge (Grantz et al., 2011). The green circle indicates the location of paleomagnetic data from the Kuparuk Formation (Valanginian–Hauterivian). Black arrows, first phase extensional deformation of the proto-Canada Basin (Grantz et al., 2011); red thrust fault, postulated compressional deformation along the Northwind Ridge required by the proposed clockwise rotation of the Borderland (Grantz et al., 2011); black and red dashed lines, gravity and magnetic anomalies (Brozena et al., 2002) indicating the second phase deformation "relict mid-ocean ridge" in the central Canada Basin; filled pattern indicates the large igneous province (Drachev and Saunders, 2006) which includes the Mendeleev and Alpha Ridges. Yellow lines indicate 2011 tracks of *R/V Marcus Langseth*, multi-channel seismic (MCS) reflection profiles that were acquired and interpreted for this study. Also shown are the Crackerjack (C) and Popcorn (P) exploration wells (Sherwood et al., 2002). CP, Chukchi Plateau; HT, Hanna Trough; NB, Northwind Basin; NCB, North Chukchi Basin; NR, Northwind Ridge; TB Toll Basin. **(b)** Bathymetry of the deepwater areas northwest of Alaska (Jakobsson et al., 2012). The 1000 m depth contour outlines the Chukchi Borderland and adjacent major basins, highs, and pertinent structural elements of the study area, normal faults mapped from MCS profiles (Ilhan and Coakley, in review), contractional deformation fronts to the south (Drachev et al., 2010 after Grantz et al., 2009), and Cretaceous (green arrows) and Cenozoic (yellow arrows) sediment dispersion patterns flanking the Chukotka–Brooks Range (Houseknecht and Bird, 2011). Yellow lines, MCS profiles from ION Geophysical; bold orange lines, figures shown in this paper. Abbreviated labels same as in a. **(c)** Tectono-stratigraphic sketch A–A'. This schematically illustrates border faults and basin stratigraphy across the southern Chukchi Borderland (modified from Ilhan and Coakley, in review). Unconformities: syn-rift, SRu; upper Paleocene, UPu; mid-Eocene, MEu; Miocene, Mu; Plio-Pleistocene, PPu. Colors used for the sequences in this figure are also used for the MCS profiles.

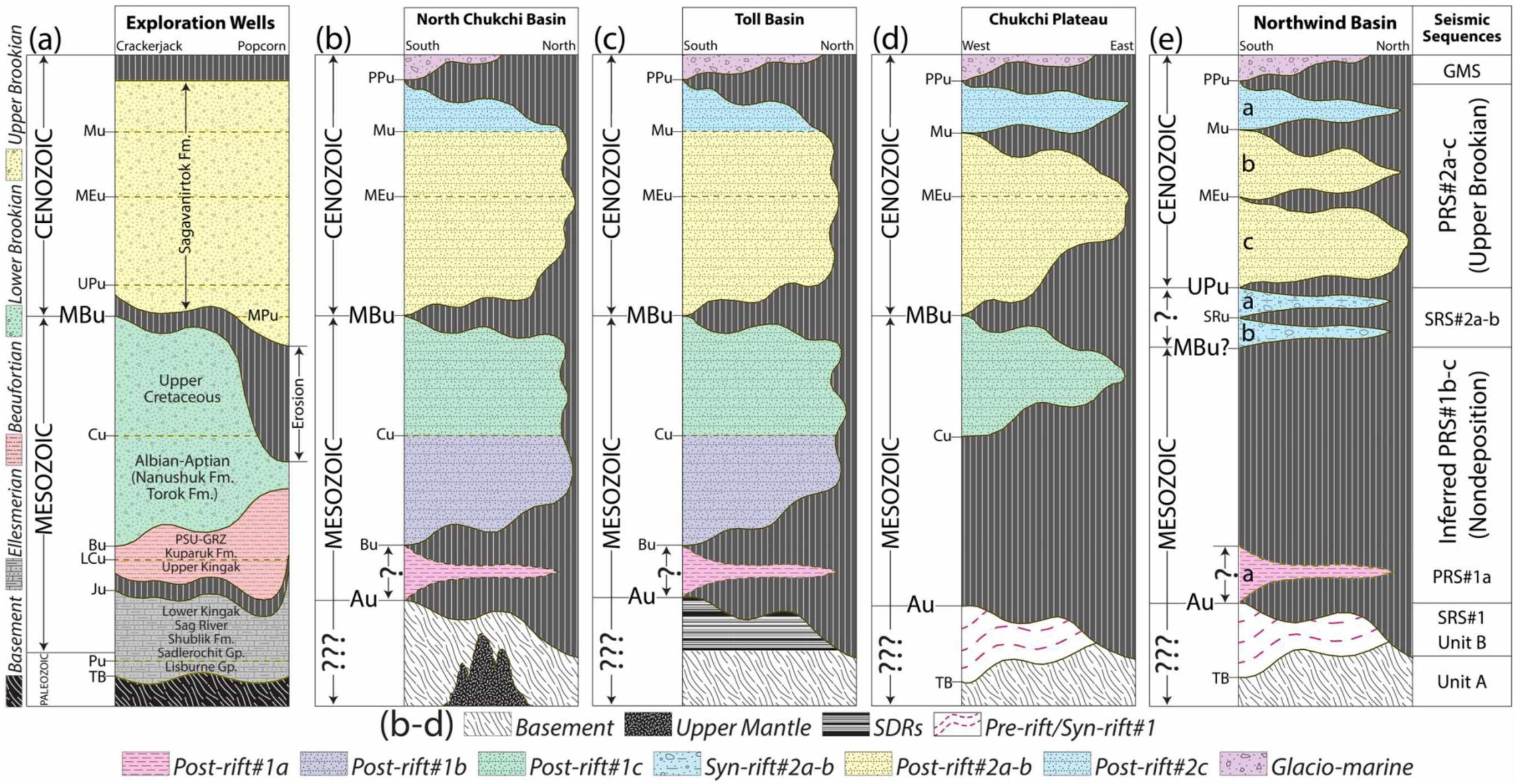

Figure 3.2 Simplified stratigraphic sections of the study area and adjacent areas
(**a**) Chukchi Shelf Crackerjack and Popcorn exploration wells (modified from Sherwood et al., 2002); (**b**) North Chukchi Basin; (**c**) Toll Basin; (**d**) Chukchi Plateau; (**e**) Northwind Basin. Interpreted seaward dipping reflections (SDRs) are shown in the Toll Basin. TB, top basement; unconformities: Permian, Pu; Jurassic, Ju; Lower Cretaceous, LCu; Brookian, Bu; Cenomanian, Cu; mid-Brookian, MBu; mid-Paleocene, MPu; upper Paleocene, UPu; mid-Eocene, MEu; Miocene, Mu; Plio-Pleistocene, PPu; Angular, Au; and Syn-rift, SRu.

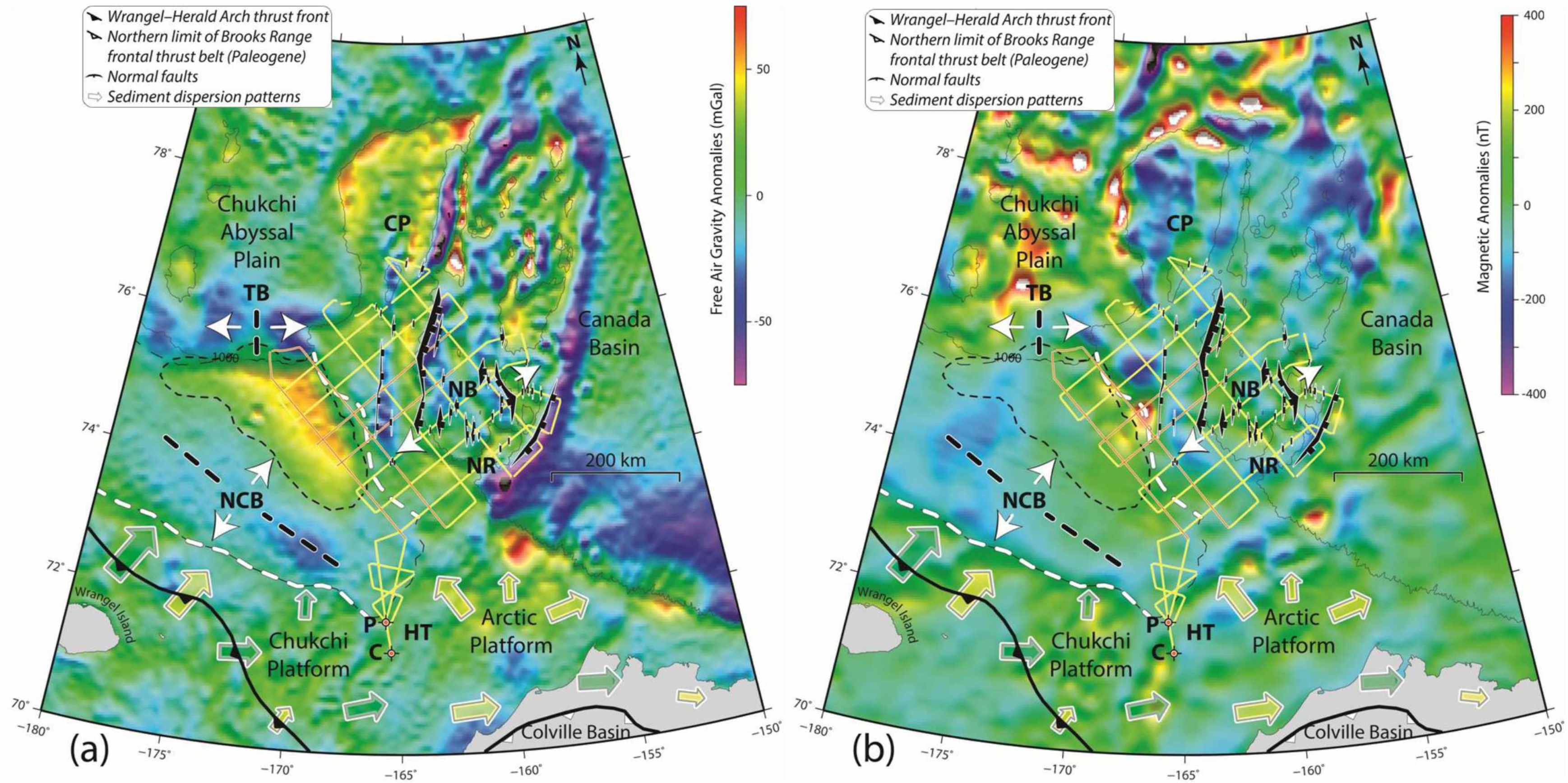

Figure 3.3 Potential field anomaly maps

(**a**) Free air gravity anomaly map (Bonvalot et al., 2012). (**b**) Magnetic anomaly map (Maus et al., 2009). North-striking normal faults (Ilhan and Coakley, in review) superimposed on these maps discordant to northwest-trending gravity anomaly (>50 mGal, outlined with a black-dashed polygon) and relatively scattered magnetic (>200 nT) positive anomalies along the north-bounding boundary of the North Chukchi Basin. The irregular high magnetic anomalies over the Chukchi Abyssal Plain are part of the large igneous province (Drachev and Saunders, 2006; Grantz et al., 2011). The axis of the North Chukchi and Toll Basins are indicated with black-dashed lines. Arrows illustrate orientations of crustal deformation. Orange lines highlight the featured MCS profiles shown in figures 3.4-8.

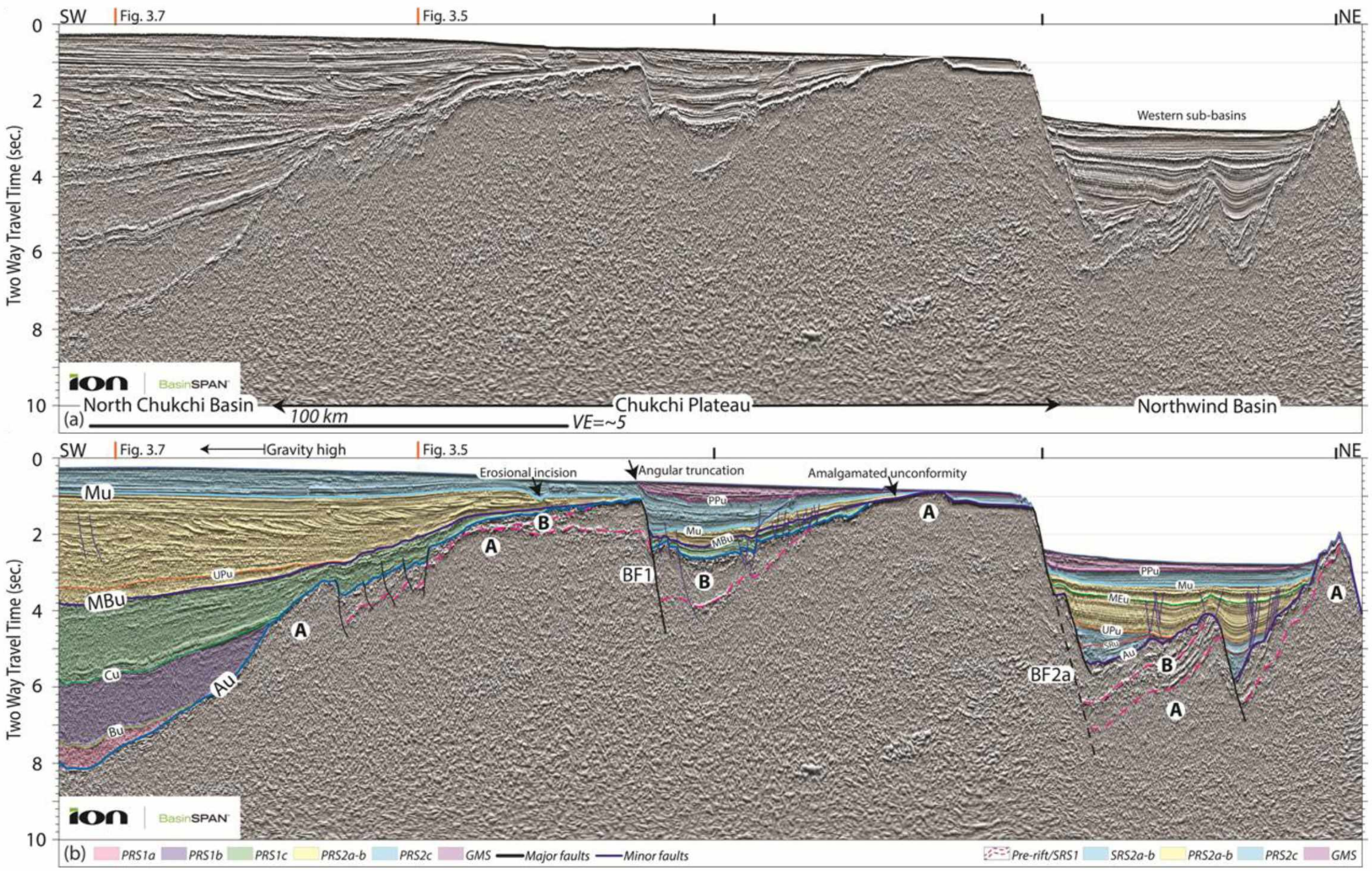

Figure 3.4 MCS profile-1

(a) MCS profile crossing the northeastern margin of the North Chukchi Basin, southern Chukchi Plateau and western sub-basins of the Northwind Basin. See Fig. 3.1b for location. **(b)** Interpreted section illustrates two of the border faults (BF) dissecting the Chukchi Plateau into rotated fault blocks and subdivision of the stratigraphy across these basins. Note the arrow for outline of gravity high mentioned in Fig. 3.3a. Dashed lines indicate areas of uncertainty. SRS, syn-rift; PRS, post-rift; and GMS, glacio-marine sequences. See Fig. 3.2 for sequence subdivisions and bounding unconformities.

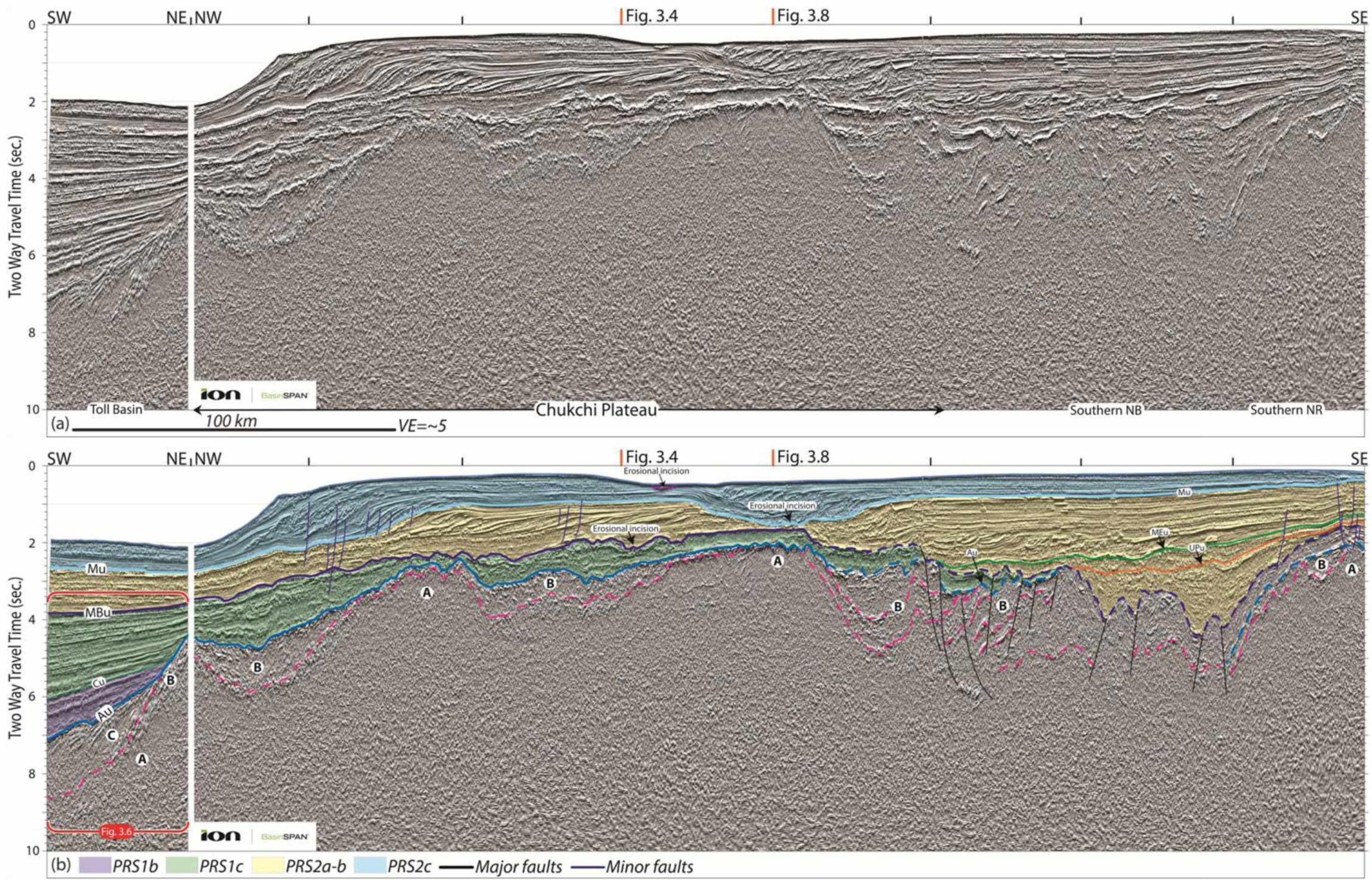

Figure 3.5 MCS profile-2

(a) MCS profile crossing the southeastern margin of the Toll Basin, and the southern Chukchi Plateau, Northwind Basin and Northwind Ridge. See Fig. 3.1b for location. **(b)** Interpreted section illustrates prominent, angular (Au) and erosional, mid-Brookin (MBu) unconformities. These two amalgamate from west to east, forming a composite surface in the southern Northwind Basin. Dashed lines indicate uncertainty of the interpretation. Note the largest amplitude of the scattered positive magnetic anomalies mentioned in Fig. 3.3b coincides with the crossing Fig. 3.4. PRS, post-rift sequence. See Fig. 3.2 for sequence subdivisions and bounding unconformities.

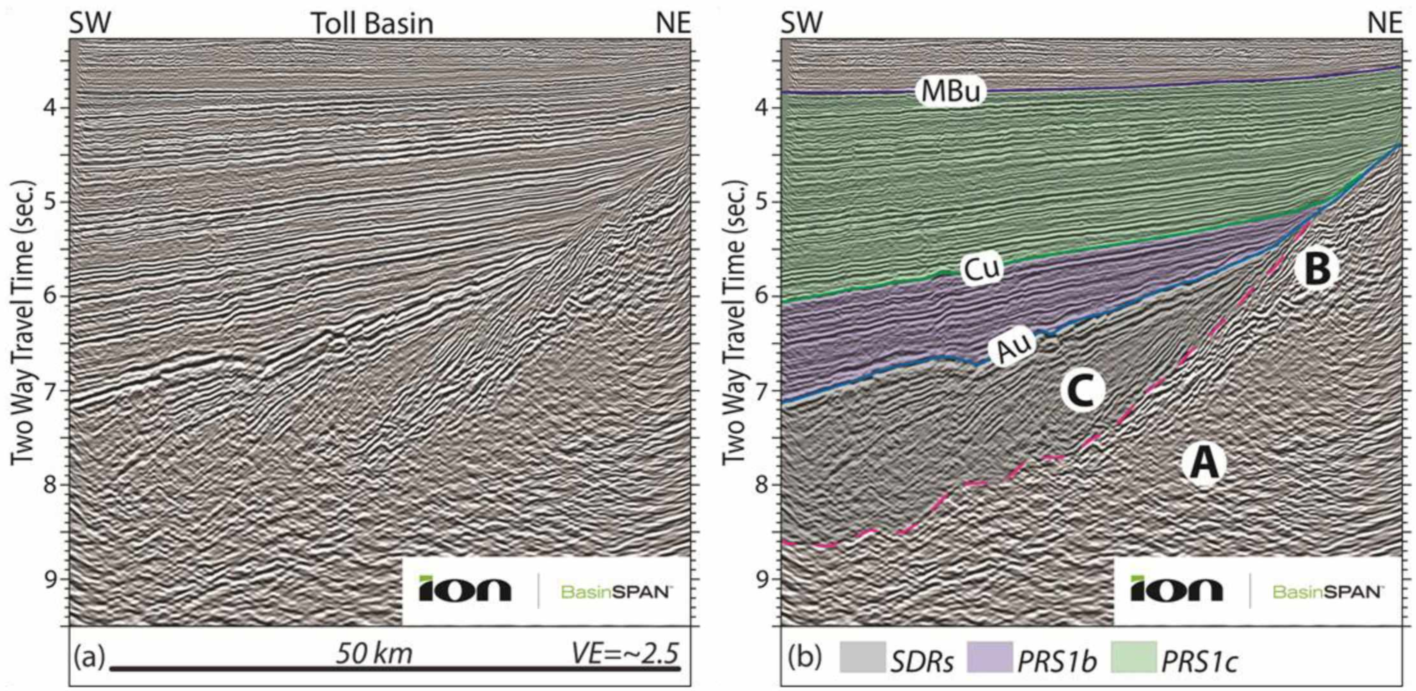

Figure 3.6 MCS profile-3
(a) Enlarged MCS section of Fig. 3.5. This section images the stratigraphy of the southwestern Chukchi Borderland between the Chukchi Plateau and Toll Basin. See Fig. 3.1b for location. **(b)** Interpreted section illustrates seaward dipping reflections (SDRs; unit C), a volcanic accrecionary sequence or stratified magmatic rocks underlying the angular unconformity (Au). Strata overlying the Au onlap the SDRs and the Chukchi Plateau. PRS, post-rift sequence. See Fig. 3.2 for sequence subdivisions and bounding unconformities.

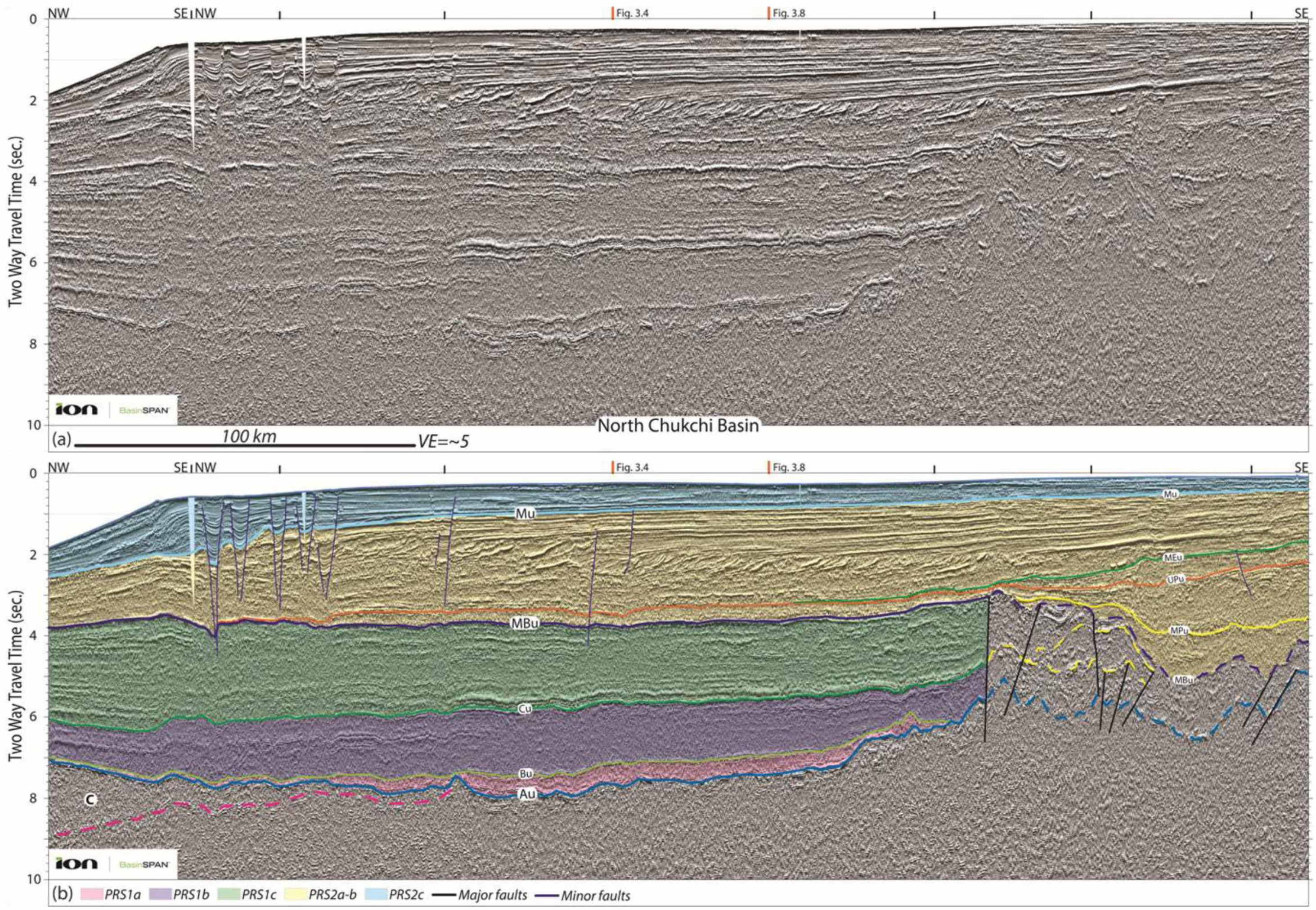

Figure 3.7 MCS profile-4

(a) MCS profile crossing the juncture between the Toll and North Chukchi Basins, the northeastern margin of the North Chukchi Basin, and the southern Northwind Ridge. See Fig. 3.1b for location. **(b)** Interpreted section illustrates Cretaceous through Cenozoic subdivision of the post-rift sequences (PRS). The wedge below the Au toward the northwest is a strike image of the SDRs seen on Fig. 3.6. Dashed lines indicate uncertainty with the interpretation. See Fig. 3.2 for sequence subdivisions and bounding unconformities.

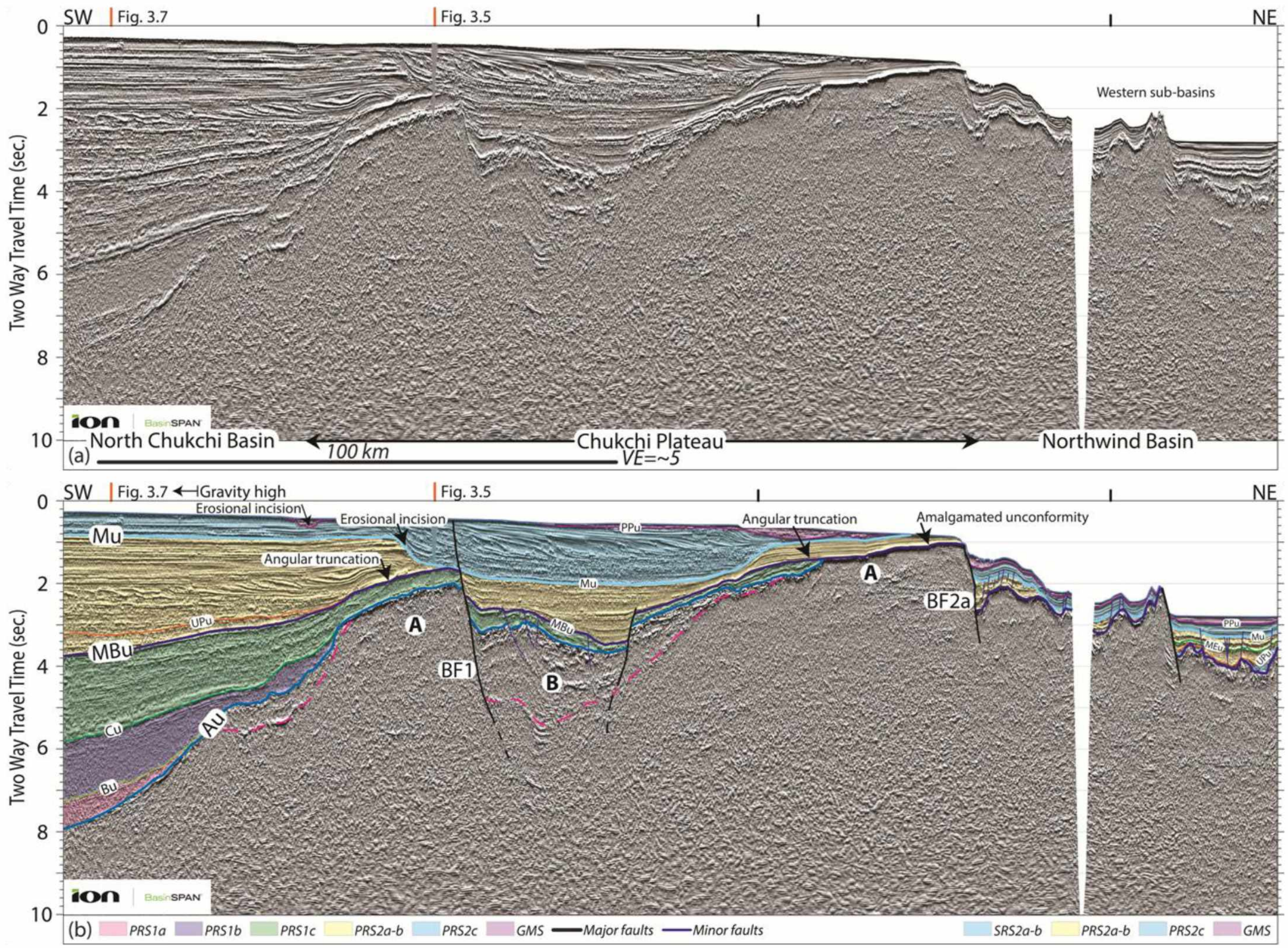

Figure 3.8 MCS profile-5

(a) MCS profile crossing the northeastern North Chukchi Basin, Chukchi Plateau and the western sub-basins of the Northwind Basin. See Fig. 3.1b for location. **(b)** Interpreted section illustrates subdivision of the stratigraphy across the basins. Note the arrow for location of gravity high outlined in Fig. 3.3a. SRS, syn-rift; PRS, post-rift; and GMS, glacio-marine sequences. See Fig. 3.2 for sequence subdivisions and bounding unconformities.

4 Northwind Ridge–Canada Basin: Structural and stratigraphic constraints for tectonic development of the Amerasia Basin, Arctic Ocean[1]

4.1 Abstract

A restorable plate-tectonic reconstruction of the Canada Basin requires matching the margins to reproduce the pre-breakup geometry. Commonly the continent-ocean boundary (COB) is used to delimit the pre-existing crust from the oceanic crust formed during basin opening, uniquely identifying the products of extension. Uncertainty about the position of the COB, plus questions about the origin of the pre-existing crust, complicate the use of this constraint to define the history of the Canada Basin. New constraints on this basin history can be derived from both the application of tectonic principles and from new multi-channel seismic reflection (MCS) data acquired in the region.

The continental blocks of the Chukchi Borderland (e.g. Chukchi Plateau and Northwind Ridge) strike north from the Chukchi Shelf forming one margin of the Canada Basin. These blocks pre-date the basin opening and must be accommodated in any reconstruction model. Understanding the history of relative motion between the Northwind Ridge and western margin of the Canada Basin is necessary to provide new constraints for the Amerasia Basin history.

A relict mid-ocean ridge (MOR) lies in the central Canada Basin, but the Canada Basin may be more complex than other ocean basins. It appears that the basin is floored in part by oceanic crust, but much of the basin may be underlain by continent-ocean transitional (COT) crust. This complicates the plate-tectonic reconstruction. There are no a priori constraints that can be applied to restore the pre-opening geometry. But other constraints can be used. The tectonic setting of

[1] Ilhan, I., Coakley, B.J., will be submitted for publication. Structure and stratigraphy of the Northwind Basin, Chukchi Borderland: Constraints on the tectonic development of the Amerasia Basin, Arctic Ocean. "Tectonophysics."

this MOR suggests that it may have formed by slow or ultra-slow seafloor spreading. The unique tectonics of slow seafloor spreading may offer additional constraints for understanding the history of this basin.

MCS reflection profiles acquired across the Northwind Ridge–Canada Basin constrain the history of relative motion through observation of the structure and stratigraphy. Besides the extension, the absence of obvious deformation between the two suggest that there has not been any relative motion since the events that formed the basin. Other critical observations of the MCS include seaward dipping (SDRs) and diapiric reflections within unit (D) of the western margin of the Canada Basin and a stratigraphic unit (C) characterized by downlap onto the underlying unit. Unit C is interpreted as a clinoform sequence, which is inferred to correlate with the Jurassic-Lower Cretaceous Kingak shale unit of the Alaska North Slope. This implies that the COT crust, supported by SDRs and parabolic reflections, which may indicate diapirs, within unit D, of the western Canada Basin occurred no later than the Middle Jurassic. This constrains models of the Amerasia Basin that require significant relative motion between the two since the Middle Jurassic.

4.2 Introduction

Chukchi Borderland, a block of extended continental crust (Grantz et al., 1998; Brumley et al., 2015; O'Brien et al., 2016) embedded in the Amerasia Basin, figures prominently in all tectonic models proposed for opening of the Amerasia Basin (Fig. 4.1a). While there are other examples of continental crust stranded within oceanic crust (e.g., Jan Mayen Ridge), the Borderland is unique in its areal extent (~200,000 km^2). Its size, position, and orientation preclude simple geometric reconstruction to any of the nearby continental shelves.

The uncertainty about origin and evolution of the Chukchi Borderland has been, in part, due to the limitations (e.g. remoteness and ice conditions) on collecting geophysical data in the Arctic

Ocean. In the last decade, this situation has changed dramatically. New data acquired by airplanes, icebreakers, and submarines has dramatically improved maps of the Arctic Ocean. These data have made it possible to formulate specific, testable hypotheses about the origin and structure of the ridges and basins that make up the Amerasia Basin. Existing data sets are, as yet, inadequate to resolve many of these questions, but provide new observations sufficient to reject some models for its development and to constrain the basin history.

The objective of this paper is to use the history of deformation of the Chukchi Borderland to constrain the evolution of the Canada Basin. The approach taken in this study is to investigate the structural and stratigraphic development of the Northwind Ridge-Canada Basin based on interpretation of 2D multi-channel seismic (MCS) reflection profiles and integration with the existing knowledge to link the history of the area to the Borderland. Our investigation uses a Meso-Cenozoic stratigraphic framework to develop a coupled model of the extensional history of the Chukchi Borderland and Canada Basin.

4.3 Background

4.3.1 Amerasia Basin

To accommodate the Chukchi Borderland in an oceanic basin requires plate boundaries along its margins (Coakley and Ilhan, 2012). Many models for the formation of the Amerasia Basin take the rotational model (Carey, 1958) as a starting point. Rotational models for the formation of the basin solve the problem of the Borderland by rotating, displacing, and/or distorting this block to make a restorable plate model of basin formation.

Carey's model (1958), which pre-dates mapping of the Borderland, proposed counter-clockwise rotation of Arctic Alaska away from the Canadian Arctic Islands around a pole in the Mackenzie Delta (Fig. 4.1a). Implications of rotational opening of the Amerasia Basin include: (1) extension along Arctic continental margins of Canada and Alaska; (2) the presence of a transform fault along the Amerasia Basin margin of Lomonosov Ridge (Cochran et al., 2006); and (3) contraction across the southern margin of the Arctic Alaska, which was accommodated by the formation of the Chukotka and Brooks Range orogens (Moore et al., 1994; Sokolov et al., 2002). This model is controversial (Lane, 1997; Embry, 2000; Doré et al., 2016), but forms the basis for most contemporary understanding of the tectonic history of the Amerasia Basin.

One of the largest uncertainties is how and where to restore the continental block of the Chukchi Borderland. Proposed reconstructions place it adjacent to the Canadian Arctic Islands, anywhere from the MacKenzie Delta margin in the Beaufort Sea, to the Sverdrup Basin along the northern Canadian coast near Ellesmere Island. Most models assume that the eastern margin of the Northwind Ridge is conjugate to some part of Arctic Canada or Alaska. Miller et al. (2006) proposed that the northern margin of the Borderland reconstructs to the Sverdrup Basin. The most recent suggestions place the northern margin of the Borderland against Stefansson Basin and adjacent to Sever Spur (O'Brien et al., 2016; Hutchinson et al., 2017).

Canada Basin is the southern part of the Amerasia Basin, surrounded by margins of the "Arctic Alaska–Chukotka microplate" (Miller et al., 2010) and Alpha–Mendeleev Ridge (Fig. 4.1a). One popular model (Grantz et al., 2011) attempts to explain the Canada Basin history with multiple phases of rotation. This begins with Jurassic counter-clockwise rotation of the microplate away from the Canadian Arctic Islands around a pole in the Mackenzie Delta, initiating the extension in the proto-Canada Basin. The counter-clockwise rotation of the microplate is supported by Halgedahl and Jarrard (1987), who documented 65–70 degrees of rotation since deposition of the Kuparuk formation on the Alaska North Slope (Fig. 4.1a). While this supports the rotational model for the formation of the basin, the age of the Kuparuk is estimated to be Early Cretaceous

(Valanginian–Hauterivian; Masterson and Eggert, 1992). Since the full rotation necessary to create the basin must post-date deposition of the Kuparuk, this constraint contradicts the Jurassic rotation of the microplate proposed by Grantz et al. (2011).

The Grantz et al. (2011) model further proposes that the counter-clockwise rotation of the Arctic Alaska–Chukotka microplate was followed by pre-Valanginian clockwise rotation of the Chukchi Borderland away from the East Siberian Shelf around a pole along the southern Northwind Ridge (Fig. 4.1a; Grantz et al., 2011). This requires substantial convergence between the Borderland and Canada Basin. Ilhan et al. (in review) infers that the Borderland was in the present-day position relative to the Chukchi Shelf since the earliest Cretaceous. The age inference is based on the stratigraphic framework of the southwestern Borderland, where probable pre-Aptian section is identified in the northeastern North Chukchi basin (e.g. PRS1a, Figs. 4, 7, 8 in Ilhan and Coakley, 2018). This unit is interpreted to be composed of condensed sediments accumulated during basin starvation similar to the composite pebble shale unit and gamma-ray zone (Hauterivian to Aptian) of the North Slope of Alaska and perhaps the Jurassic upper Kingak shale of the Chukchi Shelf (Houseknecht and Bird, 2011). This section suggests the North Chukchi basin subsided no later than the earliest Cretaceous. Observed seaward dipping reflections (SDRs) at the juncture between the North Chukchi and Toll Basins, and the Chukchi Plateau revealed the rifted margin of the southwestern Borderland. The rifting is inferred to have occurred between Middle Jurassic and earliest Cretaceous. Also, the absence of substantial shortening or east-directed thrust faults along the Northwind Ridge–Canada Basin (e.g. Fig. 5 in Ilhan and Coakley, in review and Fig. 5 in Hutchinson et al., 2017) seems to suggest that there has been no deformation along the Northwind Ridge since the formation of the Canada Basin.

According to Grantz et al. (2011), a mid-ocean ridge formed in the central Canada Basin during the Barremian. During the Barremian–

Campanian northward propagation of the MOR resulted in the formation of the Alpha–Mendeleev large igneous province (LIP; Drachev and Saunders, 2006; Fig. 4.1a). Based on P-wave velocities of 6.5–7.5 km/s obtained from seismic refraction data from the Canada Basin, about 1 km change in the basement morphology, and roughly-defined, bi-laterally symmetric magnetic anomalies indicated a change in the underlying basement of the Canada Basin (Grantz et al., 2011). This has been supported by Chian et al. (2016) who documents two types of crust, continent-ocean transitional and oceanic crust.

4.3.2 Canada Basin

The Canada Basin is composed of continental-ocean transitional (COT) and oceanic (mid-ocean ridge; MOR) crust (Grantz et al. 2011; Chian et al. 2016). This basin is surrounded by the northern margins of Alaska and Canada, and the Northwind Ridge. A relict MOR is recognized from a linear gravity low and associated bilaterally-symmetric magnetic anomalies in the central basin (Fig. 4.1a; Brozena et al., 2002). Approximately 300 km separates the outermost magnetic anomalies, which appear to define the limits of the MOR (Grantz et al., 2011; Fig. 4.1a).

A change in crustal composition is consistent with geophysical observations of the Canada Basin basement. Between the relict MOR and basin margins, there appears to be COT crust. Acoustic velocities of extended continental crust for the rifted margin of the eastern Grand Banks of Newfoundland, Canada ranged between 5 to 6.5 km/s (Van Avendonk et al., 2006). Velocities between 6.3 to 7.7 km/s were interpreted as COT crust (exhumed or serpentinized mantle). Velocities ranging between 7.8 to 8.2 km/s were interpreted as unroofed mantle with very thin incipient oceanic crust. The range of P-wave velocities observed in the Canada Basin (Chian et al., 2016) distinguish continental (5.5–6.6 km/s) and oceanic (6.7–7.6 km/s combined range for COT and MOR) is consistent with the observations of Van Avendonk et al. (2006).

The proposed relict MOR stands about 1 km above the adjacent, COT crust (Grantz et al., 2011). Gravity modeling constrains the density of the inferred COT crust to be about 2.6 g/cm^3. The region of inferred MOR was modeled as 2.85 g/cm^3 (Grantz et al., 2011). These observations and models were compared to the Newfoundland rifted margin (Grantz et al., 2011), where a broad COT has been observed. This observation supports separation of the basement of Canada basin into COT and MOR domains. The two types of crust recognized by Grantz et al. (2011) appear to have been confirmed by sonobuoy seismic refraction data (Chian et al., 2016), which distinguishes COT and MOR domains of similar extent to that inferred by Grantz et al. (2011).

The magnetic anomalies formed at the relict MOR are not distinct and do not appear to simply correlate with reversal chronologies. As a result, there are no simple or direct means to date the crustal formation. As a result, age estimates of the formation of the deeply buried MOR and COT crust must rely on indirect estimates.

Two oriented well cores from the Early Cretaceous Kuparuk Formation on the North Slope of Alaska (Fig. 4.1a) document consistent paleomagnetic pole orientations distinct from contemporaneous poles for the North American craton. The two poles can be brought into alignment by 65-70 degrees of counter-clockwise rotation of the "Arctic Alaska-Chukotka microplate" with respect to the North American craton (Halgedahl and Jarrard, 1987). The age of the Kuparuk is estimated to be Valanginian-Hauterivian (Masterson and Eggert, 1992). This rotation accounts for the complete opening of the Canada Basin as first described by Carey (1958). As a result the entire opening of the Canada basin by extension across the COT and spreading of the MOR must postdate the Kuparuk deposition.

Age constraint on the MOR comes from the magnetic anomalies of the Canada Basin (Fig. 4.1a). Grantz et al. (2011) highlighted the apparent absence of the Early-Late Cretaceous "long normal" chronozone C34N in this basin. This has been interpreted as an indication that seafloor spreading must have taken place prior to the "long normal" anomaly. Two normal magnetic anomalies (Fig. 4.1.a; M04n and M02n; Cande et al., 1989) have been interpreted to have formed during the late Hauterivian and late Barremian. Grantz et al. (2011) estimated that the MOR formed in 4 Ma (131–127 Ma). This requires that spreading rate on formation of the MOR is approximately 7.5 cm/year (300 km in 4 Ma). Given the tectonic setting of the spreading center and the proximity of its pole of opening in the MacKenzie Delta, the inferred spreading rate seems unlikely.

4.3.3 Gakkel Ridge - Canada Basin connection

This relict MOR of the Canada Basin appears to share the tectonic setting of the Gakkel Ridge (Michael et al., 2003), an ultra slow MOR. Spreading rates on this ridge range from 1.25 cm/yr near Fram Strait to 0.5 cm/yr full rate, where the ridge disappears below the Laptev Shelf (Coakley and Cochran, 1998) as it approaches its pole of opening on mainland Eurasia.

The southern terminus of the Canada Basin MOR approaches the pole of opening defined by Halgedahl and Jarrard (1987) for the Canada Basin. This ridge also disappears beneath the MacKenzie Delta. On this basis, a more likely spreading rate for formation of the relict MOR is 2 cm/yr or less. If this rate is taken into account for the duration of spreading, it would require at least 15 Ma to form 300 km (~340 km in Chian et. al., 2016) of oceanic crust in the central Canada Basin.

If the Valanginian–Hauterivian age constraint for the Kuparuk Formation (Masterson and Eggert, 1992) and post-Kuparuk rotation of Halgedahl and Jarrard (1987) are consistent with Grantz et al.'s (2011) interpretation of the Canada Basin history, there are only 5 Ma post-Kuparuk to the beginning of the "long normal" anomaly (C34; Cande et al., 1989). The absence of the "long normal" anomaly is agreed, but the length of time to form this MOR at a likely spreading rate exceeds the 5 Ma available to form the entire post-Kuparuk basin. Thus the Canada Basin MOR must have formed after the "long normal" anomaly, perhaps in the Campanian. This argument is consistent with seafloor spreading having occurred during the latter half of the Late Cretaceous.

The other possibility is that the MOR of the Canada Basin could have formed as part of the COT crust and be older than the Hauterivian. This would contradict the Halgedahl and Jarrard's (1987) constraints for the basin history. In this case, inferred age and stratigaphy of the Northwind Ridge-Canada Basin would provide new constraints on timing of the COT, and perhaps the MOR, crust of the Canada basin.

4.4 Data and methods

MCS data were acquired to image the subsurface geology of the southern Chukchi Borderland, tie the seismic data with the well from the Chukchi Shelf and constrain ages of tectonic events and sedimentary processes of this region. The ultimate goal was to indirectly test hypotheses for the formation of the Amerasia Basin. To accomplish these scientific objectives, approximately 5300 km of MCS profiles were acquired in 2011 by the *R/V Marcus G. Langseth* across the transition from the Chukchi Shelf to Borderland.

The MCS profiles were interpreted based on sequence stratigraphic principles of Vail et al. (1977). By interpreting the patterns of reflections throughout the region and integrating the other geophysical and geological constraints, structural and stratigraphic constraints have been developed for the Northwind Ridge and Canada Basin.

For the MCS data acquisition, a tuned array of ten airguns with total volume of 1830 cubic inches was used. These guns produced a simple, nearly dipole, total source signature. The spectrum of the returned signals, reflected from the subsurface interfaces, ranges between 5 and 125 Hz and falls off rapidly at both ends. The streamer included 468 hydrophones spaced 12.5 m apart recorded the returns. Each shot was recorded 10 seconds of returns with a sampling rate of 2 msec. The distance between the source and first hydrophone group was 37.5 m. The source and streamer were towed at 6 and 9 m depths, respectively. The shots were triggered every 12.5 m along the track. The resulting nominal maximum fold, the number of recorded signals that sampled, hypothetically, the same geometric location at depth, was 78.

After initial data processing at the University of Alaska, a preliminary interpretation was completed. Subsequently, the data set was reprocessed by ION Geophysical and those reprocessed MCS profiles were used for this work. Objectives of the MCS data processing were to attenuate various kinds of random, linear, and coherent noise, in particular multiples, to enhance the deeper returns, and to optimize the source signature. These objectives were accomplished by methods that include: (1) reformat SEG-D to ProMAX format and resample data from 2 to 4 ms, geometry merge, source and streamer static corrections, source system delay correction; (2) source residual bubble energy removal and zero phase application, velocity analysis (4^{th} order), source spherical spreading and absorption corrections, noise attenuation (swell noise, high amplitude noise bursts, etc.), external seismic source interference attenuation, side-scattered energy and refracted linear noise attenuation, receiver amplitude correction; and (3) multiple attenuation: SPMA (short period multiple attenuation) and SRME (surface related multiple elimination), high-resolution radon demultiple, apex-shifted demultiple (ASMA), F-X deconvolution (common offset), "Larner" noise removal (common offset), and pre-stack time migration. These methods enhanced primary signals and attenuated random, coherent, and linear noise. All of the MCS profile images shown in this paper are from pre-stack time-migrated profiles reprocessed by ION.

This data set images the boundary between the Northwind Ridge and Canada Basin providing constraints on the history of formation of the eastern margin of the Chukchi Borderland. Correlation of the interpreted reflections to the regional stratigraphic framework (Ilhan and Coakley in review and 2018) made it possible to estimate the age of sequences observed over the Northwind Ridge and develop a Cenozoic stratigraphic framework. Ages of older units have been constrained from stratigraphy observed elsewhere and from piston cores (Grantz et al. 1998) that penetrated the pelagic drape to obtain chips from the underlying indurated rock. Interpreting the details of this history has given us insight into the regional tectonic history and offers constraints on tectonic models for opening of the Amerasia Basin.

4.5 Results and discussion

The north-trending normal fault of the Northwind Ridge forms the western margin of the Canada Basin (Figs. 4.1b and 4.2). Critical to understanding this region are the ages of the strata over the Northwind Ridge and in the western margin of the Canada Basin (Figs. 4.2-4). The following sections address age constraints for these rocks, followed by descriptions and interpretations of the main seismic stratigraphic units.

4.5.1 Northwind Ridge

An MCS profile crossing the Northwind Ridge and Canada Basin contains ~3 seconds of two-way-travel (TWT) stratigraphic section (unit A, B and C; Fig. 4.2). Underlying this combined section is unit D, of uncertain age and composition. All of these units (A–D) are cut by planar normal faults, but thrust faults are confined to unit D (Figs. 4.2 and 4.3).

At the southwestern end of the seismic image in Fig. 4.2, strata shallower than 2.5 seconds (unit A) have been correlated directly to the Popcorn and Crackerjack wells (Ilhan and Coakley in review). Seismic-to-well correlations using public-domain check-shot surveys, regional stratigraphic correlations (Sherwood et al., 2002), and biostratigraphic data from the wells (Mickey et al., 2006; J. Bujak, 2018 personal comm.) indicate that the succession shallower than ~2.5 seconds is Cenozoic. This unit (A) is characterized by foreset and topset facies towards the southwestern part of the MCS profile (in between MEu and Mu markers on Fig. 4.2). The bottomset facies onlap laterally onto sides of underlying surfaces of discordance (e.g. Au and MBu on Figs. 4.2 and 4.4). In between the Crackerjack and Popcorn wells and the North Chukchi basin, lower Paleocene strata downlap onto the Mid-Brookian unconformity (MBu; Thurston and Theiss, 1987; Sherwood et al., 2002; Drachev et al., 1999, 2010; Kumar et al., 2011; Granath et al., 2015; and Nikishin et al., 2014, 2017; Ilhan and Coakley, 2018) or bottomset facies of unit A onlap the irregular surface of the angular (Au) unconformity beyond the eastern flank of the North Chukchi basin (Fig. 2 in Ilhan and Coakley, in review). These observations are characteristic of the Paleocene to Miocene upper Brookian sequence (Sherwood et al., 2002; Drachev et al., 2010; Houseknecht and Bird, 2011; Kumar et al., 2011; Hegewald and Jokat, 2013a, b; Granath et al., 2015; Nikishin et al., 2014, 2017) and across the entire Chukchi Borderland (Ilhan and Coakley, in review and 2018). A correlative surface of the middle Eocene (MEu) unconformity (Ilhan and Coakley, in review) of the Northwind basin terminates by onlap onto the western slope of the Northwind Ridge (Fig. 4.4) indicating the strata over the Northwind Ridge range from middle Eocene to present (Fig. 4.2; PRS2a-b and GMS units of Ilhan and Coakley, in review).

The section (units B, C, and D; Fig. 4.2) deeper than ~2 seconds cannot be directly tied to well control. Constraining the ages of these units relies on reflection character and similarity of stratigraphic relationships observed elsewhere in the Chukchi region. In addition to the seismic reflection observations, these units may have been sampled directly by piston coring (Fig. 1b). The cores contain chips that have been interpreted to be pieces of lithified rock underlying a sedimentary drape. Grantz et al. (1998) were able to date these chips and constrain the ages of the near surface stratigraphy along the Northwind Ridge.

Unit B is characterized by alternating high and low amplitude, parallel-continuous reflections above the Au. Unit B reaches a maximum of 0.5 seconds of thickness. This unit pinches out in all directions and is only observed in the northeastern part of the MCS grid (Fig. 4.2 and e.g. unit above the Au on Fig. 5 in Ilhan and Coakley, in review). According to Ilhan and Coakley (2018), the inferred Aptian-Albian and Upper Cretaveous sections of the lower Brookian sequence (PRS1b-c) pinch out by onlap onto the Chukchi Plateau, the northeastern flank of the North Chukchi basin. The inferred pre-Aptian condensed section (PRS1a) is restricted to the deepest part of the North Chukchi basin. These observations support that the unit B does not appear to have physical connection with the lower Brookian sequence. Piston cores collected over the Northwind Ridge are the closest constraint for the age of unit B. This may be consistent with the Upper Cretaceous unit (e.g. UK unit on Fig.4 in Grantz et al., 1998 and Fig. 4.1b for piston core locations).

Unit C contains mostly low-amplitude, transparent and moderately continuous reflections across the Northwind Ridge (Fig. 4.2). The basal reflections of this unit onlaps the underlying high-amplitude and folded reflection surface that is consistent with the unit B observed on Fig. 5 in Ilhan and Coakley (in review). The upper most reflections of this unit are discordant with the Au. This unit is about 0.7 seconds over the Northwind Ridge, pinching out to the south and north.

Unit C underlies the regional Au unconformity (Fig. 4.2). According to the stratigraphic framework of Ilhan and Coakley (2018), the Aptian–Albian strata (PRS1b) pinch out on the eastern flank of the North Chukchi basin and the underlying pre-Aptian condensed section (PRS1a) has been interpreted to be coeval with the Hauterivian pebble shale unit and perhaps the Jurassic upper Kingak shale of the Chukchi Shelf and Alaska North Slope (Sherwood et al., 2002) deposited in this basin along its eastern margin (e.g. Fig. 4 in Ilhan and Coakley, 2018). These sequences are restricted to high accommodation areas to the south, thus are presumed to be absent over the Northwind Ridge. As a result, the Au over the Northwind Ridge can be correlated to either the Hauterivian LCu or the Jurassic (Ju) unconformity, which is considered to be Mid-Jurassic on the Chukchi Shelf and Alaska North Slope (Sherwood et al., 2002). All of these suggest that the unit C is pre-Hauterivian in age. According to Grantz et al. (1998), the unit below this surface (Au; Fig. 4.2) is upper Lower Triassic and part of the upper Ellesmerian megasequence (Upper Devonian to Middle Jurassic; Sherwood et al., 2002).

The sag basin geometry and low amplitude of unit C indicate that the strata deposited in a deep marine depositional setting, mostly composed of fine-grained sedimentary rocks (Fig. 4.2). According to Grantz et al. (1998), the upper Lower Triassic, part of the upper Ellesmerian megasequence has been sampled by piston cores (Fig. 1b) beneath a prominent unconformity (e.g. Fig.4 in Grantz et al., 1998). Sherwood et al. (2002), interpret the upper Ellesmerian sequence (Permian to Middle Jurassic) as sag phase deposits. If a part of the Beaufortian megasequence (Upper Jurassic to Lower Cretaceous rift sequence of Sherwood et al., 2002; or Kingak shale unit of Houseknecht and Bird, 2004) is absent and the Au correlates to the Ju over the Northwind Ridge (Fig. 4.2), the youngest strata that can be correlated to unit C is the lower Kingak shale (Lower to Middle Jurassic) of the Chukchi Shelf and Alaska North Slope (Sherwood et al., 2002).

Unit D is characterized by folding, north-, east- and west-directed thrust faults (Figs. 4.2 and 4.4), and capped by a high-amplitude reflection surface (Fig. 4.2). This high-amplitude reflector is consistent across the Northwind Ridge, Canada Basin and, in part, across the Northwind Basin (Figs. 4.2-4). Reflections within unit D are terminated by the Au (Figs. 4.2 and 4.4). Unit D contains 3-4 seconds of deformed rocks, which taper to 1.5 seconds on both sides of the Northwind Ridge (Fig. 4.4).

There are two possibilities for unit D, it is either part of the Ellesmerian (Upper Devonian–Middle Jurassic; Grantz et al., 1994;

Sherwood et al., 2002) or the Franklinian (Proterozoic–Upper Devonian; Sherwood et al., 2002; Kumar et al., 2011) megasequence. The high-amplitude contrast is consistent with a substantial change in lithology, suggesting that the underlying section could be crystalline or carbonate rocks. The absence of a significant magnetic anomaly may rule out igneous, volcanic or intrusive rocks. The low amplitude, inferred lower Kingak shale (unit C) could account for the high-amplitude contrast with a carbonate unit of either the Ellesmerian or Franklinian megasequence (Fig. 4.2). The separating surface, a prominent unconformity, between unit C and D can be correlated to the Permian (Pu) unconformity (Sherwood et al., 2002).

A high-amplitude reflection surface is observed from MCS data at Crackerjack, which displays growth strata (e.g. Fig. 9 in Ilhan and Coakley, in review; Fig. 3a in Craddock and Houseknecht, 2016). This unit correlates to the lower Ellesmerian sequence at Crackerjack well (Sherwood et al., 2002). At that location, the lower Ellesmerian sequence is offset by planar normal faults. Fig. 3.4 shows planar normal faults that are restricted to one half of the Northwind Ridge (west of the unit A and D color bar) and offset the rocks within unit D without apparent stratigraphic thickness changes. According to Grantz et al. (1998) the presence of pre-Triassic rocks, possible lower Ellesmerian sequence, is questionable along the eastern Northwind Ridge. This may support Northwind Ridge being composed of deformed rocks of both the Ellesemerian and Franklinian megasequences. The depositional units of the Ellesmerian megasequence are known to pinch out to the north beneath the Chukchi Shelf (Figs. 6 and 7 in Sherwood et al., 2002). Yet the carbonate platform units of the Ellesmerian megasequence may lie beneath the Northwind Basin.

The pre-Missssissipian rocks underlying the Ellesmerian megasequence are characterized by east-directed thrust faults on the Arctic Platform (e.g. Fig. 4 in Kumar et al., 2011) and north-directed thrust faults along the Alaska margin of the Canada Basin (e.g. Fig. 3a in Craddock and Houseknecht, 2016). These faults are restricted to the Franklinian megasequence (Proterozoic–Upper Devonian). This megasequence was deformed during the Ellesmerian orogeny (Early to Middle Devonian). As a result the eastern part of the Northwind Ridge could be composed of Franklinian rocks that lie along a N-S trend, including the Arctic Platform and North Chukchi High (Fig. 4.1b). Although the east-directed thrust faults of Kumar et al. (2011) appear to be consistent with the east-directed thrust faults of the Northwind Basin (Fig. 4.4), the intra-Franklinian reflectors of the Arctic Platform (Sherwood 1994 and Kumar et al., 2011) are absent beneath the Au across the Northwind Basin (Fig. 4.4 and e.g. unit A on Figs. 3-5 in Ilhan and Coakley, in review). This reasoning implies that the western part of the Northwind Ridge (unit D west of black and yellow color bar on Fig. 4.2) could be composed of the carbonate platform sequence of the Ellesmerian megasequence, which may have deformed during another phase of contractional deformation. The distinction between the possible Ellesmerian and Franklinian megasequences is pending further investigation of the sub-Au rocks across the Chukchi Borderland.

Within unit D, three sub-units have been observed on the eastern Northwind Ridge beneath the Au (Fig. 4.4). D1 is characterized by eastward inclined and flat-lying reflections that are topped with relatively high-amplitude continuous reflections. The dipping reflections terminate by downlap onto the underlying unit (D2). Unit D2 is composed of low-amplitude transparent and high-amplitude continuous reflections from bottom to top. This unit can be characterized as growth strata, pinching out to the west (Fig. 4.4). An identical unit lies beneath the Au in the eastern half-graben of the Northwind Basin (e.g. unit B on Fig. 7 in Ilhan and Coakley, in review), where a transparent seismic unit is capped by very high-amplitude reflections. Unit D3 has a tabular geometry, relatively, and is also capped by distinctively high-amplitude reflections. Both unit D2 and D3 are folded.

Based on stratigraphic position and observations described above, the inclined and flat-lying reflections of unit D1 are interpreted as foreset and topset facies, indicating a clinoform-clastic sequence. This implies a shallow marine depositional environment. Within the Franklinian megasequence, which lies directly below the LCu, a clinoformal clastic unit is identified from MCS data in the northeast Chukchi basin, northwest of the Arctic Platform (e.g. Fig. 3 in Sherwood, 1994). The growth strata within unit D2 are interpreted as foreland deposits, deformed by contractional deformation, prior to development of the Au in the Northwind Basin (Ilhan and Coakley, in review). The tabular geometry of unit D3 is identical to the unit between the high-amplitude intra-Franklinian reflectors of D and F (e.g. Fig. 8 in Kumar et al., 2011). This unit (D3) is interpreted to be carbonate platform sequence (e.g. Fig. 3 in Sherwood, 1994). All of the above observations and interpretations imply that the rocks of the Franklinian megasequence, in part, lie beneath the Northwind Ridge and Northwind Basin.

4.5.2 Canada Basin

Stratigraphic section (units A, B and C) in the Canada Basin is about 3 seconds (Fig. 4.3). This section is defined by a high-amplitude reflection surface below well-stratified sediments. According to Grantz et al. (2011) age correlation from the McKenzie Delta, unit A is Cenozoic (e.g. Fig. 4 in Grantz et al., 1998) and onlaps the 65 Ma surface towards the Northwind Ridge at about 6 seconds (e.g. Profile A in Grantz et al., 2011). Unit B, equivalent to combined unit B-1 (Upper Cretaceous) and B-2 (Hauterivian–Albian) of Grantz et al. (1998), cannot be directly correlated to any wells along the margins of the Canada basin.

Unit A is characterized by parallel-continuous, alternating high-and-low amplitude reflections that onlap unit B (Figs. 4.2 and 4.3). This unit contains 1 second of strata along the western margin of the Canada Basin, thickening northward towards the central Canada Basin. Unit A is separated from the underlying unit (B) along a well-developed onlap surface. Unit B is characterized by parallel-continuous, alternating high-and-low amplitude reflections that onlap unit C (Figs. 4.2 and 4.3). Unit B contains 0.5 seconds of strata along the Northwind margin of the Canada Basin, pinching out towards the west and south onto lower slope of the Northwind Ridge (Figs. 4.2, 4.3 and 4.4).

The Aptian–Albian, lower Brookian strata were restricted to the south of the northern margin of Beaufort rift shoulder of the Canada Basin (Houseknecht et al., 2009). This unit also pinches out by onlap onto the Chukchi Plateau along the northeastern flank of the North Chukchi Basin (PRS1b; Ilhan and Coakley, 2018). But the upper Cretaceous strata stepped into the Canada Basin (Houseknecht and Bird, 2011). Strata within unit A and B are interpreted to be mostly coeval with the Aptian(?) through Upper Cretaceous (lower Brookian) and Paleocene-Miocene (upper Brookian) strata, which form a clinothem on the Chukchi Shelf and Alaska North Slope (Sherwood et al., 2002; Houseknecht et al., 2009). Seismic data show that the foreset and topset facies of the clinothem (e.g. clinoform orientations on Fig. 1 in Houseknecht et al., 2009) grade into exclusively bottomset facies along the western flank of the Canada Basin. Therefore, these units are interpreted in the study area to comprise exclusively deep water facies, likely including mudstone and sandstone deposited in basin-floor fan and related environments. The onlap pinchout of these units indicates these deep water deposits were banked against the flanks of the Northwind Ridge as well as the intra-basin highs of the Northwind Basin (Fig. 4.4), consistent with the sediment dispersion patterns (Fig. 3.1b; Houseknecht and Bird, 2011) and depositional history of the southwestern Chukchi Borderland (Ilhan and Coakley, 2018 and in review). Sediment thickness decreases from McKenzie Delta northward and westward into the central Canada Basin and Northwind Ridge by about fifty percent (8 seconds on Fig. 2 to 4 seconds on Fig. 7 in Mosher et al., 2012) consistent with south and westward pinch out of unit B (Figs. 4.2-4).

Unit C is characterized by subparallel and semi-continuous reflections (Figs. 4.2 and 4.3). This unit reaches maximum of a 1.4 seconds along the western margin of the Canada Basin. Three sub-units recognized in unit C: C1, high-amplitude, sub-parallel and semi-continuous reflections; C2, low-amplitude, sub-parallel and discontinuous reflections; and C3, alternating high and low amplitude, moderately continuous and parallel reflections. The sub-parallel reflections within subunit C1 and C2 terminate by downlap onto underlying high-amplitude reflections that cap unit D (Fig. 4.3). Besides the capping high-amplitude reflections, unit D shows two seismic reflection facies. These are high-amplitude northward-dipping and diapiric (concave down/dome-shaped) reflections (Fig. 4.3), which appear to be distinct from unit D of the Northwind Ridge (Fig. 4.2).

Based on stratigraphic position and inferred Aptian age of the overlying unit (B), unit C is inferred to be pre-Aptian in age. Considering that the lower Cretaceous (Hauterivian) strata are either restricted to the central grabens of Canada Basin (Mosher et al., 2012) or absent and/or beyond the imaging of the seismic resolution at the western margin of the Canada Basin, unit C may be pre-Hauterivian in age. This interpretation is consistent with poorly imaged unit C of Grantz et al. (1998). If true, the onlap surface between unit B and C may be correlated to the Hauterivian (LCu) unconformity. The sub-parallel reflections of unit C1 and C2 are interpreted as foreset facies, whereas the parallel, flat-lying, reflections of C3 are interpreted as topset facies. These sub-units define a clinoform sequence, indicating a change from shallow marine to deep marine depositional setting. An identical sequence in the National Petroleum Reserve in Alaska has been documented beneath the Hauterivian (LCu) unconformity (e.g. K1-3 on Fig. 4 in Houseknecht and Bird, 2004). Considering the stratigraphic position of unit C and depositional contrasts (e.g. basinward downlap of unit C and landward onlap of unit B onto a surface of discordance), this unit (C) is interpreted to correlate to the equivalent of the Kingak shale unit (Upper Jurassic to Lower Cretaceous) of the Beaufortian megasequence (Houseknecht and

Bird, 2004). This interpretation implies that the Northwind Ridge was a passive margin since deposition of unit C, suggesting the continent-ocean transitional crust of the Canada Basin may have formed no later than the Middle Jurassic. If the MOR of the Canada Basin was part of this extension, this interpretation contradicts the age constraints of Halgedahl and Jarrard (1987) and suggests that either the age of the Kuparuk is incorrect or that the paleomagnetic results are somehow suspect.

The anomalous, high-amplitude reflections of unit D can be explained by the existence of a carbonate platform sequence either part of the Ellesmerian or Franklinian megasequence underlying the low-amplitude unit C (Fig. 4.3). Unit D of the western Canada Basin does not appear to be folded as unit D of the Northwind Ridge (Fig. 4.2). The northward-dipping reflections within unit D can be interpreted as an accretionary sequence of volcanic rocks known as seaward dipping reflections (SDR; Mutter, 1985; Pindell et al., 2014; Paton et al., 2017). The diapiric reflections can be interpreted as intrusive rocks, similar to the diapiric reflection observed within the crust beneath the western margin of the Canada Basin (e.g., Profile E and Fig. 50.12 in Grantz et al., 2011). These interpretations reveal an extended continental crust of the western margin of the Canada Basin and are consistent with previous investigations (Grantz et al., 2011; Chian et al., 2016).

4.6 Conclusions

Structural and stratigraphic observations from MCS data constrain the geologic history of the Chukchi Borderland and tectonic models proposed for the Amerasia Basin, Arctic Ocean.

The Aptian-Albian and Upper Cretaceous sections of the lower Brookian sequence pinch out by onlap onto the Chukchi Plateau, the northeastern flank of the North Chukchi Basin. The inferred pre-Aptian condensed section is restricted to the deepest part of the North Chukchi Basin (Ilhan and Coakley, 2018). Thus these sections are presumed to be absent (or very thin) over the Northwind Ridge. Based on this reasoning, the angular (Au) unconformity observed over the Northwind Ridge can be correlated to the Middle Jurassic (Ju) unconformity. Based on this reasoning, the Au separates the stratigraphic section into Cretaceous through Cenozoic (units A and B) and pre-Cretaceous (units C and D).

Unit A is inferred to include the Eocene to present section of the upper Brookian clinothem and glacio-marine sediments (Fig. 4.2). The basal strata onlap the middle Brookian unconformity (MBu), consistent with Ilhan and Coakley (in review).

Unit B is only observed at the northern limit of the MCS grid on the Northwind Ridge (Fig. 4.2; Fig. 5 in Ilhan and Coakley, in review). This unit (B) pinches out in all directions and is not continuous with or connected to the Upper Cretaceous section of the lower Brookian sequence. Based on piston cores collected along the Northwind Ridge (Grantz et al., 1998), it is constrained to include Upper Cretaceous stata.

Internal stratal relations and the structure of unit C (Fig. 4.2) are consistent with the sag phase deposits of the Triassic to Lower Jurassic upper Ellesmerian sequence (lower Kingak shale unit(?); Sherwood et al., 2002) and piston cores collected along the Northwind Ridge (Grantz et al., 1998).

Unit D is composed of three sub-sections (D1-3) over the Northwind Ridge (Fig. 4.4 and unit B on Fig. 7 in Ilhan and Coakley, in review) that are consistent with the sub-Mississippian rocks of the Franklinian megasequence (Sherwood, 1994) that were deformed during the Ellesmerian orogeny (Early to Middle Devonian). Yet, the absence of stratification within unit D beneath the Northwind Basin (Fig. 4.4) similar to those of Kumar et al. (2011) observed in the Arctic Platform (e.g. intra-Franklinian reflectors) implies the sub-Au rocks of the Northwind Basin may include the Mississippian lower Ellesmerian sequence. Thus the east and west directed thrust faults of the

Northwind Basin and western part of the Northwind Ridge (Fig. 4.4) could have formed by another phase of contraction.

Based on regional sediment dispersion patterns of Cretaceous through Cenozoic sediments of the Alaska margin of the Canada Basin (Houseknecht and Bird, 2011), combined unit A and B that onlap onto a well-developed unconformity and the lower slope of the Northwind Ridge (Figs. 4.2 and 4.3) are inferred to be distal facies of the lower Brookian clinothems. These strata are likely to include mudstone and sandstone deposited in basin-floor fan and related environments. The unconformity underlying this unit is inferred to be the Hauterivian (LCu).

Unit C is interpreted to be a passive-margin clinoform sequence (Fig. 4.3) similar to the one observed in the National Petroleum Reserve in Alaska (e.g. K1-3 on Fig. 4 in Houseknecht and Bird, 2004), documented beneath the Hauterivian (LCu) unconformity. Considering the stratigraphic position of unit C and depositional contrasts (e.g. basinward downlap of unit C and landward onlap of unit B onto a surface of discordance), we believe that this unit (C) correlates to the equivalent of the Kingak shale unit (Upper Jurassic to Lower Cretaceous) of the Beaufortian megasequence. This interpretation implies that the Northwind Ridge was a passive margin since deposition of unit C.

The anomalous, high-amplitude reflections of unit D can be explained by the existence of a carbonate platform sequence either part of the Ellesmerian or Franklinian megasequence underlying the low-amplitude unit C (Fig. 4.3). The northward-dipping reflections within unit D can be interpreted as an accretionary sequence of volcanic rocks known as seaward dipping reflections (SDRs; Mutter, 1985; Pindell et al., 2014; Paton et al., 2017). The diapiric reflections can be interpreted as intrusive rocks, similar to the diapiric reflection observed within the crust beneath the western margin of the Canada Basin (e.g., Profile E and Fig. 50.12 in Grantz et al., 2011). These interpretations reveal an extended continental crust of the western margin of the Canada Basin and are consistent with previous investigations (Grantz et al., 2011; Chian et al., 2016). The inferred age of the overlying unit C implies that the continent-ocean transition crust of the Canada Basin may have formed no later than the Middle Jurassic.

All tectonic models make predictions about the connection between the Chukchi Borderland, the Chukchi Shelf basins and the Canada Basin. The predictions of existing models for formation of the Canada Basin have been constrained. The inferred Uppper Jurassic-Lower Cretaceous passive-margin clinoform sequence (unit C) along the western margin of the Canada Basin, continuity of the Cretaceous sediments along the margins of the Chukchi Borderland, and the absence of east-directed thrust faults along the Northwind Ridge-Canada Basin margin invalidate most of these models that require significant relative motion between the Chukchi Shelf basins, Chukchi Borderland and Canada Basin, in particular, the model of Grantz et al. (2011). Following up on these observations, a new set of constraints for the opening of the Canada Basin has been developed, arguing both from the history constrained by the MCS data and from geologic processes observed in analogous settings.

The tectonic setting of the apparent extinct MOR that bisects the basin argues that it was likely formed by ultra-slow seafloor spreading, analogous to the presently active Gakkel Ridge. Given the time required to explain the amount of seafloor delimited by paired magnetic anomalies, accepting the constraint imposed by the Halgedahl and Jarrard (1987) estimates of the rotational opening of the basin and the apparent absence of the Cretaceous long normal interval in the magnetic anomalies (Grantz et al., 2011) seafloor spreading would be younger than currently conceived, occurring no earlier than the Cenomanian.

The other possibility is that the MOR may have formed during development of the COT crust of the Canada Basin as single event and is likely to be much older than the Hauterivian. Considering the observations presented here and rejecting the constraints of Halgedahl and Jarrard (1987), the COT crust of the Canada Basin should have formed no later than the Middle Jurassic. The absence of observable significant deformation along the western margin of the Canada Basin constrains the opening of the Canada Basin.

In strategic locations, direct sampling, seismic imaging and analysis of the sub-Au rocks of the Chukchi Borderland would constrain the deformation history. This investigation, if well-planned, would provide a set of new constraints for the development of the Amerasia Basin, Arctic Ocean.

4.7 References

Brozena, J., Lawver, L., Kovacs, L., Childers, V., 2002. Aerogeophysical evidence for the rotational opening of the Canada Basin. AAPG Bull 86, 1138.

Brumley, K., Miller, E.L., Konstantinou, A., Grove, M., Meisling, K.E., Mayer, L.A., 2015. First bedrock samples dredged from submarine outcrops in the Chukchi Borderland, Arctic Ocean. Geosphere 11, 76-92, doi:10.1130/GES01044.1.

Cande, S. C., LaBreque, J.L., et al., compilers. 1989. Magnetic Lineations of the World's Ocean Basins. American Association of Petroleum Geologists, DD0023, Tulsa, OK.

Carey, S., 1958. WA tectonic approach to continental drift, in continental drift: a symposium. Australia: University of Tasmania.

Coakley, B.J., Cochran, J.R., 1998. Gravity evidence of very thin crust at the Gakkel Ridge (Arctic Ocean). Earth and Planetary Science Letters 162, 81-95.

Chian, D., Jackson, H.R., Hutchinson, D.R., Shimeld, J.W., Oakey, G.N., Lebedeva-Ivanova, N., Li, Q., Saltus, R.W., Mosher, D.C., 2016. Distribution of crustal types in Canada Basin, Arctic Ocean. Tectonophysics 691, 8-30, http://dx.doi.org/10.1016/j.tecto.2016.01.038.

Cochran, J.R., Edwards, M.H., Coakley, B.J., 2006. Morphology and structure of the Lomonosov Ridge, Arctic Ocean. Geochemistry, Geophysics, Geosystems 7, doi:10.1029/2005GC001114.

Craddock, W.H., Houseknecht, D.W., 2016. Cretaceous–Cenozoic burial and exhumation history of the Chukchi shelf, offshore Arctic Alaska. AAPG Bulletin 100, 63-100, doi:10.1306/09291515010.

Doré, A.G., Lundin, E.R., Gibbons, A., Sømme, T.O., Tørudbakken, B.O., 2016. Transform margins of the Arctic: a synthesis and re-evaluation. Geological Society, London, Special Publications 431, 63-94, http://doi.org/10.1144/SP431.8.

Drachev, S.S., Malyshev, N.A., Nikishin, A.M., 2010. Tectonic history and petroleum geology of the Russian Arctic Shelves: an overview, Geological society, London, petroleum geology conference series. Geological Society of London, pp. 591-619, doi:10.1144/0070591.

Drachev, S., Saunders, A., 2006. The Early Cretaceous Arctic LIP: its geodynamic setting and implications for Canada Basin opening, Proc. Fourth Int. Conf. on Arctic Margins, Dartmouth, Nova Scotia, pp. 216-223.

Drachev, S., Johnson, G., Laxon, S., McAdoo, D., Kassens, H., 1999. Main structural elements of Eastern Russian Arctic continental margin derived from satellite gravity and multichannel seismic reflection data, Land-Ocean Systems in the Siberian Arctic. Springer, pp. 667-682.

Embry, A., 2000. Counterclockwise rotation of the Arctic Alaska Plate: best available model or untenable hypothesis for the opening of the Amerasia Basin. Polarforschung 68, 247-255.

Granath, J.W., McDonough, K.-J., Sterne, E.J., Horn, B.W., 2015. Contrasting extensional basin styles and sedimentary fill across the eastern Russian Arctic shelf as imaged in crustal-scale PSDM reflection data. American Association of Petroleum Geologists Datapages, Search and Discovery Article 10811.

Grantz, A., Hart, P.E., Childers, V.A., 2011. Geology and tectonic development of the Amerasia and Canada Basins, Arctic Ocean, in Spencer, A.M., Embry, A.F., Gautier, D.L., Stoupakova, A.V., Sørensen, K. (Eds.), Arctic Petroleum Geology: Geological Society, London, Memoirs 35, 771-799, doi:10.1144/M35.50.

Grantz, A., Clark, D.L., Phillips, R.L., Srivastava, S.P., Blome, C.D., Gray, L.B., Haga, H., Mamet, B.L., McIntyre, D.J., McNeil, D.H., Mickey, M.B., Mullen, M.W., Murchey, B.I., Ross, C.A., Stevens, C.H., Silberling, N.J., Wall, J.H., Willard, D.A., 1998. Phanerozoic stratigraphy of Northwind Ridge, magnetic anomalies in the Canada basin, and the geometry and timing of rifting in the Amerasia basin, Arctic Ocean. Geological Society of America Bulletin 110, 801-820.

Grantz, A., May, S.D., Hart, P.E., 1994. Geology of the Arctic continental margin of Alaska, in Plafker, G., Berg, H.C. (Eds.), The Geology of North America, The Geology of Alaska. Geological Society of America G-1, 17-48.

Halgedahl, S., Jarrard, R., 1987. Paleomagnetism of the Kuparuk River Formation from oriented drill core: Evidence for rotation of the Arctic Alaska plate, in Tailleur, I., Weimer, P. (Eds.), Alaskan North Slope Geology, Pacific Section, Society for Sedimentary Geology, Santa Barbara, CA, 581-617.

Hegewald, A., Jokat, W., 2013a. Tectonic and sedimentary structures in the northern Chukchi region, Arctic Ocean. Journal of Geophysical Research: Solid Earth 118, 3285-3296.

Hegewald, A., Jokat, W., 2013b. Relative sea level variations in the Chukchi region - Arctic Ocean - since the late Eocene. Geophysical Research Letters 40, 803-807.

Houseknecht, D.W., Bird, K.J., 2011. Geology and petroleum potential of the rifted margins of the Canada Basin, in Spencer, A.M., Embry, A.F., Gautier, D.L., Stoupakova, A.V., Sørensen, K. (Eds.), Arctic Petroleum Geology: Geological Society, London, Memoirs 35, 509-526, doi:10.1111/j.1365-2117.2008.00392.x.

Houseknecht, D.W., Bird, K.J., Schenk, C.J., 2009. Seismic analysis of clinoform depositional sequences and shelf-margin trajectories in Lower Cretaceous (Albian) strata, Alaska North Slope. Basin Research 21, 644-654.

Houseknecht, D.W., Bird, K.J., 2004. Sequence stratigraphy of the Kingak Shale (Jurassic–Lower Cretaceous), National Petroleum Reserve in Alaska. AAPG bulletin 88, 279-302.

Hutchinson, D.R., Jackson, H.R., Houseknecht, D.W., Li, Q., Shimeld, J.W., Mosher, D.C., Chian, D., Saltus, R.W., Oakey, G.N., 2017. Significance of Northeast-Trending Features in Canada Basin, Arctic Ocean. Geochemistry, Geophysics, Geosystems 18, 4156-4178, http://doi.org/10.1002/2017GC007099.

Ilhan, I., Coakley, B.J., 2018. Meso–Cenozoic evolution of the southwestern Chukchi Borderland, Arctic Ocean. Marine and Petroleum Geology 95, 100-109, https://doi.org/10.1016/j.marpetgeo.2018.04.014.

Ilhan, I., Coakley, B.J., in review. Structure and stratigraphy of the Northwind Basin, Chukchi Borderland: constraints on the tectonic development of the Amerasia Basin, Arctic Ocean. AAPG Bulletin.

Jakobsson, M., Mayer, L., Coakley, B., Dowdeswell, J.A., Forbes, S., Fridman, B., Hodnesdal, H., Noormets, R., Pedersen, R., Rebesco, M., Schenke, H.W., Zarayskaya, Y., Accettella, D., Armstrong, A., Anderson, R.M., Bienhoff, P., Camerlenghi, A., Church, I., Edwards, M., Gardner, J.V., Hall, J.K., Hell, B., Hestvik, O., Kristoffersen, Y., Marcussen, C., Mohammad, R., Mosher, D., Nghiem, S.V., Pedrosa, M.T., Travaglini, P.G., Weatherall, P., 2012. The International Bathymetric Chart of the Arctic Ocean (IBCAO) Version 3.0. Geophysical Research Letters 39, L12609, doi:10.1029/2012GL052219.

Kumar, N., Granath, J.W., Emmet, P.A., Helwig, J.A., Dinkelman, M.G., 2011. Stratigraphic and tectonic framework of the US Chukchi Shelf: exploration insights from a new regional deep-seismic reflection survey, in Spencer, A.M., Embry, A.F., Gautier, D.L., Stoupakova, A.V., Sørensen, K. (Eds.), Arctic Petroleum Geology: Geological Society, London, Memoirs 35, 501-508, doi:10.1144/M35.33.

Lane, L.S., 1997. Canada Basin, Arctic Ocean: evidence against a rotational origin. Tectonics 16, 363-387.

Masterson, W., Eggert, J., 1992. Kuparuk River Field--USA North Slope, Alaska. AAPG Special Volumes, A025, 257-284.

Michael, P., Langmuir, C., Dick, H., Snow, J., Goldstein, S., Graham, D., Lehnert, K., Kurras, G., Jokat, W., Mühe, R., 2003. Magmatic and amagmatic seafloor generation at the ultraslow-spreading Gakkel ridge, Arctic Ocean. Nature 423, 956.

Mickey, M.B., Haga, H., Bird, K.J., 2006. Micropaleontology of selected wells and seismic shot holes, northern Alaska: U. S. Geological Survey Open-File Report 2006-1055, CDROM, http://pubs.usgs.gov/of/2006/1055/.

Miller, E.L., Gehrels, G.E., Pease, V., Sokolov, S., 2010. Stratigraphy and U-Pb detrital zircon geochronology of Wrangel Island, Russia: Implications for Arctic paleogeography. AAPG Bulletin 94, 665-692, doi:10.1306/10200909036.

Miller, E.L., Toro, J., Gehrels, G., Amato, J.M., Prokopiev, A., Tuchkova, M.I., Akinin, V.V., Dumitru, T.A., Moore, T.E., Cecile, M.P., 2006. New insights into Arctic paleogeography and tectonics from U-Pb detrital zircon geochronology. Tectonics 25, TC3013, doi:10.1029/2005TC001830.

Moore, T.E., Wallace, W.K., Bird, K.J., Karl, S.M., Mull, C.G., Dillon, J.T., 1994. Geology of northern Alaska, in Plafker, G., Berg, H.C., (Eds.), The Geology of Alaska: Boulder, CO, Geological Society of America, Geology of North America G-1, 49-140, doi:10.1130/DNAG-GNA-G1.49.

Mosher, D.C., Shimeld, J., Hutchinson, D., Chian, D., Lebedova-Ivanova, N., Jackson, R., 2012. Canada Basin revealed, OTC Arctic Technology Conference. Offshore Technology Conference, OTC 23797.

Mutter, J.C., 1985. Seaward dipping reflectors and the continent-ocean boundary at passive continental margins. Tectonophysics 114, 117-131.

Nikishin, A.M., Petrov, E.I., Malyshev, N.A., Ershova, V.P., 2017. Rift systems of the Russian Eastern Arctic shelf and Arctic deep water basins: link between geological history and geodynamics. Geodynamics & Tectonophysics 8, 11-43.

Nikishin, A.M., Malyshev, N.A., Petrov, E.I., 2014. Geological structure and history of the Arctic Ocean. EAGE Publications, Houten, The Netherlands 88 pp.

O'Brien, T.M., Miller, E.L., Benowitz, J.P., Meisling, K.E., Dumitru, T.A., 2016. Dredge samples from the Chukchi Borderland: Implications for paleogeographic reconstruction and tectonic evolution of the Amerasia Basin of the Arctic. American Journal of Science 316, 873-924, doi: 10.2475/09.2016.03.

Paton, D.A., Pindell, J., McDermott, K., Bellingham, P., Horn, B., 2017. Evolution of seaward-dipping reflectors at the onset of oceanic crust formation at volcanic passive margins: Insights from the South Atlantic. Geology 45, 439-442, doi:10.1130/G38706.1.

Pindell, J., Graham, R., Horn, B., 2014. Rapid outer marginal collapse at the rift to drift transition of passive margin evolution, with a Gulf of Mexico case study. Basin Research 26, 701-725, doi:10.1111/bre.12059.

Sherwood, K.W., Johnson, P.P., Craig, J.D., Zerwick, S.A., Lothamer, R.T., Thurston, D.K., Hurlbert, S.B., 2002. Structure and stratigraphy of the Hanna Trough, U.S. Chukchi Shelf, Alaska, in Miller, E.L., Grantz, A., Klemperer, S.L. (Eds.), Tectonic Evolution of the Bering Shelf-Chukchi Sea-Arctic Margin and Adjacent Landmasses, Geological Society of America, Boulder, CO, Special Papers 360, 39-66.

Sherwood, K., 1994. Stratigraphy, structure, and origin of the Franklinian, northeast Chukchi basin, Arctic Alaska plate, 1992 Proceedings International Conference on Arctic Margins: US Minerals Management Service OCS Studies, pp. 94-0040.

Sokolov, S.D., Bondarenko, G.Y., Morozov, O.L., Shekhovtsov, V.A., Glotov, S.P., Ganelin, A.V., Kravchenko-Berezhnoy, I.R., 2002. South Anyui suture, northeast Arctic Russia: facts and problems, in Miller, E.L., Grantz, A., Klemperer, S.L. (Eds.), Tectonic Evolution of the Bering Shelf-Chukchi Sea-Arctic Margin and Adjacent Landmasses, Geological Society of America, Boulder, CO, Special Papers 360, 209-224.

Thurston, D., Theiss, L., 1987. Geologic Report for the Chukchi Sea Planning Area, Alaska-Regional Geology. Petroleum Geology, and Environmental Geology: Minerals Management Service, Alaska OCS Region, OCS Report, MMS, 87-0046, 193 p.

Vail, P. R., Mitchum, R. M., Thompson, S., III, 1977. Seismic stratigraphy and global changes of sea level, Part 3: Relative changes of sea level from coastal onlap, Application of seismic reflection configuration to stratigrapic interpretation: AAPG Memoir 26, 63-81.

Van Avendonk, H.J.A., Holbrook, W.S., Nunes, G.T., Shillington, D.J., Tucholke, B.E., Louden, K.E., Larsen, H.C., Hopper, J.R., 2006. Seismic velocity structure of the rifted margin of the eastern Grand Banks of Newfoundland, Canada. Journal of Geophysical Research: Solid Earth 111, B11404, doi:10.1029/2005JB004156.

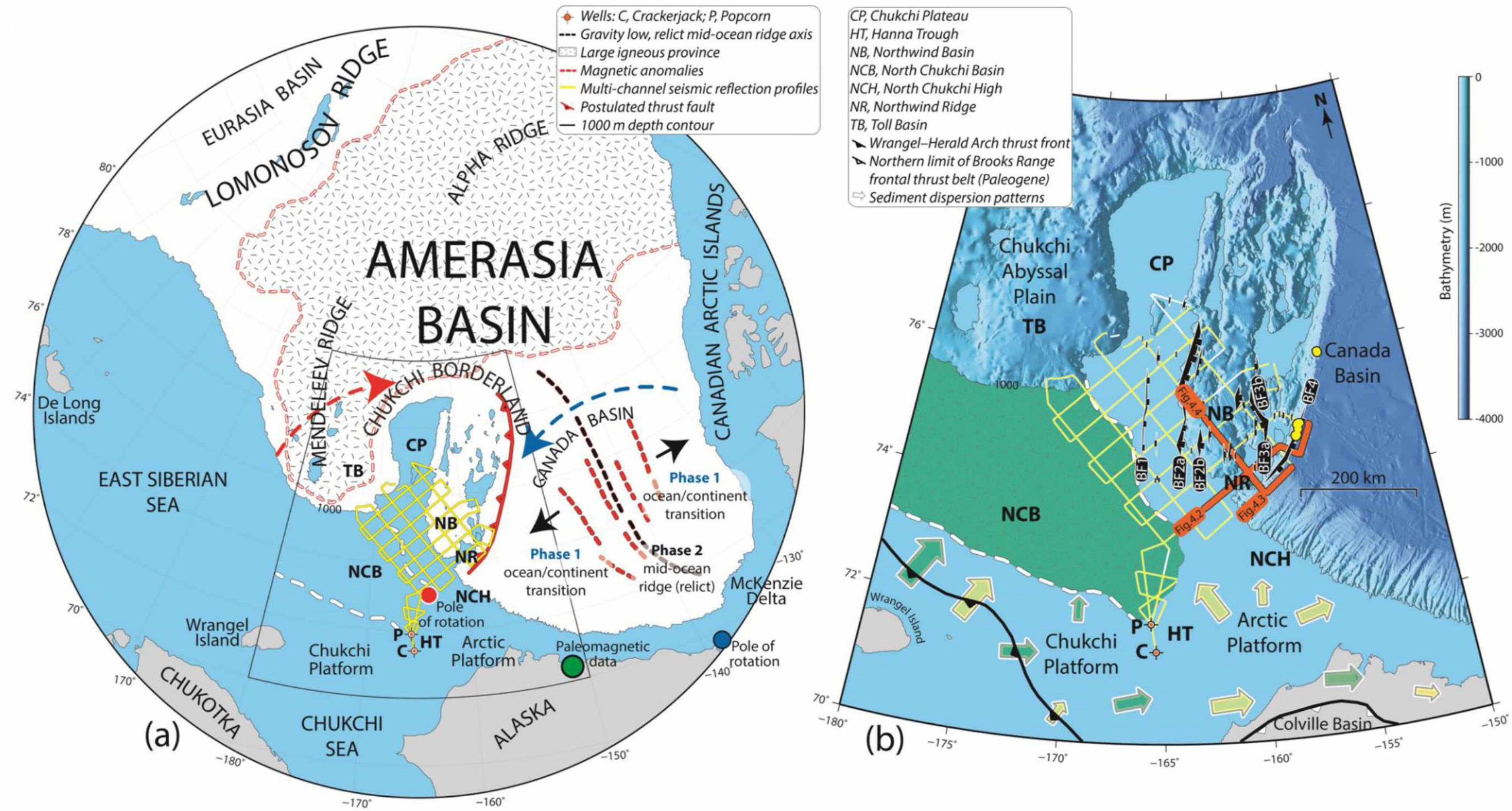

Figure 4.1 Overview of the study area
(a) Physiographic and tectonic elements of the Amerasia Basin, Arctic Ocean (modified from Grantz et al., 2011). The 1000m contour (basinward boundary of blue; Jakobsson et al., 2012) approximates the present-day shelf edge and is a proxy for northern boundary of the Arctic Alaska-Chukotka microplate (Miller et al., 2010), the Arctic Canada and Lomonosov Ridge. Blue and red arrows track proposed counter-clockwise and clockwise rotations of the microplate away from the Canadian Arctic Islands around a pole in the McKenzie Delta, and of the Chukchi Borderland away from the East

Figure 4.1 cont.
Siberian Shelf around a pole south of the Northwind Ridge (Grantz et al., 2011). The green circle indicates the location of paleomagnetic data from the Kuparuk Formation (Valanginian–Hauterivian). Black arrows, first phase extensional deformation of the proto-Canada Basin (Grantz et al., 2011); red thrust fault, postulated compressional deformation along the Northwind Ridge required by the proposed clockwise rotation of the Borderland (Grantz et al., 2011); black and red dashed lines, gravity and magnetic anomalies (Brozena et al., 2002) indicating the second phase deformation "relict mid-ocean ridge" in the central Canada Basin; filled pattern indicates the large igneous province (Drachev and Saunders, 2006) which includes the Mendeleev and Alpha Ridges. Yellow lines indicate 2011 tracks of *R/V Marcus Langseth*, multi-channel seismic (MCS) reflection profiles that were acquired and interpreted for this study. Also shown are the Crackerjack (C) and Popcorn (P) exploration wells (Sherwood et al., 2002). CP, Chukchi Plateau; NB, Northwind Basin; NR, Northwind Ridge; NCH, North Chukchi High; HT, Hanna Trough; NCB, North Chukchi Basin; TB, Toll Basin. **(b)** Bathymetry of the deepwater areas northwest of Alaska (Jakobsson et al., 2012). The 1000m depth contour outlines the Chukchi Borderland and adjacent major basins, highs and pertinent structural elements of the study area. Also shown are piston core locations (yellow circles; Grantz et al., 1998), normal faults (Ilhan and Coakley, in review), contractional deformation fronts to the south (Drachev et al., 2010), and Cretaceous (green arrows) and Cenozoic (yellow arrows) sediment dispersion patterns flanking the Chukotka-Brooks Range (Houseknecht and Bird, 2011). Yellow lines, MCS profiles from ION Geophysical; bold orange lines, figures shown in this chapter.

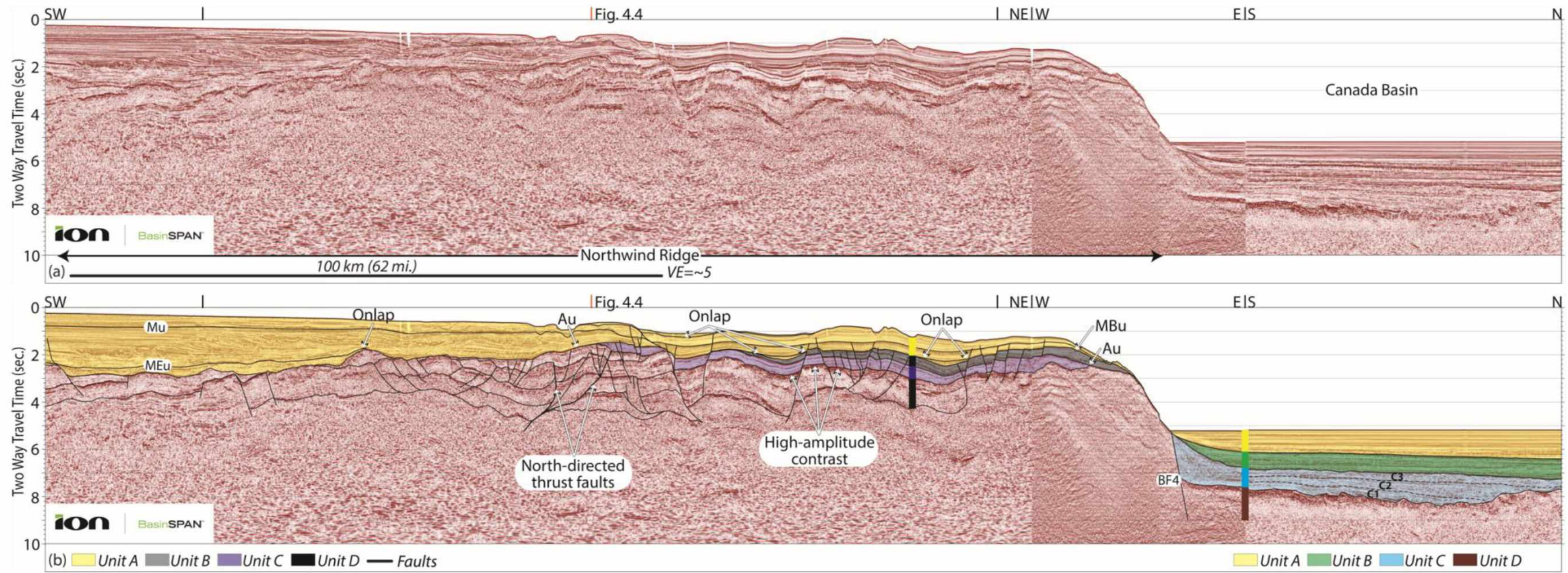

Figure 4.2 MCS profile-1

(a) Northeasterly oriented MCS profile crossing the Northwind Ridge and the western margin of the Canada Basin. This is a crooked profile and the annotated directions indicate changes in profile directions (Fig. 4.1b). Black and orange bars indicate crossing points of the other MCS profiles. **(b)** Interpreted section illustrates subdivision of the stratigraphy across the profile and extensional and contractional deformations, depicted by normal and thrust faults. Unconformities include: Angular, Au; mid-Eocene, MEu; Miocene, Mu (Ilhan and Coakley, in review).

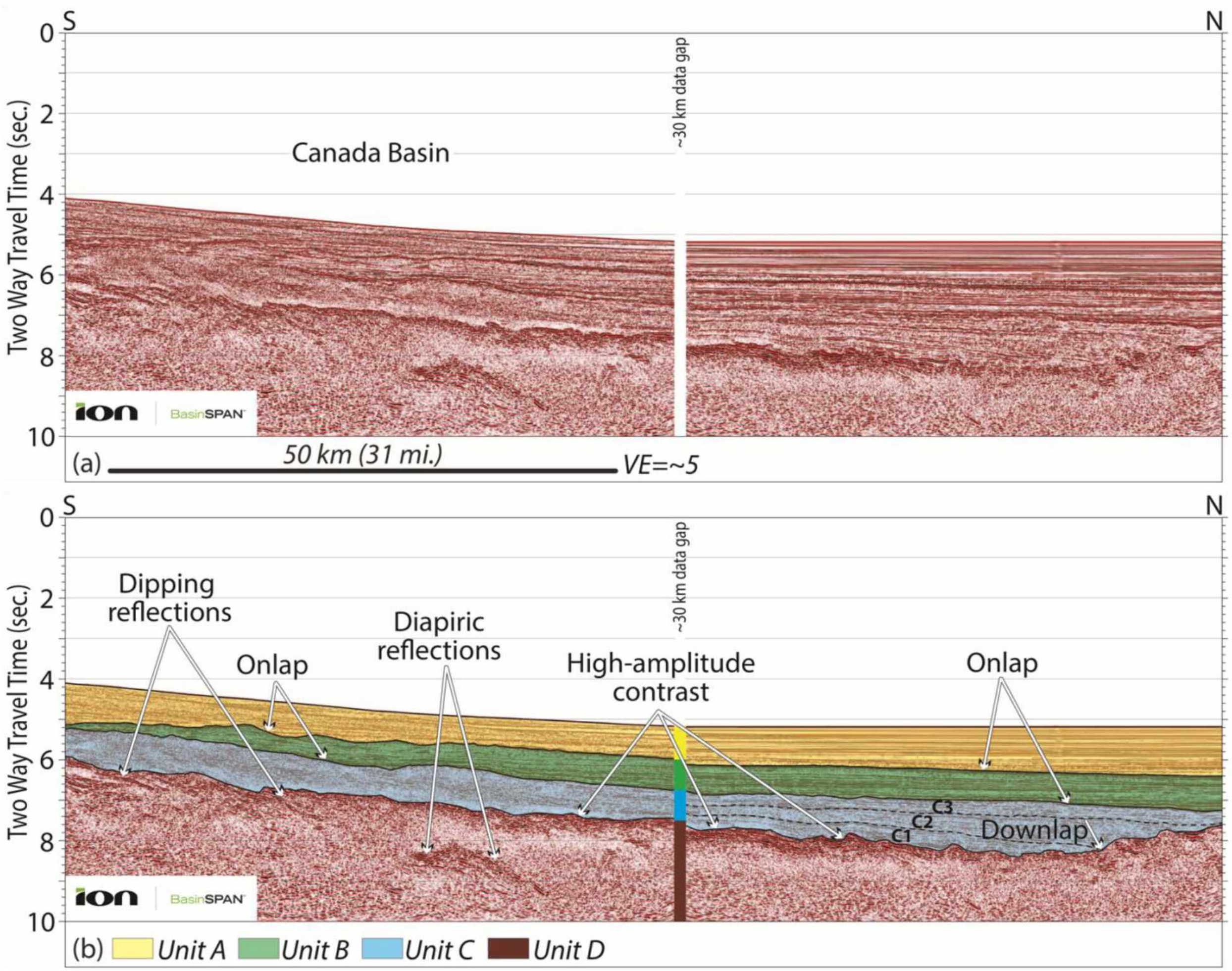

Figure 4.3 MCS profile-2

(a) North-oriented MCS profile crossing the western margin of the Canada Basin. See Fig. 4.1b for location. **(b)** Interpreted section illustrates subdivision of the stratigraphy (unit A-C) defined by onlap and downlap terminations and extensional deformation of the extended continental crust (unit D). Dipping (seaward dipping reflections) and diapiric reflections are interpreted as a volcanic accrecionary sequence (or stratified magmatic) and intrusive igneous rocks respectively.

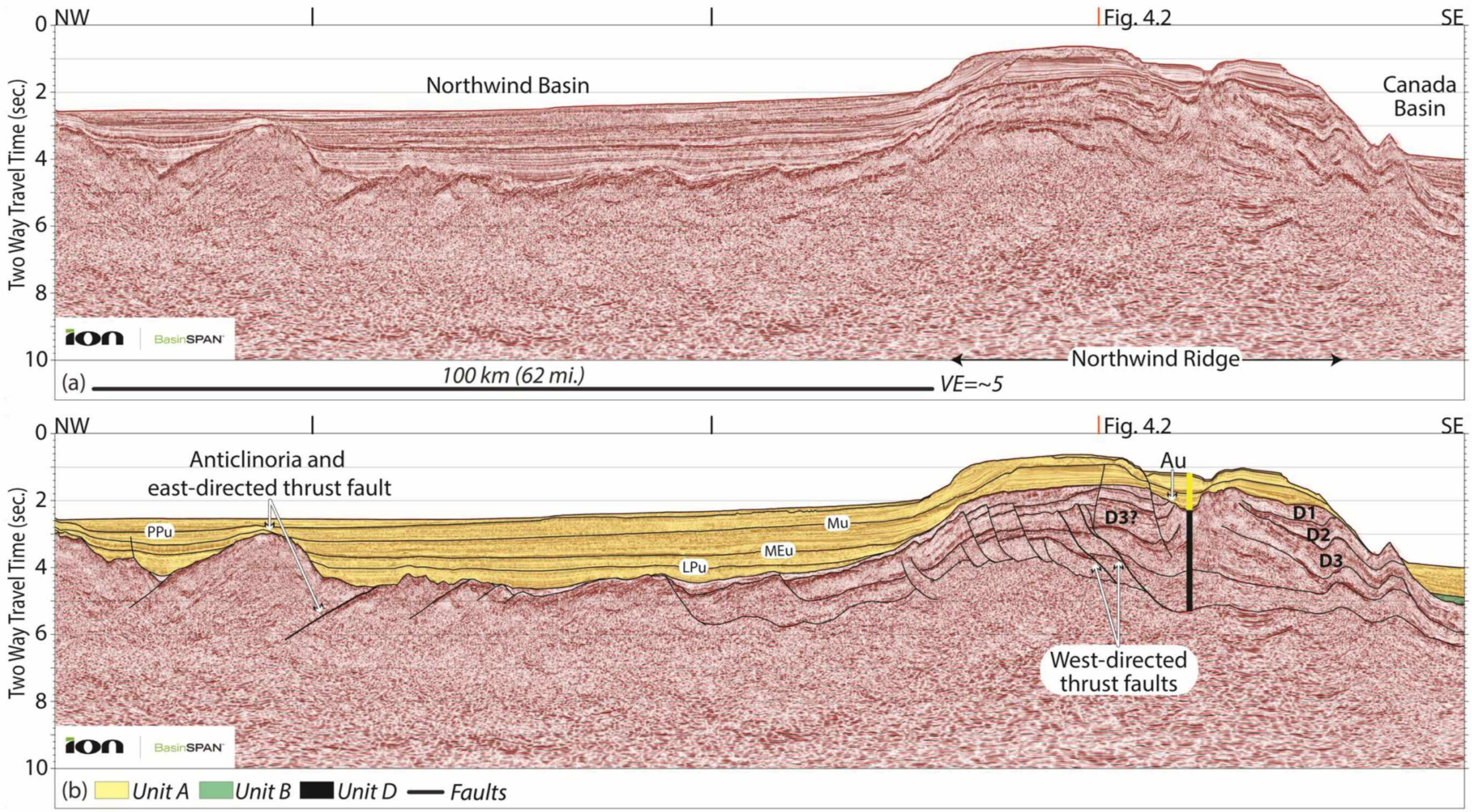

Figure 4.4 MCS profile-3

(a) NW-SE oriented MCS profile crossing the western sub-basins of the Northwind Basin, the Northwind Ridge, and the western margin of the Canada Basin. Black and orange bars indicate crossing points of the other MCS profiles. See Fig. 4.1b for location. **(b)** Interpreted section illustrates subdivision of the stratigraphy across the profile and extensional and contractional deformations, depicted by normal and thrust faults, and folding of D2 and D3 sub-units. Unconformities include: Angular, Au; late-Paleocene, LPu; mid-Eocene, MEu; Miocene, Mu; Plio-Pleistocene, PPu (Ilhan and Coakley, in review).

5 Conclusions

All tectonic models for the Amerasia Basin make predictions about the relationship between the Chukchi Borderland, the structures beneath the Chukchi Shelf basins and the Canada Basin. These predictions for formation of the Canada Basin have been tested by using multi-channel seismic data. A new set of constraints for the opening of the Canada Basin has been developed.

The tectonic setting of the extinct mid-ocean ridge (MOR) that bisects the Canada Basin argues that it was formed by ultra-slow seafloor spreading. Given the time required to explain the amount of seafloor delimited by paired magnetic anomalies and the apparent absence of the Cretaceous long normal interval in the magnetic anomalies, seafloor spreading must be younger than currently conceived, occurring no earlier than the Cenomanian. The other possibility is that the MOR of the Canada Basin could have formed as part of the continent-ocean transitional (COT) crust and be older than the Hauterivian.

The absence of significant deformation along Northwind Ridge suggests that the current structure was formed in the events that created the Canada Basin. Along the western margin of the Canada Basin, a clinoform sequence (unit C), which is inferred to correlate with the Jurassic-Lower Cretaceous Kingak shale unit of the Alaska North Slope and the underlying COT crust (unit D), supported by seaward dipping and parabolic reflections imply that the COT and, perhaps the MOR, crust of the Canada Basin formed no later than the Middle Jurassic.

While the observations and crude kinematics outlined in this dissertation present testable hypotheses for future work, they fall short of a complete model for the development of the Canada Basin. In strategic locations, direct sampling, seismic imaging and analysis of the sub-Au rocks of the Chukchi Borderland would constrain the history of the Amerasia Basin, Arctic Ocean.